ALEKSI HÄNNINEN
CELL SEEDING OF POROUS POLYMER-BASED SCAFFOLDS
WITH HUMAN ADIPOSE-DERIVED STEM CELLS
Master of Science Thesis

ABSTRACT

ALEKSI HÄNNINEN: Cell seeding of porous polymer-based scaffolds with human adipose-derived stem cells
Tampere University of Technology
Master of Science Thesis, 84 pages, 7 Appendix pages
April 2015
Master's Degree Programme in Biotechnology
Major: Tissue Engineering
Examiner: Professor Minna Kellomäki

Keywords: Cell seeding, biomaterials, adipose-derived stem cells, tissue engineering

Tissue engineering aims to regenerate or create damaged or lost organs and tissues by utilizing biodegradable scaffolds, cells and growth factors. One promising tissue engineering strategy involves seeding cells into a porous scaffold and culturing it *in vitro*, which is followed by implantation into the defect site. Cell seeding should result in a uniform distribution of cells inside the scaffold - otherwise the functionality and mechanical properties of the engineered construct can be compromised. Also a high seeding efficiency is appreciated to avoid wasting valuable cells and to enable faster tissue formation.

The aim of this study was to test six different cell seeding methods in order to find an optimal method for supercritical carbon dioxide (ScCO$_2$) processed scaffolds. Of these scaffolds, one was a copolymeric poly(L-lactide-co-ε-caprolactone) 70/30 (PLCL) scaffold, whereas the other one was a composite of PLCL and β-tricalcium phosphate. The functionality of the cell seeding methods was verified with two scaffold types that were manufactured from poly-L/D-lactide 96L/4D (PLDLA 96/4) fibers. In addition, a novel cell seeding model utilizing iron-labeled microspheres with diameters of 15 μm and 100 μm was proposed. Adipose-derived stem cells (ASC) were used in the experiments due to their potential in hard-tissue engineering.

The study revealed that the microsphere seeding model is functional, offering useful information about the seedability of the ScCO$_2$ processed scaffolds. The microsphere distributions were noticed to be more uniform compared to the corresponding cell seeding results. The microsphere model also suggested more challenging seedability of the composite scaffolds compared to the PLCL substrates. Applying micro-computed tomography (micro-CT) imaging and seeding ASCs fed with iron oxide nanoparticles, it was noted that the uniformity of the cell distribution in ScCO$_2$ processed PLCL scaffolds can be enhanced by forcing the cell suspension into the scaffold with a syringe.

Due to technological limitations, evaluating cell seeding in the composite scaffolds was more challenging. However, the cell experiments supported the microsphere model, indicating a more difficult seedability compared to the PLCL scaffolds. A static pipetting of cells on top of the PLDLA fabrics was enough to provide desirable cell distribution and cell numbers in those scaffold types.

TIIVISTELMÄ

Kudosteknologia pyrkii korjaamaan tai luomaan uusia kudoksia ja elimiä vaurioituneiden tilalle. Se hyödyntää biohajoavia tukirakenteita (skaffoldeja), soluja ja kasvutekijöitä yksinään tai yhdessä. Eräs lupaava kudosteknologian menetelmä alkaa solunsyötöllä, jossa huokoiseen skaffoldiin istutetaan soluja ja rakennetta kasvatetaan *in vitro* ennen sen implantoimista vaurioalueelle. Solunsyötön pitäisi johtaa tasaiseen solujakaumaan skaffoldin sisällä - muuten rakennetun kudoksen toiminnollisuus ja mekaaniset ominaisuudet saattavat jäädä odotettua huonommiksi. Jotta arvokkaita soluja ei hukattaisi, solunsyöttöprosessin tulisi olla myös tehokas. Tämä edesauttaa myös nopeampaa kudoksen muodostumista.

Työssä testattiin kuutta erilaista solunsyöttömenetelmää tarkoituksena optimoida syöttömenetelmä kahdelle ylikriittisellä hiilidioksidilla prosessoidulle skaffoldityypille. Näistä toinen oli poly(L-laktidi-ko-ε-kaprolaktoni) 70/30 (PLCL) -kopolymeeristä valmistettu ja toinen PLCL:n sekä β-trikalsiumfosfaattikeraamin komposiitti. Solunsyöttömenetelmien toimivuus varmistettiin kahdella poly-L/D-laktidi 96L/4D (PLDLA 96/4) kuiduista valmistetulla skaffoldityypillä. Lisäksi tutkittiin uudenlaista solunsyöttömallia, joka pohjautuu rautaa sisältäviin mikropartikkeleihin. Mallissa soluja jäljiteltiin halkaisijaltaan 15 µm ja 100 µm kokoisilla partikkeleilla. Aikuisen rasvan kantasoluja käytettiin solukokeissa, koska niillä on valtava potentiaali ruston ja luun kudosteknologiassa.

Tutkimuksissa mikropartikkelisolunsyöttömallin huomattiin toimivan ja tarjoavan hyödyllistä tietoa skaffoldien rakenteesta ja sen soveltuvuudesta solujen istutukseen. Rautapartikkelien jakaumat vaikuttivat tosin tasaisemmilta kuin vastaavien solunsyöttökokeiden tulokset. Solunsyöttömalli osoitti myös komposiittiskaffoldien rakenteen olevan solunsyötön suhteen haasteellisempi kuin vastaavien PLCL skaffoldien. Mikro-CT kerroskuvauksen avulla pystyttiin havaitsemaan myös nanokokoluokan rautaoksidipartikkeleilla leimattujen solujen sijainti skaffoldien sisällä. Tämän perusteella huomattiin, että tavallisella ruiskulla voitiin pakottaa solususpensiota PLCL skaffoldien sisään ja parantaa siten solujen tasaista jakautumista verrattuna muihin menetelmiin.

Johtuen teknologisista rajoitteista solunsyötön onnistumisen arviointi komposiittiskaffoldeissa oli haasteellista. Solunsyöttöä rautapartikkeleilla mallinnettaessa huomattiin niiden rakenteen olevan kuitenkin hieman vaikeampi solujen istutusta ajatellen. Perinteinen staattinen solujen pipetointi skaffoldin pinnalle oli riittävä PLDLA kuituskaffoldeissa, tuottaen tasaisen solujakauman ja tyydyttävän solumäärän skaffoldeissa.

PREFACE

This study was performed as a collaboration between the Biomaterials Science and Tissue Engineering Group of Tampere University of Technology and the Adult Stem Cell Group of the Institute of Biosciences and Medical Technology (BioMediTech) at the University of Tampere.

First, I would like to express my deepest gratitude to Professor Minna Kellomäki for offering me this fantastic opportunity and for her professional comments regarding the study. I am also very grateful to Docent Susanna Miettinen for providing the facilities for this study and for her valuable advices throughout the project. My supervisor Ph.D. Kaarlo Paakinaho has counseled and challenged me in a most instructive way, for which I am highly thankful. In addition, I would like to thank Ph.D. Kaarlo Paakinaho and M.Sc. Laura Johansson for providing materials for this project.

I am extremely grateful to M.Sc. Sanna Pitkänen for her patient, precise and thorough guidance during this work, as well as for her valuable feedback throughout the project. Also laboratory technicians Anna-Maija Honkala, Miia Juntunen and Sari Kalliokoski have advised me a lot during this work, for which I am very thankful. I owe my gratitude to M.Sc. Markus Hannula for sharing his expertise in imaging and data analysis with me and for providing the 3D images and scaffold porosity analyses for this work. I also would like to thank the rest of my colleagues at BioMediTech for their help during this project. Finally, I want to thank my family and friends for their support. Especially, I want to thank Maaria for her love.

Tampere, 20.05.2015

Aleksi Hänninen

TABLE OF CONTENTS

Appendix 1: Well plate images of COMP50 scaffolds

Appendix 2: Live/Dead experiments 1 & 2

Appendix 3: PLCL & COMP50 CyQUANT results

Appendix 4: PLCL Micro-CT Experiments 1 & 2

Appendix 5: Prussian blue results

ABBREVIATIONS

°C	Celsius degree
2D	Two-dimensional
3D	Three-dimensional
APC	Allophycocyanin
ASC	Adipose-derived stem cell
BioMediTech	Institute of Biosciences and Medical Technology (Tampere, FIN)
BMP	Bone morphogenetic protein
BMSC	Bone marrow-derived mesenchymal stem cell
β-TCP	Beta-tricalcium phosphate
Calcein AM	Calcein acetoxymethyl
CD	Cluster of differentiation
CO_2	Carbon dioxide
COMP50	Composite of PLCL and β-TCP in a weight ratio of 50:50
DNA	Deoxyribonucleic acid
DMEM	Dulbecco's Modified Eagle Medium
DPBS	Dulbecco's Phosphate Buffered Saline
ECM	Extracellular matrix
ESC	Embryonic stem cell
EthD-1	Ethidium acetoxymethyl homodimer-1
FITC	Fluorecein isothiocyanate
g	Standard gravity
GPa	Gigapascal
hASC	Human adipose-derived stem cell
HCl	Hydrochloric acid
HFSC	Human Fat Stem Cell
HLA-DR	Human leukocyte antigen-DR
H_2O	Water
IFATS	International Federation for Adipose Therapeutics
iPSC	Induced pluripotent stem cell
ISCT	International Society for Cellular Therapy
kPa	Kilopascal
Micro-CT	Micro-computed tomography
MSC	Mesenchymal stem cell
PCL	Poly(ε-caprolactone)
PDL	Poly-D-lysine
PE	Phycoerythrin
PE-Cy7	Phycoerythrin-Cyanine
PLCL	Poly(L-lactide-co-ε-caprolactone)
PLGA	Poly(lactide-co-glycolide)
PLA	Polylactide
PLDLA	Poly-L/D-lactide
PLLA	Poly-L-lactide
Rpm	Revolutions per minute
$ScCO_2$	Supercritical carbon dioxide
T_g	Glass transition temperature
T_m	Melting temperature
USPIO	Ultrasmall superparamagnetic iron oxide
VEGF	Vascular endothelial factor

1. INTRODUCTION

Severely injured or diseased tissues and organs are often reconstructed using artificial tissues or organ transplants. These kinds of alternatives do not always repair the function of the lost tissue and there are problems related to immune rejection and limited number of donated organs. Described as an ultimately ideal treatment, tissue engineering strives for regenerating new organs and tissues without any of the listed problems. (Ikada 2006; Chapekar 2000)

Currently, autografts are the golden standard for bone repair due to their osteoconductive and osteoinductive properties and thus dominate the bone grafting business that has sales of over 2.5 billion dollars per year. The problems with autografts are related to their limited availability, donor-site morbidity and cost. Bone tissue engineering as a leading field in multidisciplinary tissue engineering can provide a functional biological substitute to bone grafts. The most promising strategy in bone tissue engineering involves seeding adult stem cells or osteoblasts into a 3D scaffold, culturing the construct *in vitro* and implanting it into the defect site. (Pina et al. 2015; Costa-Pinto et al. 2011; C.M. Murphy et al. 2013)

Adipose-derived stem cells have been considered as a suitable alternative for tissue engineering due to their multilineage differentiation capacity. Regardless of the target tissue, large engineered tissue constructs require uniform and efficient cell seeding in order to achieve functional tissue equivalents. (Tirkkonen et al. 2012; Vunjak-Novakovic et al. 1998) In this work, different cell seeding methods were compared with respect to cell viability, number and distribution. Four different scaffold types were examined by seeding human adipose-derived stem cells into them, using six cell seeding methods.

THEORETICAL PART

2. CELL SEEDING

Tissue engineering utilizes three basic components, namely cells, biomaterial templates called scaffolds and signals such as growth factors. These three can be applied together or individually. (Ikada 2006) One tissue engineering approach involves *in vitro* generation of engineered tissue, which generally begins with the attachment of cells on three-dimensional (3D) scaffolds. This phase is referred to as cell seeding. (Bueno et al. 2007) This chapter explains the rationale behind successful cell seeding and presents some of the most typical cell seeding parameters and methods that have previously been used.

2.1   The purpose and requirements of successful cell seeding

Being the first step of the process, optimal cell seeding is essential in successful cultivation of large *in vitro* tissue constructs (Vunjak-Novakovic et al. 1998). The *in vitro* development of engineered tissues is highly enhanced by uniform distribution of the attached cells and an optimal initial cell concentration. The deficiencies in cell seeding are generally hard to compensate later during the tissue cultivation period. (Vunjak-Novakovic & Radisic 2004)

Uniformly distributed cells enable uniform extracellular matrix (ECM) deposition, which leads to uniform tissue growth that affects the functionality of the tissue. High seeding efficacy, meaning a high ratio of attached cells to seeded cells is important for rapid tissue regeneration. A successful cell seeding process includes also fast cell attachment to scaffolds and a high cell survival percentage. Thus, evaluating cell seeding should be done by determining cell distribution, the amount of deoxyribonucleic acid (DNA) and viability of the cells. (Bueno et al. 2007; Kinner & Spector 2002; Vunjak-Novakovic & Radisic 2004)

After cell seeding, the resulting cell-scaffold construct can be cultivated under applicable conditions to enable tissue formation (Vunjak-Novakovic & Radisic 2004). Ultimately, the newly engineered tissue could be integrated into functional tissue and the biodegradable scaffold should be slowly replaced by cell migration, proliferation and ECM production (Thevenot et al. 2008). Even though cell seeding has been studied widely using different scaffolds and cell types, the studies are typically narrowed to a specific application and thus cannot be generalized to other tissue engineering cases (Bueno et al. 2007).

In order to permit a higher rate of tissue development, optimal initial construct cellularity is appreciated. Also user independence and high reproducibility should be considered. Although these requirements apply to most tissue engineering cases, their criticality ranges between different types of cells and scaffolds. Hence, the conditions and duration of the seeding process need to be cautiously selected. Anchorage-dependent and shear-

sensitive cells for example should be seeded with a high kinetic rate in order to minimize their time in a suspension culture. (Vunjak-Novakovic et al. 1998; Vunjak-Novakovic & Radisic 2004; Soletti et al. 2006; Bueno et al. 2007)

Facilitating fast cell attachment not only enhances the survival of anchorage-dependent cells, but also accelerates tissue ingrowth in the scaffolds. On the other hand, many polymeric scaffolds are typically hydrophobic and possess small pore sizes, for which the capillary resistance is larger. In such cases longer seeding times are required - cellular penetration can be even completely hindered. In order to fasten the seeding process, external forces can be applied, but it is possible that mechanical forces like shear stress lead to shear-mediated membrane lysis or trigger apoptotic pathways. (Bueno et al. 2007; Li et al. 2007; Nguyen et al. 2012; Dardik et al. 2005)

A high cell density, in other words the number of cells per construct or volume unit, can be favorable for tissue formation in 3D constructs by affecting cell-cell and cell-scaffold interactions. Thereby one of the key parameters in obtaining a decent seeding result is the cell seeding density, which can be thought as the number of cells per cubic centimeter introduced to the scaffold. The effect of different seeding densities depend on the tissue type and the culture conditions. Low seeding densities can prolong the time needed to obtain a well-populated scaffold ready for implantation, which can prevent their use in bioengineering applications. (Bueno et al. 2007; Shimizu et al. 2007; Grayson et al. 2008; Godbey et al. 2004)

Even though low seeding densities have also been linked to loss of mechanical integrity and limited cell proliferation, the properties of the seeded construct cannot automatically be increased by increasing the seeding density. For example, in a prior study no improvement in bone formation of tissue engineered bone was seen, although a more homogenous cell distribution was reported, when seeding densities of 1×10^6 cells per cm^3 and 10×10^6 cells per cm^3 were compared. Moreover, indicating scaffold saturation, the seeding efficiency and the survival of cells seem to decrease when seeding density is increased. Anyhow, better understanding of the effects of initial cell density is needed. (Bueno et al. 2007; Holy et al. 2000; Grayson et al. 2008)

Along with cell seeding density and the seeding method, also cell source contributes considerably to the seeding efficiency (Kinner & Spector 2002). The cells used in tissue engineering have certain general requirements like isolation from a tissue, *in vitro* proliferation in order to increase the cell mass for seeding large 3D scaffolds and the capacity to differentiate into functional target tissues (Vunjak-Novakovic & Radisic 2004). Fast proliferating stem cells might compensate low scaffold cellularity, but seeding slowly proliferating mature cells like chondrocytes or osteoblasts in an inefficient manner leads to catastrophic consequences in terms of tissue development. Obtaining differentiated mature cells in sufficient numbers for a tissue engineering scaffold is also difficult, but on the other hand there are ethical considerations with the stem cells. (Bueno et al. 2007)

2.2   Cell seeding methods

There are many different cell seeding methods and various ways to classify different seeding strategies. The methods can be divided into active and passive (Solchaga et al. 2006), surface and bulk seeding (Soletti et al. 2006) or static and dynamic (Buizer et al. 2013; Melchels et al. 2010; Zhu et al. 2010) seeding. Here, a view modified from (Burg et al. 2000) is used, where three main seeding strategies are distinguished. These are static, dynamic (external forces are applied but bioreactors are excluded) and bioreactor (such as spinner flask and perfusion systems) seeding.

2.2.1   Scaffold pre-wetting

Common to all cell seeding methods is that the scaffolds need to be pre-wetted with culture medium before the seeding process. The reason lies in displacing air in the scaffold, which could prevent the migration of cells and medium to the center of the scaffold. Pre-wetting also permits proteins from the culture medium to adsorb to the surface of the scaffold. This makes the surface of polymers like poly(ε-caprolactone) (PCL) less hydrophobic, which enhances cell attachment. Pre-wetting can be done for example by applying vacuum or pressure on scaffolds sunk in culture medium. (Vunjak-Novakovic & Radisic 2004; Wang et al. 2006; Melchels et al. 2010)

2.2.2   Static cell seeding

Static seeding is the most frequently used cell seeding method. It means mixing cell seeding suspension with a scaffold without applying external forces. (Buizer et al. 2013) Two common static seeding methods are schematically illustrated in Figure 1. Typically cell suspension is spread on top of the scaffold using a pipette. Static cell seeding can be applied to every cell type and scaffold structure, although it is thought to be the least efficient approach. The scaffold is incubated with the seeded cells from hours to days in order to maximize cell seeding efficiency. (Adebiyi et al. 2011; Villalona et al. 2010)
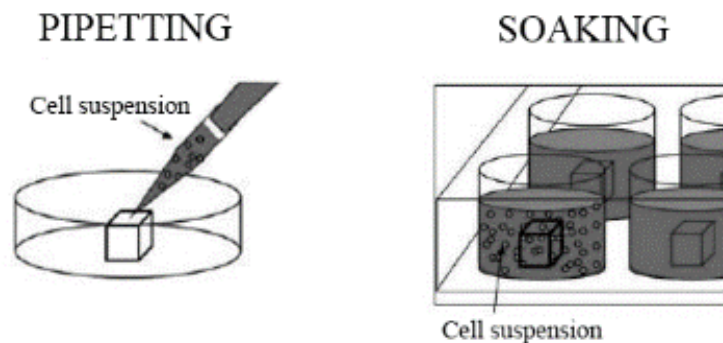

Figure 1. *Pipetting and soaking are two common static cell seeding methods. After cell seeding, the cell-scaffold constructs can be cultivated in growth medium alone. Modified from (Hasegawa et al. 2010).*

Static seeding relies on gravitational forces alone and requires large pore sizes that allow cell penetration throughout the scaffold. Owing its popularity mostly to its simplicity, it also does not require costly equipment or expose cells to possibly damaging forces. The problems of static seeding include low seeding efficiencies and inhomogeneous spatial cell distribution in the scaffold. (Li et al. 2007; Ji et al. 2011; Dai et al. 2009; Buizer et al. 2013) Seeding small cell suspension volumes (100 µl) with a large number of cells might lead to formation of cell aggregates on the scaffold surface. These aggregates may cover the pores and prevent other cells from migrating to the inner parts of the scaffold. After the seeding process, the cells in the center of the scaffold might be too far from the surfaces and become necrotic due to lack of nutrients or oxygen. An open pore network facilitates nutrient and oxygen transport during static culture phase that follows cell seeding. (Ding et al. 2008; Melchels et al. 2010) On the other hand, this might be the case with any cell seeding method followed by static culture phase.

In many cases the penetration of cells depends on the material and porosity of the scaffold (Villalona et al. 2010) and there are thus different views about the recommendable appliance of static seeding techniques. According to Vunjak-Novakovic and Radisic, static seeding can be successfully used if the scaffolds are thinner than 2 mm (Vunjak-Novakovic & Radisic 2004). Schliephake et al. claim penetration of cells to a maximum depth of 500 µm depending on the material of the scaffold (Schliephake et al. 2009), while Zhu et al. recommend static seeding to scaffolds with a thickness less than 1.2 mm (Zhu et al. 2010). Dong et al. suggest that the seeding efficiency is always low, even with excellent scaffolds containing large pores. The reason presented was the presence of air in the pores, which emphasizes the importance of pre-wetting. (Dai et al. 2009)

The seeding efficiency might increase if the scaffold is flipped at timed intervals like every hour. In addition to the static seeding method where the cell suspension is spread on top of the scaffold with a pipette, there are other alternatives to seed scaffolds statically with cells. For example, the cell suspension can be injected into multiple evenly divided points using an injection needle or small cuts can be applied to the scaffold surface using a scalpel. Injection seeding is beneficial especially if cell seeding needs to be performed in a specific area within the scaffold, but at the same time it damages the scaffold. Another static seeding method involves soaking scaffold granules in cell suspension. (Vunjak-Novakovic & Radisic 2004; Vitacolonna et al. 2013; Thevenot et al. 2008; Buizer et al. 2013)

2.2.3 Dynamic cell seeding

There are numerous articles where spinner flasks, rotating vessel and perfusion bioreactors are described as dynamic cell seeding methods (Burg et al. 2000; Melchels et al. 2010; Vunjak-Novakovic & Radisic 2004). In this text, bioreactor systems like this are excluded from dynamic cell seeding techniques and form their own chapter. The reason for this lies in the fact that such bioreactors are often used also for culturing the cells after

the seeding process, which can lead to very different seeding results compared to static culture. In dynamic seeding an external force is applied to seed cells to the scaffold, which distinguishes it from static seeding. (Burg et al. 2000; Buizer et al. 2013)

The most common strategies of dynamic cell seeding utilize hydrostatic forces as for example in centrifugation, or create pressure differentials (Villalona et al. 2010). Further examples include methods using electric or magnetic fields as driving forces. Although dynamic seeding might yield in more homogenous and efficient seeding results compared to static seeding, the methods are more complex and possibly lead to prolonged seeding time. In addition, all the dynamic seeding methods have their own specific disadvantages. One relatively easy way to improve seeded cell density and uniformity of the cell distribution is to apply mild suction to help the cells to permeate through the scaffold. For elastomeric scaffolds like poly(L-lactide-co-ε-caprolactone) (PLCL) sponges, it is possible to use compression forces to induce suction that has helped rabbit chondrocytes to infiltrate to the scaffold. Multiple cycles of compression-induced suction were reported to increase the uniformity of the cell distribution, but also to slightly decrease cell viability. (Soletti et al. 2006; Buizer et al. 2013; Melchels et al. 2010; Xie et al. 2006) An illustration of this method is presented in Figure 2.
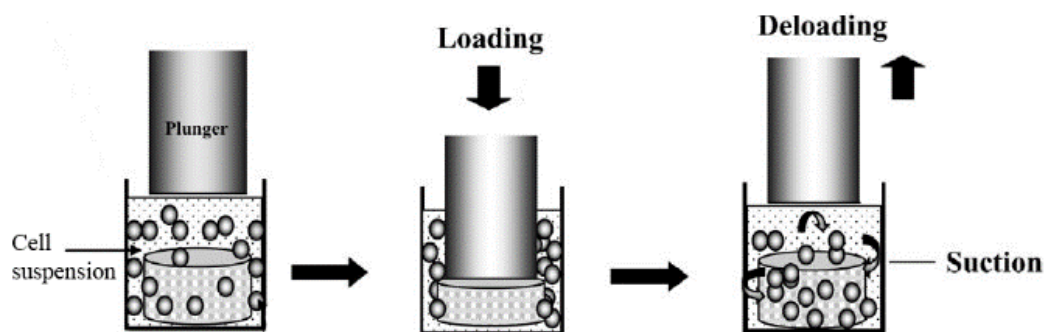
Figure 2. Elastomeric scaffolds can be seeded in a dynamic manner by applying compression-induced sectional forces. Modified from (Xie et al. 2006).

Rotational seeding is a common strategy used for example in vascular tissue engineering. In addition to rotational bioreactor systems, dynamic cell seeding method involving centrifugal forces has been investigated. This requires fewer cells and less time in comparison to spinner flask bioreactors. As a consequence, cell media and other resources are needed in lesser quantities and the time from cell seeding to cell proliferation phase is shorter. Although cell viability is generally maintained in centrifugal cell seeding, there are concerns whether cell morphology remains unaffected in the process. With too high rotation speeds, also cell lysis has been reported. (Villalona et al. 2010; Godbey et al. 2004)

Godbey and his colleagues investigated different rotation speeds within the range of 0-6000 rpm using murine bladder smooth muscle cells or human foreskin fibroblasts and polyglycolide (PGA) fiber scaffolds with porosities of 95%. Since the centrifuges used

did not allow smooth rotation below 2000 rpm and unbalanced centrifugation resulted in unwanted cell shearing, the rotor speed was set constant to 2500 rpm for the experiments. In this case, this translates to 35.0 times gravitation ($\times$ g) at the inner surface of the scaffold and 52.5 $\times$ g at the outer surface. In comparison, spinner flasks typically utilize seeding conditions up to 500 rpm. From different centrifugation times tested, 10 minutes was found to be the optimal choice with even better results if the centrifugation time was broken into one minute segments. The cellular distribution and seeding efficiency were superior compared to static and spinner flask seeding. The method was reported to be especially efficient at low cell concentrations (1.33×10^5 cells/ml) and recommended to be used for planar and cylindrical scaffolds. (Godbey et al. 2004; Villalona et al. 2010)

Later, different conditions were tested by spinning PGA fiber mesh sheets and ovine bone marrow stromal cells 5×2 minutes at 2500 rpm. After each cycle, the unattached cells were re-suspended. Again, improved seeding efficiency and cell distribution were reported. (Roh et al. 2007) Seeding fibroblasts on 0.7 mm thick porous fibrin scaffolds by centrifuging them for 5 minutes at 1000 rpm was investigated by Lam et al. in 2007. The centrifuge method was found to be superior compared to an orbital shaker method, where the cell-scaffold constructs were placed on a shaker for 4 hours at 60 rpm. Nevertheless, neither of these methods nor the combined centrifuge and orbital shaker method was able to deliver cells deeply into the scaffold. (Lam et al. 2007)

Seeding techniques applying pressure differentials have been investigated in vascular tissue engineering for decades (Villalona et al. 2010). Low pressure or vacuum have commonly been used in tissue engineering to remove air from inside the scaffolds (Dai et al. 2009; Hasegawa et al. 2010; Vunjak-Novakovic & Radisic 2004). Using hydroxyapatite scaffolds and rat bone-marrow derived osteoblasts, Dong et al. concluded that this induced cell suspension flow into the pores and thus increased bone tissue formation in rats. Their system consisted of a vacuum pump, desiccator and a controller. The low pressure method can naturally be integrated into other seeding systems as well. (Dong et al. 2001)

Two different low pressure methods were tested by Hasegawa et al. for scaffold degassing prior to seeding rat bone marrow-derived stem cells into ceramic scaffolds. The actual seeding was done by simply soaking the scaffolds into cell suspension. In the other low pressure method, the scaffolds in growth medium were first exposed to pressure of 100 kilopascals (kPa) and soaked then in cell suspension. The second method applied a syringe for creating the same pressure of 100 kPa by closing the syringe tip, pulling its plunger back, vibrating the syringe and letting the air out. This was repeated a couple of times, after which the scaffolds were also soaked in cell suspension. This syringe method was noticed to result in higher amount of cells in the scaffold than the other low pressure system or two static groups, where the scaffolds were either soaked in cell suspension or the cells pipetted on top of the scaffolds. (Hasegawa et al. 2010)

Syringes have been applied in low pressure cell seeding also directly and not only for scaffold degassing. One way is to set the scaffolds into the syringe, draw cell suspension and some air into the syringe, after which the syringe is closed with a cap. By pulling the plunger back, low pressure is created within the syringe – this step can be repeated a few times. Named "a 1-min method for homogenous cell seeding", the method was noticed to result in a homogenous cell distribution with a cell seeding efficiency equivalent to that of static seeding. The scaffolds used included both polymeric and ceramic scaffolds. (Tan et al. 2012)

Another syringe method involving a stopcock can be used to create low pressure first and then add cell suspension, or bone marrow as done by Yoshii and his colleagues. A schematic illustration of the method is presented in Figure 3. The β-tricalcium phosphate (β-TCP) scaffolds were transplanted into intramuscular sites of rabbit and bone formation was observed at 5 and 10 week time points. Seeding under low pressure led to significantly higher amount of newly formed bone compared to seeding under atmospheric pressure. (Yoshii et al. 2009)
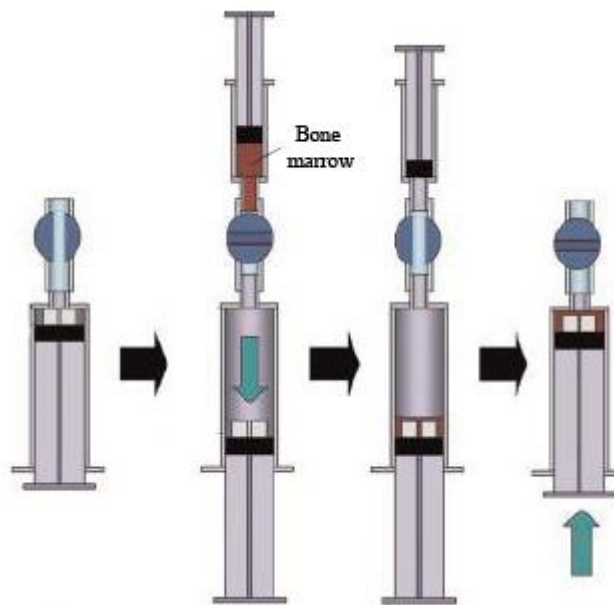
Figure 3. An illustration of a cell seeding method applying low pressure in a syringe system. Modified from (Yoshii et al. 2009).

Despite promising results, the effects of the low pressure treatment on cell viability and genetic mutations as well as cell differentiation, de-differentiation and function should also be followed (Dai et al. 2009). Moreover, not all publications confirm the efficiency of low pressure methods on cell seeding. When comparing low (45%) and high (90%) porosity tricalcium phosphate scaffolds, Buizer et al. noticed that the seeding outcome was more homogenous with static seeding than with vacuum seeding. Although the vacuum method resulted in a higher number of seeded cells on the low porosity scaffolds,

after 7 days the cell numbers were comparable regardless of the seeding method. (Buizer et al. 2013)

In addition to the more common dynamic cell seeding methods, less frequently used techniques include for example using cells labeled with magnetite nanoparticles and applying magnetic forces (Shimizu et al. 2007) and employing surface acoustic waves (Li et al. 2007). With very highly porous scaffolds, cell seeding can be challenging because the cells might end up to the bottom of the culturing plate. Cell seeding efficiencies of more than 90% have been achieved by delivering the cells inside a hydrogel where they are entrapped. Despite the possible advantages in dynamic cell seeding methods, these conditions do not ensure a uniform cell distribution. (Hong et al. 2014; Andersen et al. 2013; Bueno et al. 2007)

2.2.4 Bioreactors

Not only the cell seeding method, but also the following cell proliferation environment has been shown to have an effect on the seeding outcome. Bioreactors can be used for both dynamic seeding and culturing of the cells. Culturing cells in bioreactors reduces problems with mass-transfer limitations. In addition, the behavior and biochemical activity of the seeded cells can be modified by altering the culturing technique. Seeding scaffolds in a bioreactor offers often an automated and controlled process with an effective and reproducible outcome. Different bioreactor types include for instance spinner flask, rotating wall and perfused chamber bioreactors, which are presented in Figure 4. (Burg et al. 2000; Martin & Vermette 2005; Schliephake et al. 2009; Zhu et al. 2010; Martin et al. 2004)
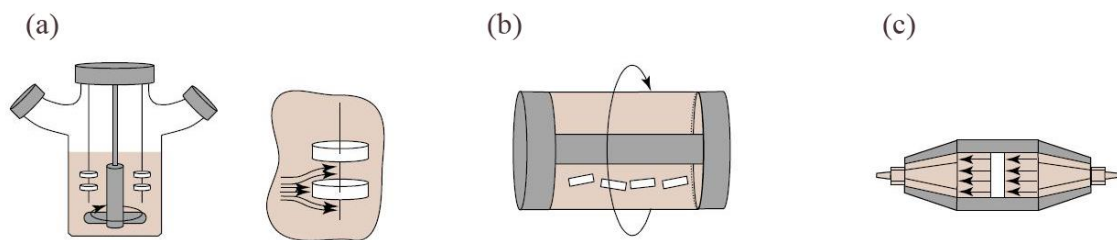
Figure 4. Three common bioreactor types: a) spinner flask, b) rotating wall and c) perfusion chamber. The scaffolds are shown in white. Modified from (Martin et al. 2004).

Rotational systems like spinner flask (or stirred-flask) bioreactors are a well-accepted and commonly used cell seeding method. In such a system the scaffold is attached to a needle that is placed into a spinner flask with cell suspension. A spinner in the flask rotates the medium, which drives the cells into the scaffold. The following culture period in the flask ranges generally from 12 to 72 hours. With low-speed rotation, spinner flasks have not

indicated to affect cell morphology. Since the method requires seeding times of approximately 24 hours, its practicality is limited especially in applications where the seeded scaffold should be implanted the same day. (Godbey et al. 2004; Villalona et al. 2010)

Perfusion bioreactors are used to prevent diffusional limitations in mass transfer. Perfusing scaffolds with culture medium allows the transport of oxygen to the cells through both diffusion and convection. (Vunjak-Novakovic & Radisic 2004) Both cell seeding and the subsequent cultivation phases can be performed using a perfusion bioreactor. These kinds of bioreactors have been originally designed for vascular grafts, but are used also for example in cartilage and cardiac tissue engineering. The medium flow rate can affect the results of direct perfusion. (Martin & Vermette 2005) Also the prolonged culture period required with perfusion bioreactors leads to a growing risk of fungal and bacterial contamination. Also the complexity of such bioreactors reduce their suitability for clinical applications. (Villalona et al. 2010)

The rotating wall bioreactors comprise of a stationary inner cylinder providing for gas exchange and a rotating outer cylinder. In some applications also the inner cylinder can be rotated independently from the outer cylinder. The space between these two cylinders is filled with culture medium and the scaffolds are placed there after they are seeded with cells. Rotating-wall vessels are used for dynamic culturing with low shear stress and high mass-transfer rates. In some cases rotating wall bioreactors have shown effectiveness, but problems arise for example from random collisions of scaffolds between themselves and the culture chamber. Rotating wall bioreactors have been shown to promote osteogenic differentiation. Even so, the positive effect of perfusion systems on osteogenic differentiation has been shown to be greater than that of the rotating wall bioreactors. (Yeatts & Fisher 2011; Martin & Vermette 2005; Zhang et al. 2010)

3. BIOMATERIALS IN TISSUE ENGINEERING

Reconstructing tissues or organs by a simple cell injection is possible only in few cases. In order to form tissues with distinct three-dimensional shapes, support is usually needed. Biomaterial scaffolds provide this support by functioning similarly to natural ECM and thus promoting cell proliferation and differentiation. (Ikada 2006) When it comes to scaffolds, there are two main strategies in tissue engineering. The first approach involves using scaffolds as supporting constructs upon which cells are seeded *in vitro*. Secondly, they can be used as devices for growth factor/drug delivery. These two strategies can also be combined. The scaffold should degrade over a period of time that would allow tissue formation concurrently – ideally the scaffold disappears leaving behind regenerated tissue. (Howard et al. 2008; C.M. Murphy et al. 2013)

3.1   Natural bone and cartilage

Bone has a high regeneration potential, for which it is the most investigated tissue in tissue engineering. It is also a core theme when it comes to biomaterials in this work. The hierarchical structure of bone is so complex that it is still not very well understood. Nevertheless, in order to choose the right biomaterials for bone tissue engineering, it is essential to understand the composition and properties of bone. The role of this dynamic tissue is to function as mechanical support, which provides mineral homeostasis at the same time. (Pina et al. 2015; Reznikov et al. 2014; Jang et al. 2009; Costa-Pinto et al. 2011)

Bone is a family of hierarchically organized complex materials with a network of interconnected cells. The four main components of bone include the mineral phase (consisting of carbonated hydroxyapatite crystals), collagen (with type I being the most abundant protein), non-collagenous macromolecules (such as osteocalcin and osteonectin) and water. In bone, these components are arranged in a hierarchical way that can be divided into multiple different levels. An elementary unit of bone is the mineralized collagen fibril, which, together with water and non-collagenous proteins is responsible for the mechanical properties of bone. The organic matrix constitutes 35% of the mineralized bone ECM. The remaining 65% is composed of the mineral matrix. (Reznikov et al. 2014; Costa-Pinto et al. 2011)

As seen in Figure 5, bone constitutes of an outer layer called compact or cortical bone and an inner layer, which is referred to as spongy or cancellous bone (Nguyen et al. 2012; Bose et al. 2012). Both of these layers are highly vascularized, although the compact bone is much denser with a porosity of 10-30%. The highly porous spongy bone typically has porosities between 30-90%. Correspondingly, the mechanical properties of spongy and compact bone vary as well: Young's modulus of spongy bone ranges between 0.1 and

2 GPa whereas that of compact bone lies in the range of 15 and 20 GPa. High vasculature within the compact bone is enabled by functional units called osteons. These osteons contain central haversian canals, inside which blood vessels and nerves are located. At the same time, spongy bone is porous enough to allow vascularization without osteons. A connective, also highly vascularized connective tissue called the periosteum covers the surface of most bones. (Bose et al. 2012; Nguyen et al. 2012)
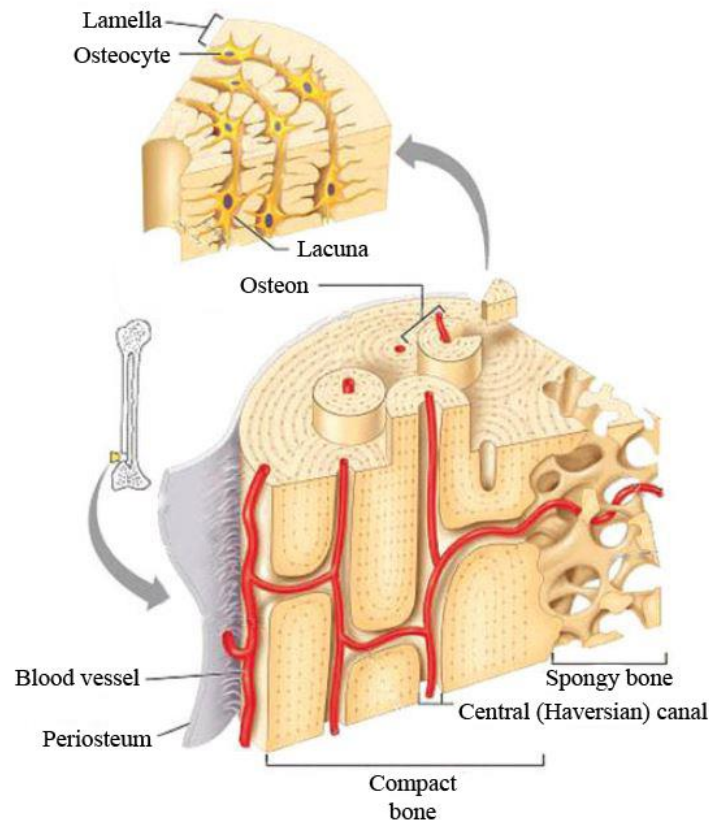
Figure 5. Anatomy of the bone tissue in a nutshell. Modified from (Nguyen et al. 2012).

The different cell types related to bone maintenance include osteocytes that are terminally differentiated and entrapped in the bone ECM, mesenchymal stem cells found in the bone marrow, bone-lining cells covering all bone surfaces, osteoblasts that are able to synthesize organic non-mineralized bone matrix, and finally osteoclasts being capable of resorbing bone tissue which is the first step of bone remodeling. As a living tissue, most of the bone fractures and other defects can be healed through spontaneous regeneration. Defects beyond a critical size cannot heal this way. (Costa-Pinto et al. 2011; Puppi et al. 2010; Fernandez-yague et al. 2014)

In synovial joints that connect two bones with each other allowing movement, the bone ends are covered by a cushioning cartilage layer. In addition, a capsule in the joint with lubricating synovial fluid protects the bone ends. The state when the cartilage layer in the bone ends has been worn away is called osteoarthritis. (Starr & McMillan 2015) Mechanical stimulation is part of the development and maintenance of natural cartilage, which

should be noticed in tissue engineering as well. Cartilage is an avascular tissue with highly differentiated chondrocyte cells present at low concentrations in the ECM. The chondrocytes are supplied with nutrients only by diffusion and fluid flow caused by joint loading. The cartilage has thus poor self-healing capacity, so even a small cartilage defect can result in progressive damage and joint instability. (Jung et al. 2008; Vunjak-Novakovic & Radisic 2004; Ohyabu et al. 2010)

3.2   Scaffold materials

In tissue engineering, the three typically used biomaterial groups are synthetic polymers, natural polymers and ceramics. Due to the design flexibility of synthetic polymers and the structural similarity of ceramics with the mineral phase of bone, these two biomaterial groups are in focus in this work. (O'Brien 2011; Vergroesen et al. 2011) Especially polylactide (PLA) and its copolymers like poly(L-lactide-co-caprolactone) (PLCL) are discussed from the group of synthetic polymers. Most of the attention in the group of ceramics is paid on β-tricalcium phosphate (β-TCP).

3.2.1   Polylactide and its copolymers

Polylactides are thermoplastic polyesters from the family of poly-α-hydroxy acids, which is the most widely used polymer group in clinical surgeries. Lactide monomers, which are dimers of lactic acid, form the polymer backbone of polylactides. They can be polymerized via direct polycondensation of lactic acid monomers or by ring-opening polymerization of lactide. The ring-opening of lactide (presented in Figure 6) is a better route for achieving high molecular weight PLA. Since lactic acid exists as two different enantiomers, L- and D-lactic acid, PLA refers to a group of polymers depending on the form of lactic acid units used to produce lactide dimers and PLA polymers. Of the two enantiomers, L-lactic acid exists in the metabolism of animals and microorganisms. Therefore, this degradation product of PLA is non-toxic. (Paakinaho et al. 2009; Tirkkonen et al. 2012; Huttunen 2013; Lasprilla et al. 2012; Kricheldorf 2001)
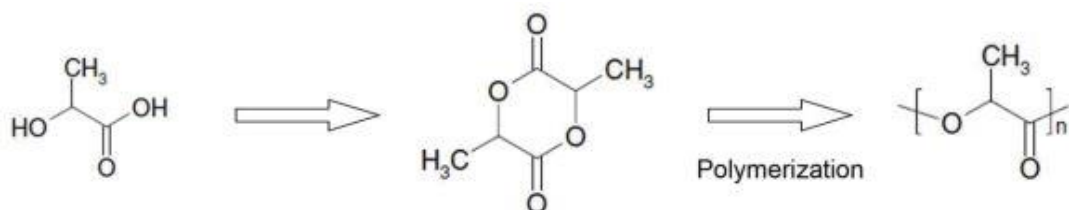

Figure 6. A schematic illustration of PLA synthesis by ring-opening polymerization of lactide. Starting from the lactic acid monomers (available in L- and D-form), their lactide dimers (with possible forms L-, D- and L/D lactide) are polymerized into PLA. Modified from (Paakinaho 2013).

Especially poly-L-lactide (PLLA) and poly-L/D-lactide (PLDLA) are widely studied in the biomedical field due to their biocompatibility and adjustable mechanical and degradation properties (Fonseca et al. 2014; Lasprilla et al. 2012; Ashammakhi et al. 2001). These two have different properties: PLLA is crystalline but PLDLA with a smaller L/D ratio than 87.5/12.5 is amorphous and has thus weaker mechanical properties. The glass transition temperature (T_g) of PLLA is between 60-65°C and melting temperature (T_m) 175°C and it degrades slower than a 50L/50D PLDLA that has a T_g in a lower range from 50°C to 60°C. (Fonseca et al. 2014; Vert et al. 1981; Nair & Laurencin 2007; Paakinaho 2013)

Polylactides degrade mainly by hydrolytic degradation, where the ester bonds in the polymer backbone are cut in a reaction with water. Due to the methyl groups in the polymer backbone, high molecular weight polylactide-based materials are hydrophobic. Still, in an aqueous environment water can diffuse into the polymer matrix in small quantities leading to bulk erosion of the polymer. Following hydrolysis, the molecular weight decays immediately. After reaching a certain molecular weight threshold region, a rapid loss of the mechanical properties takes place. In addition to the chemical structure of the polymer and its water permeability, the degradation rate depends on many factors, such as the sterilization method, sample size and the degradation environment. (Huttunen & Kellomäki 2013; Ashammakhi et al. 2001; Paakinaho 2013)

Different polylactide types have been successfully applied in many different clinical applications, including resorbable sutures and wound dressings (Kricheldorf 2001), small joint reconstructions (Honkanen et al. 2010; Ellä et al. 2011) as well as internal bone fixation devices like plates and screws (Rokkanen et al. 2000). In tissue engineering, they have been considered as drug delivery devices (Nair & Laurencin 2007), non-woven scaffold source materials (Ellä et al. 2007) and other porous 3D scaffolds for reconstruction of ligaments, tendon, bone, muscle and cardiovascular tissues (Coutu et al. 2009; Lasprilla et al. 2012; Van Alst et al. 2009). The limitations of PLA in tissue engineering are related to its acidic degradation products and the lack of reactive side chains for attachment of peptides and other biological cues (Coutu et al. 2009).

Besides their rare properties that are suitable for bone fixation devices, polylactides owe part of their popularity to their processability. For tissue engineering purposes, many different kinds of porous PLA scaffold structures can be produced. The mechanical properties of PLA can also be adjusted via different processing methods, as in the case of drawing fibers which leads to molecular orientation and higher strength in this direction. Melt processing methods are often used in manufacturing of bioabsorbable biomedical devices, but the sensitivity of biodegradable polymers to thermal degradation might lead to varying polymer molecular weights, and thus into variation in the degradation rates. (Rokkanen et al. 2000; Ellä et al. 2007; Lasprilla et al. 2012; Ashammakhi et al. 2001; Paakinaho et al. 2011)

Copolymerization is another efficient way to tailor mechanical, thermal and degradation properties of polylactides and other polymers (Paakinaho 2013). Especially the structures of the comonomers as well as their molar ratio and sequences have an effect on the copolymer properties. Not only are different types of lactide monomers copolymerized with each other to achieve PLDLA, they are also copolymerized with other monomer types, most typically glycolide and ε-caprolactone. For drug delivery applications, incorporating glycolide into the copolylactides is often desirable due to its enhancing effect on hydrolytic degradation. Correspondingly, copolymerizing lactides with ε-caprolactone results in a decreased degradation rate compared to PLLA and PLDLA polymers. The poly-ε-caprolactone (PCL) resulting from the ring-opening polymerization of ε-caprolactone is highly processable due to its low T_g (-60°C) and T_m (55-60°C) and solubility to a number of organic solvents. PCL has an excellent biocompatibility and a high elongation at breakage (>700%), but its low strength properties require enhancement by copolymerization or blending. (Nair & Laurencin 2007; Ellä et al. 2007; Kricheldorf 2001; Lasprilla et al. 2012)

PLLA and PCL are both biocompatible and biodegradable polymers, but their degradation rates and mechanical properties are totally different. Copolymers of lactide and ε-caprolactone combine the properties of the respective homopolymers in a way that leads to a material showing elasticity, good drug-releasing properties and processability resulting from the ε-caprolactone monomer, as well as improved mechanical properties and faster degradation rate compared to PCL homopolymer. (Ahola et al. 2012; Larrañaga et al. 2014) These properties can be tailored by changing the monomer ratio - thus it must be taken into account when comparing the results of different studies. In tissue engineering, PLCL has been widely used in different applications such as drug delivery vehicles, scaffolds for cartilage reconstruction or cell culturing substrates for endothelial and smooth muscle cell culturing. However, especially in bone tissue engineering, the lack of bioactivity in polyesters such as PLCL has led to adding bioactive ceramic fillers into the polymer matrix to form composites with enhanced properties. (Puppi et al. 2010; Jung et al. 2008; Xie et al. 2006; Ahola et al. 2012; Larrañaga et al. 2014)

3.2.2 β-tricalcium phosphate

Ceramics are crystalline, non-metallic compounds that are typically stiff and brittle with a slow degradation rate. Due to their chemical similarity with the inorganic part of natural bone, calcium phosphates such as hydroxyapatite (HA) and beta-tricalcium phosphate (β-TCP) are among the most investigated bone tissue engineering scaffold materials. Both HA and β-TCP can be synthetically produced and are highly biocompatible osteoconductive materials without toxic or immunogenic side effects. However, HA might remain in the regenerated bone, whereas β-TCP is completely resorbable. (C.M. Murphy et al. 2013; Bose et al. 2012; Pina et al. 2015; Kolk et al. 2012)

Having the same calcium/phosphate ratio than the inorganic amorphous phase of natural bone, β-TCP is used as granules and blocks to substitute bone grafts. During their degradation, β-TCP and other calcium phosphate ceramics release calcium and phosphate ions that can used as raw materials for new bone formation. These ions can also induce bone cell activity and induce similar biological responses that are generated in bone remodeling. By forming a strong interface between host bone tissue via direct bonds, calcium phosphates stimulate osteoblastic new bone formation and osteoclastic bone resorption. Still, their mechanical properties are not sufficient enough for load-bearing applications. (Ahola et al. 2012; C.M. Murphy et al. 2013; Kolk et al. 2012; Pina et al. 2015)

3.2.3   Composite biomaterials

Composites of calcium phosphate ceramics and polymers combine the advantages of these two material classes, including mechanical integrity and bioactivity of calcium phosphates as well as toughness, compressive strength and processability of polymers. At the same time, it needs to be noted that bioactive ceramic fillers might have an accelerating or hindering effect on the degradation rate. This kind of composites has been in focus especially in bone tissue engineering. When it comes to osteogenesis, 60 weight-% of β-TCP in PLLA is said to have the same activity than pure β-TCP. (Ahola et al. 2012; Bose et al. 2012; Kolk et al. 2012; Huttunen & Kellomäki 2013; Larrañaga et al. 2014; Aunoble et al. 2006)

3.3   Scaffold fabrication

Not only selecting the appropriate biomaterial, but also selecting a suitable and reproducible processing method is important in optimizing the scaffolds for each application (Vunjak-Novakovic & Radisic 2004; Nguyen et al. 2012). Biodegradable polymers can be processed into similar shapes than any other thermoplastics, but the hydrolytic sensitivity of the polymer bonds needs to be taken into account. In practice, the presence of moisture needs to be minimized to avoid degradation during processing. Otherwise the final polymer properties and molecular weight can be altered. Common processing methods include extrusion, compression molding, solvent casting and injection molding. (Middleton & Tipton 2000) This work focuses on supercritical carbon dioxide ($ScCO_2$) processing and technologies related to polymer fibers.

3.3.1   Scaffold design requirements

Along with the general requirements like providing temporary mechanical support with mechanical properties comparable to host tissue, producing non-toxic degradation products while degrading in a controlled manner and not generating a chronic inflammatory response, a crucial feature for a scaffold is interconnected porosity (Bose et al. 2012;

Romagnoli et al. 2013). As a highly vascularized tissue, bone regeneration should be better when scaffolds enabling greater mass transport are used. The pores are thus essential in bone tissue engineering since they allow bone in-growth and vascularization. Porous scaffold structure also allows the diffusion of nutrients and oxygen to the cells. Moreover, the pores should be interconnected to enable cellular infiltration and growth as well as matrix deposition. (Mitsak et al. 2011; Romagnoli et al. 2013; Bose et al. 2012; C.M. Murphy et al. 2013; Romagnoli & Brandi 2014)

Despite its vitality, porosity of the scaffold has also a downward effect on compressive strength and other mechanical properties, which leads to a trade-off situation (Karageorgiou & Kaplan 2005; Costa-Pinto et al. 2011; Mitsak et al. 2011; Bose et al. 2012). When it comes to pore sizes, too large pores limit scaffold surface area and thus cell adhesion, but on the other hand small enough pore sizes hinder cell migration. This can lead to formation of cellular aggregations around the periphery of the scaffold, inhibiting nutrient diffusion and waste removal. The hypoxic conditions tend to result in an osteochondral process before osteogenesis. Another concern in this kind of a case is premature core degradation of the construct. The optimal pore size in bone tissue engineering is still controversial and pore sizes ranging all the way from 20 to 1500 μm have been used. Not only the application, but also the chosen biomaterial has an influence on the optimal pore size. (C.M. Murphy et al. 2013; Costa-Pinto et al. 2011; Loh & Choong 2013)

3.3.2 Supercritical CO$_2$ processing

Many processing methods used to produce tissue engineering scaffolds require the use of organic solvents such as dichloromethane. The removal process can be difficult and toxic residues can be left behind. Supercritical CO$_2$ processing is a method avoiding the use of organic solvents. As a non-toxic, non-flammable, readily available and inexpensive solvent with a tunable density, ScCO$_2$ is an attractive solvent. Under mild conditions, CO$_2$ is a poor solvent for most high molecular weight polymers, but at high pressures CO$_2$ has a solvating power comparable to typical organic solvents. (Howard et al. 2008; Floren et al. 2011; Davies et al. 2008; Barry et al. 2006)

Once the critical temperature (31.1°C) and pressure (73.8 bar) of CO$_2$ are exceeded, a single fluid phase called supercritical CO$_2$ with properties of both liquid and gas is formed. In such case, the liquid and gaseous components are identical and further compression will not result in condensation to a liquid state. Instead, only increase in fluid density is seen along compression. The liquid-like density as well as the gas-like viscosity and compressibility of supercritical fluids allow tuning of the fluid properties by changing temperature and pressure. The properties of conventional organic solvents are much less dependent on temperature and pressure. (Barry et al. 2006; Quirk et al. 2004; Bhamidipati et al. 2013)

Processing polymers with ScCO$_2$ is based on its solubility to polymers, which causes some polymers to create porous materials by swelling or foaming. At high pressures, polymers saturated with CO$_2$ plasticize. This plasticization results from the diffusion of ScCO$_2$ into the polymer matrix: as the polymer chains are separated, also their chain rotation becomes easier. Plasticization is followed by a decrease in polymer glass transition temperature. The stronger the molecular interactions in the polymer, the greater the T$_g$ reduction. As the polymer is in this plasticized state and the gas pressure of CO$_2$ is brought down to atmospheric pressure, the gas solubility in the polymer decreases, which generates bubbles (nuclei). The growth of these bubbles result in formation of the pores in the polymer. The T$_g$ starts to rise when CO$_2$ leaves the polymer and ultimately reach a temperature near that of the equipment. As the polymer becomes glassy, the pores are locked in and cannot grow any further. The process is schematically shown in Figure 7. (Barry et al. 2006; Bhamidipati et al. 2013)
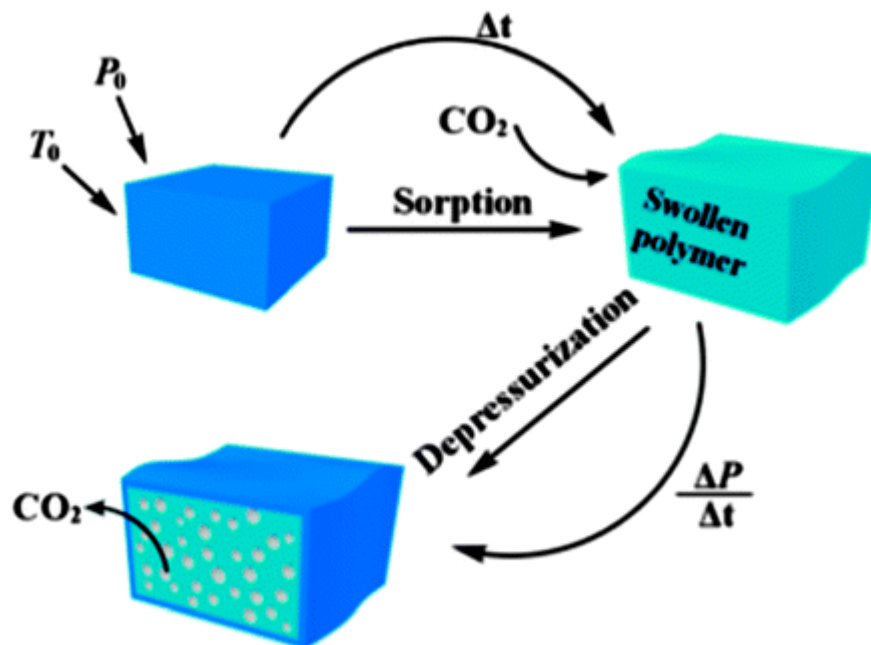
Figure 7. *Supercritical CO$_2$ processing as a schematic illustration. Modified from (Zhang et al. 2014).*

The pore size distribution can be manipulated by tuning the venting rate, which is an important parameter along with temperature and pressure. With a high venting rate, the nucleation is fast leading to a large number of nucleation sites. The pores develop fast and the effect of gas diffusion into the pores becomes insignificant, facilitating uniform pore size distribution. Slower venting rate and thus slower nucleation means that the firstly nucleated pores become larger than the others. This results from the greater amount of gas diffused from the surrounding polymer matrix, shifting the pore size distribution

to a more inhomogeneous state. (Barry et al. 2006) One major challenge in CO_2 processing of polymers has been the problems with pore interconnectivity. This problem can be overcome by controlling the processing parameters or using solid porogen particles to create an open pore network. (Bhamidipati et al. 2013)

3.3.3 Polymer fiber processing and textile technologies

Bioabsorbable polymer fibers have been used as sutures for soft tissue wounds or as reinforcing elements in composites, but they also serve as a basis for different types of textile structures (Ellä et al. 2011). In addition to non-woven scaffolds, more organized scaffold structures can be produced from fibers and yarns by knitting, weaving and braiding technologies. Possible applications of these scaffolds include tendon, cartilage, ligament and bone tissues. (Kellomäki et al. 2015)

The organized textile scaffolds should be highly porous with an interconnected pore network and a large surface area, although their surface area to volume ratio is still lower than that of the non-woven scaffolds. By producing fibers with smaller diameters, the surface area to volume ratio of the resulting textiles can be increased. On the other hand, handling very thin fibers is more difficult and their mechanical strength is weaker compared to thicker fibers. With rat mesenchymal stem cells, small fiber diameter has been also associated with lower cell attachment and spherical-shaped cells due to the big size of the cells with respect to the fiber size. (Ellä et al. 2007; Park et al. 2013; Karageorgiou & Kaplan 2005)

The chosen bioabsorbable material should possess adequate thermal and solubility properties to withstand fiber spinning. Typical methods for this are melt spinning, dry spinning and wet spinning, from which the first one is free of harmful solvents but requires a large enough temperature window for extrusion. In melt spinning, the material is first melted and then extruded into multi- or monofilaments. In order to improve the processability of the spun fibers, a stretching phase can be applied to increase their mechanical properties. By stretching the fibers above their T_g (but below T_m of semicrystalline materials), the polymer chains become oriented in this direction, leading to significant improvement in the strength, strain and Young's modulus of the filaments. PLA and other poly-α-hydroxy acids are the most widely used synthetic polymers in melt spinning, but also some natural polymers and although rarely alone, even bioactive glasses with a specific chemistry have been melt-spun into fibers. (Kellomäki et al. 2015)

By producing interlocked loops from continuous yarns, a method called knitting can be applied to produce fabric scaffolds. Depending on the direction of the series of loops, the resulting form is either weft or warp knitted. Weft knitted fabrics can be created from one continuous strand of yarn, but they unravel easily which limits their use in applications where the end-product is cut into a desired shape. Being more stable and cut-withstanding, the warp knits are more suitable for surgical use. When manufacturing warp knitted

products, the number of columns in the width of the fabric determines the number of yarns needed in the system: each needle needs its own yarn. The resulting stitching patterns are longitudinal with adjacent yarn loops being interlocked with each other. Knitted fabrics are easy to shape and elastic. They can be used in tubular or flat form. (Kellomäki et al. 2015)

Knitted structures made from multifilament polylactide 96L/4D fibers have been used for both osteoarthritis and rheumatoid arthritis patients. The function of the scaffolds is based on inducing fibroblast ingrowth into the structure, which later leads to maturation to connective tissue. As the structure cushions the bone ends, the mobility of the joint is improved. (Kellomäki et al. 2015) Shortly, after the knitting process the resulting knits are cut into the desired length depending on the wanted scaffold size. The knits are then rolled and the ends are heat sealed to avoid the running of the loop. Finally, the scaffolds are heat treated in a mold to achieve the final shape. (Ellä et al. 2011)

3.4   Scaffold analysis with micro-computed tomography

The need to evaluate the 3D scaffold structures and the destructive nature of traditional histological techniques have led to the development of improved 3D imaging methods. In the case of therapeutic applications, the cell-scaffold constructs require both evaluation of the scaffold structure and determining the distribution of the cells. When designing tissue engineering scaffolds, for example quantifying the pore sizes and interconnectivity is essential. In this kind of scaffold research, micro-computed tomography (micro-CT) is one widely applied imaging technology. One factor to its popularity is the detailed qualitative and quantitative information on sample 3D morphology. The internal structure of the scaffolds can be studied accurately without destructing the sample or using any harmful chemicals. (Appel et al. 2013; Jones et al. 2007; Ho & Hutmacher 2006)

The method is based on irradiating the sample from the sides with X-rays that are attenuated as they travel through the sample. A detector array captures these X-rays with reduced intensities. Not only the X-ray paths, but also attenuation coefficients correlating to material density can be determined from the detector measurements. As the sample is computationally divided into two-dimensional (2D) slices, each attenuation coefficient value corresponds to one pixel on 2D pixel maps created from the computations. These 2D pixel maps expose the material phases in the sample. Using a 3D modeling program, the 2D slices can be stacked to create 3D models for visualization. The scanning resolution typically ranges from 1 to 50µm. (Ho & Hutmacher 2006; Loh & Choong 2013)

The data sets resulting from micro-CT imaging are large, which is challenging in terms of data processing and storage. Other concerns include using ionizing radiation which might damage tissues and the fact that micro-CT is not applicable for scaffolds that contain metals. The metals attenuate the X-rays so heavily, that other important details are obscured by the resulting grainy artefacts. Furthermore, image thresholding affects the

visualization and subsequent analysis, but needs to be done before 3D modeling. If there are multiple scaffold materials with overlapping threshold ranges, the digital separation of them becomes problematic. (Ho & Hutmacher 2006; Appel et al. 2013)

Besides analyzing structural features of the scaffolds such as interconnectivity, porosity, pore sizes and surface area to volume ratio (Zeltinger et al. 2001; Ho & Hutmacher 2006), micro-CT applications include many more such as quantifying bone volumes, mineral densities and mineral contents from implanted scaffolds (Mitsak et al. 2011), evaluating their osteointegration in bone (Appel et al. 2013), visualizing molecular probes by means of enzyme-mediated silver deposition (Metscher & Müller 2011) or characterizing neo-vascularization with contrast agents like barium sulfate (Appel et al. 2013). The most popular application for micro-CT is characterization of tissue engineered bone in cell seeded constructs. An increasing amount of new applications in the biomedical field are explored to utilize this technique. (Appel et al. 2013; Ho & Hutmacher 2006)

4. STEM CELLS

Stem cells are described to be cells that have the potential for both self-renewal and mul-
tilineage differentiation. Thus, they can produce undifferentiated stem cells and differen-
tiated descendants including functional mature cells. Both scenarios occur in the case of
asymmetric division, where each stem cell produces one undifferentiated daughter cell
and one daughter cell with a differentiated fate. Symmetric division results in daughter
cells destined to the same fate. Stem cells can use symmetric divisions for self-renewal
or generation of differentiated progeny. Due to their ability to differentiate into multiple
cell lineages, stem cells are considered to be suitable for tissue engineering and cell ther-
apies. (Yan et al. 2014; Choumerianou et al. 2008; Morrison & Kimble 2006)

4.1 Stem cell sources and development potential

One way to classify stem cells sorts them according to their differentiation potential. An
entire organism can theoretically be created with totipotent stem cells, whereas pluripo-
tent cells have the ability to give rise to all embryonic cell types. Multipotent stem cells
are able to differentiate into a variety of cellular lineages; oligopotential denotes a more
limited number of possible developmental directions. Unipotent stem cells such as epi-
dermal stem cells can give rise to one specific cellular lineage only. (Fernández Vallone
et al. 2013; Fortier 2005; Serakinci & Keith 2006)

Stem cells can also be classified according to the developmental stage from which they
are obtained. Embryonic stem cells (ESCs) are pluripotent cells obtained from early-stage
embryos, as opposed to multipotent adult stem cells that are isolated from adult tissues.
Unlike other stem cell types, embryonic stem cells can also divide or self-renew indefi-
nitely. Potential therapeutic applications of embryonic stem cells include for example
spinal cord injuries, myocardial infarction and diabetes. However, their clinical use is
very limited because of ethical and safety concerns. (Fortier 2005; Dutta 2013; Yan et al.
2014)

Adult stem cells are the ethically least controversial stem cell type (Faulkner et al. 2014).
Found in various differentiated tissues, they are undifferentiated cells having limited self-
renewal and differentiation capacity. Examples of adult stem cells include neural stem
cells in the central nervous system, skin stem cells, various epithelial stem cells, mesen-
chymal stem cells (MSCs) and skeletal muscle stem cells in muscle fibers.
(Choumerianou et al. 2008; Fernández Vallone et al. 2013) Since their identification in
bone marrow in the 1960s, MSCs have been isolated from adipose tissue, heart, liver,
dental pulp, hair follicles and nearly every other tissue in the body. They have the ability
to differentiate at least into osteoblasts, chondrocytes and adipocytes. MSCs derived from

bone marrow and adipose tissue are the most widely studied adult stem cells. BMSCs were the first type of mesenchymal stem cells to be identified. The procedure for harvesting BMSCs is however invasive and painful. (Tsuji et al. 2014; Yan et al. 2014; Liao 2014; Romagnoli & Brandi 2014)

In addition to embryonic and adult stem cells, another interesting subgroup, namely induced pluripotent stem cells (iPSCs) has lately been studied a lot. They are adult somatic cells that have been reprogrammed into a pluripotent stage being similar to embryonic stem cells. The reprogramming can be achieved by transfection of somatic cells with specific genes. These genes activate and maintain the networks responsible for regulating the stemness of the cells. Compared to embryonic stem cells, iPSCs are morphologically and antigenically similar but lack ethical problems related to embryonic tissue sources. However, one significant limitation of iPSCs is their poor reprogramming efficiency. Homogenous differentiation to desirable cell types has also been a concern. (Yan et al. 2014; Monti et al. 2012; Sánchez Alvarado & Yamanaka 2014; Faulkner et al. 2014)

Generally, stem cells used for tissue engineering should be available in adequate quantities via minimally invasive harvesting methods. They should also differentiate into multiple cellular lineages in a reproducible manner and be safely and effectively transplanted to an autologous or allogeneic host. However, stem cells are typically found in low numbers and cell death after implantation remains a problem. The fact that large quantities of stem cells are rarely available leads to the requirement of their *ex vivo* expansion before clinical use. Furthermore, passaging reduces typically their self-renewal, proliferation and differentiation abilities. If the potential of stem cells could be maintained during *in vitro* culture, high numbers of high quality stem cells would be easily available for clinical purposes. (Bunnell et al. 2008; Yan et al. 2014; Monti et al. 2012; Romagnoli & Brandi 2014)

4.2   Adipose-derived stem cells

An excellent source for mesenchymal stem cells is the adipose tissue: it is ubiquitous and can be harvested with a minimally invasive procedure. The adipose tissue can be harvested in large quantities and more importantly, the stem cell yields from adipose tissue are higher than those from bone marrow or other stem cell sources: the number of ASCs derived from a gram of aspirated tissue ranges typically from 350 000 to 1 000 000, whereas one gram of bone marrow aspirate yields normally between 500 and 50 000 BMSCs. In addition, expanding ASCs *in vitro* is relatively easy: their average doubling time depending on passage number and culture medium is 2-5 days. ASCs can be cryopreserved without affecting their proliferation or differentiation. The transcription profiles for stem cell phenotype-related genes are practically identical between the ASCs and BMSCs. (Barba et al. 2013; Romagnoli & Brandi 2014; Tsuji et al. 2014)

4.2.1   ASC characteristics

Adipose-derived stem cells are not a homogenous population. Comparison and interpretation of studies is difficult due to the lack of standardization among isolation and culture procedures. For example, using unpurified stromal vascular fraction instead of purified ASCs is a common practice in clinical trials and sometimes used in research as well. Standardization of cell culture methods and isolation procedures would increase the reliability and reproducibility of the results, but there are also variables affecting ASC quality that cannot be standardized. These include for example donor age, gender, ethnicity, medical history and body mass index. (Tsuji et al. 2014; Romagnoli & Brandi 2014; Locke et al. 2011)

Variations in viability, immunophenotype, proliferation rate and differentiation capacities have been found depending on the donor and harvest location. For example, when comparing different anatomical sites for harvesting ASCs, it was noted that the osteogenic potential of the ASCs isolated from the omentum was higher compared to cells from other locations such as subcutaneous or intrathoracic tissue depots. (Russo et al. 2013) On the other hand, in another study the ASCs harvested from the superficial abdominal depot showed lower susceptibility to apoptosis than the cells obtained from the omental depot. (Schipper et al. 2008)

When comparing the effect of the donor age on ASC proliferation rates and apoptosis susceptibility, the youngest patients had fastest cell proliferation rates and the lowest tendency of ASCs to apoptosis. Aksu et al. (2008) noticed faster proliferation and more effective osteogenic differentiation on male ASCs than female ASCs, whereas van Harmelen and colleagues (2004) did not find any differences in ASC proliferation or preadipocyte differentiation capacities between male and female samples. (Schipper et al. 2008; Van Harmelen et al. 2004; Aksu et al. 2008)

In addition to the minimal criteria of differentiation into cartilage, bone and adipose tissues, adipose-derived stem cells have been shown to have the potential to differentiate into other mesodermal tissues, including tendon, myocardium and skeletal muscle tissues. They have also demonstrated to be capable of crossing germinal boundaries by transdifferentiating towards hepatocytes, epithelial cells and kidney cells. The possible ability of ASCs to transdifferentiate into neural cells is still somewhat controversial. (Liao 2014; Barba et al. 2013)

One additional interesting property of ASCs is their immunosuppressive potential: by secreting specific signaling proteins like prostaglandins or interleukins, ASCs can reduce the maturation of certain immune cells and suppress inflammation. Moreover, they have been shown to modulate immune responses by direct cell-cell contacts. This all makes ASCs an attractive alternative for applications related to transplantations or immune dis-

orders. Clinical trials for repairing fistula from Crohn's disease have already been per-formed. Another possible application for the immunosuppressive properties of ASCs is osteoarthritis, as inflammation is one component of the condition. The possible drawback of immunomodulation or immunosuppression is possible cancer cell development due to downregulated antitumor immune cells. (Schmitt et al. 2012; Kokai et al. 2014; M.B. Murphy et al. 2013)

4.2.2 Characterization

In 2006, the International Society for Cellular Therapy (ISCT) proposed minimal criteria to define MSCs. According to the statement, ≥95% of the cell population should express cluster of differentiation (CD) antigen surface molecules CD105, CD73 and CD90, whereas ≥2% must lack the expression of CD45, CD34, CD14 or CD11b, CD79α or CD19 and human leukocyte antigen (HLA) class II. Expression of the markers can be measured using flow cytometry. In addition, MSCs need to be plastic-adherent under standard culture conditions in tissue culture flasks and must be able to differentiate *in vitro* to adipocytes, osteoblasts and chondroblasts in standard differentiating conditions. (Dominici et al. 2006) In Figure 8, adipose-derived stem cells adhered onto a polystyrene cell culturing flask are presented.
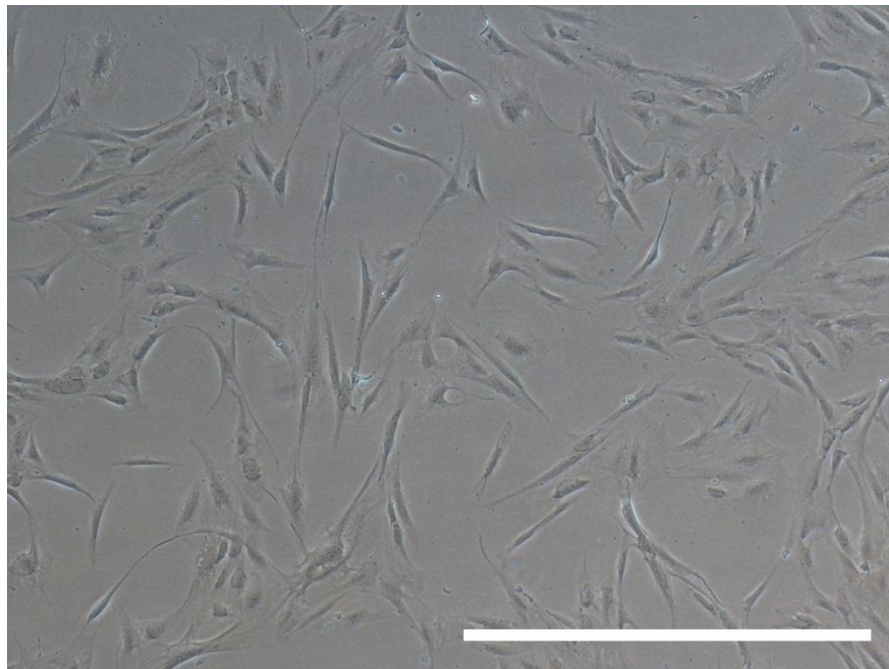
Figure 8. *Adipose-derived stem cells adhered onto a polystyrene cell culturing flask. Scale bar 1mm.*

The ISCT statement was updated in 2013, when ISCT together with the International Federation for Adipose Therapeutics (IFATS) gave guidelines for better characterizations of adipose-derived stromal and stem cells. Phenotypical identification of the stromal cells as uncultured SVF requires expression of the marker CD34 and lack of expression in the

case of markers CD45, CD235a and CD31. A viability marker and surface antigens CD13, CD73, CD90 and CD105 may provide added value for the identification. ASCs in culture remain positive for markers CD90, CD73, CD105 and CD44 which are common with other MSCs, but do not express markers CD45 and CD31. Positivity for CD36 and negativity for CD106 distinguishes ASCs from BMSCs. (Bourin et al. 2013) Table 1 summarizes the surface marker expression criteria from 2006 and 2013.

Table 1. A summary of the surface marker expression criteria for partly defining ASCs. In this work, the characterization was done using the criteria from 2006. (Bourin et al. 2013; Dominici et al. 2006)

Surface Marker	ISCT 2006 criteria (Surface marker expression)	ISCT & IFATS 2013 criteria (Surface marker expression)
CD11b or CD14	≤ 2%	-
CD19 or CD79α	≤ 2%	-
CD31	-	≤ 2%
CD34	≤ 2%	-
CD44	-	≥ 95%
CD45	≤ 2%	≤ 2%
CD73	≥ 95%	≥ 95%
CD90	≥ 95%	≥ 95%
CD105	≥ 95%	≥ 95%
HLA-DR	≤ 2%	-

4.2.3 ASC differentiation into osteogenic lineages

Although logical and sometimes functional, using readily differentiated cells like osteo-blasts for bone regeneration entails problems. One of those is the limited amount of tissue for cell isolation. For this reason, either multipotent or pluripotent stem cells have been thought to be the most suitable cell alternatives for tissue engineering. The ability of ASCs to differentiate into osteogenic lineages makes them a potential alternative for orthopedic applications. (Salgado et al. 2013; Tirkkonen et al. 2012)

A typical strategy for tissue regeneration using ASCs involves their *in vitro* differentiation before implantation (Kokai et al. 2014). The differentiation can be achieved for example

by applying chemical (Mesimäki et al. 2009; Zhang et al. 2012), electrical (Pelto et al. 2013), electromagnetic (Kang et al. 2013), mechanical (Tirkkonen et al. 2011) or scaffold (Salazar & Ohneda 2012; Yan et al. 2014) stimuli. Commonly used chemical agents for osteogenic differentiation of ASCs include ascorbic acid, dexamethasone and β-glycerophosphate. For example, Tirkkonen et al. (2013) have used a medium optimized for ASCs, which is supplemented with these substances. (Fiorentini et al. 2011; Tirkkonen et al. 2012)

Enhancing the osteogenic capacity of ASCs has largely focused on growth factors like bone morphogenetic proteins (BMPs). Yet their cost-effectiveness and safety are questioned, and there have been doubts whether these cells respond to BMPs at all. For example, Tirkkonen et al. noticed no benefit from adding growth factors BMP-2, BMP-7 or vascular endothelial factor (VEGF) into the osteogenic medium when it comes to cell number and osteoinduction of ASCs. In addition, the growth factor doses required in the clinical use are large, making their usage very expensive. (Kyllönen et al. 2013; Tirkkonen et al. 2012)

Since most of the cells are anchorage-dependent, the chemical composition and the properties of the scaffold material play an important role in tissue engineering. In scaffold-stimulated bone regeneration, the material should not only be osteoconductive thus allowing bone growth on its surface, but ideally be osteoinductive thereby stimulating osteogenic differentiation of cells. For example certain bioceramics are osteoinductive. Also the surface topography of the scaffold material is of great importance concerning stem cell differentiation. (Albrektsson & Johansson 2001; Salazar & Ohneda 2012; Yan et al. 2014)

4.2.4 ASCs in bone tissue engineering

Originally, stem cells were applied directly into the bone fracture site. Adipose-derived stem cells have been noted to have the ability to migrate towards the injured tissue, possibly by means of chemoattractants released after tissue damage. Although injecting stem cells has been demonstrated to promote bone regeneration as well, it is ineffective in cases of large defects or non-union of bone. Hence, scaffolds seeded with cells are nowadays preferred instead of cell therapy. The reason for this lies in the ability of the scaffolds to provide support for cell growth, migration and differentiation. (Romagnoli & Brandi 2014; Kokai et al. 2014; Qin et al. 2014)

When it comes to clinical applications of bone tissue engineering, adipose-derived stem cells have been used especially in reconstructing or accelerating skull and jaw defects. They were successfully used in bone tissue engineering only a few years after their discovery, when Lendeckel *et al.* applied ASCs with spongy bone and fibrin glue to large defects in a 7-year old girl's skull. Three months after the operation, nearly complete continuity of the fragments in the skull was shown. A bit later, a 65-year-old male patient

was treated with a combination of β-TCP, autologous ASCs and BMP-2. The patient's lost upper jaw was replaced with a construct of these materials that was first grown inside the patient's abdominal muscle. The healing was uneventful during the 36 months follow-up period. Ever since, multiple patients with cranio-maxillofacial defects have been treated in Finland with bioactive glass or β-TCP scaffolds seeded with ASCs. 10 out of 13 reported cases were successful with demonstrated hard-tissue integration of the seeded cell-scaffold constructs at the defect sites. (Romagnoli & Brandi 2014; Lendeckel et al. 2004; Mesimäki et al. 2009; Sándor et al. 2014)

So far, clinical studies have shown adipose-derived stem cells to be safe and to possess the potential for tissue repair. Standardizing harvest, isolation and culturing of the cells would make the comparison of different studies easier. Also the effect of different scaffolds on ASC osteogenesis has been investigated in numerous studies, suggesting the use of different materials, structures and fabrication materials. Despite their potential, further results are needed from long-term human series and animal models. (Kokai et al. 2014; Romagnoli & Brandi 2014; Sándor et al. 2014)

EXPERIMENTAL PART

5. MATERIALS AND METHODS

In this study, 6 different cell seeding methods were tested on 4 different types of porous biomaterial scaffolds. Human adipose-derived stem cells were used in the cell seeding experiments. Iron-labeled microspheres were used to estimate the structure and pore interconnectivity of two scaffold types. The viability and the distribution of the cells were evaluated qualitatively, whereas the cell number analysis was quantitative.

5.1 Scaffold fabrication

The 4 different scaffold types (diameters 10 mm or 12 mm) are presented in Figure 9. Sc-PLCL and Sc-COMP50 were processed with supercritical CO_2.
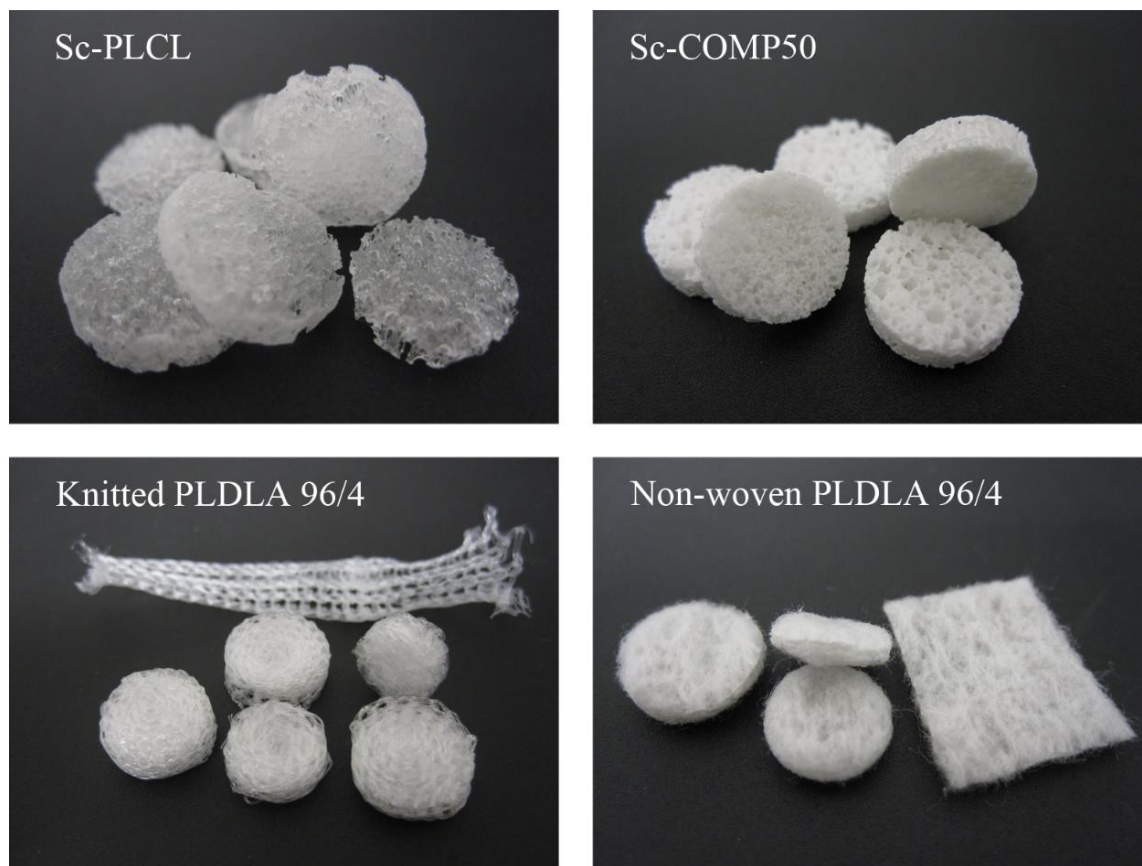
Figure 9. Different scaffold types with diameters of 10 mm and 12 mm, as used in the experiments. In the knitted PLDLA 96/4 scaffolds, an unrolled piece of knit is shown in the back. Similarly, a small piece of the non-woven fabric is seen on the right of the non-woven PLDLA 96/4 image.

The cylindrical-shaped scaffolds had heights ranging from about 2.5 mm to 3.5 mm depending on the scaffold type. All the scaffolds were sterilized before cell experiments by

gamma irradiation (BBF Sterilisationsservice GmbH, Kernen-Rommelshausen, Germany) with a minimum dose of 25 kilograys (kGy).

Copolymeric **SC-PLCL** scaffolds were processed from poly(L-lactide-co-ε-caprolactone) 70/30 (Corbion Purac, Gorinchem, The Netherlands). The general porosity of the PLCL scaffolds was 65% with an average pore size of 430±170 μm and a maximum pore size of 1100 μm, analyzed from the micro-CT data. **Sc-COMP50** composite scaffolds contained 50 weight-% PLCL 70/30 (Corbion Purac) and 50 weight-% β-tricalcium phosphate granules (Plasma Biotal, Tideswell, The United Kingdom) of sizes ranging from 100 to 300 μm. Sc-COMP50 porosity showed a similar percentage of 65% with an average pore size of 370±150 μm and the biggest pore size at 950 μm. Both supercritical CO_2 processed scaffold types were cut into their final height of approximately 3 mm using a scalpel.

The **non-woven PLDLA** fabric scaffolds were manufactured from PLDLA 96/4 (Purac Biochem; currently Corbion Purac, Gorinchem, The Netherlands). The fibers were manufactured by extrusion and had a diameter of approximately 13 μm. They were first carded and then needle punched into a non-woven fabric structure using 4 layers of card. The PLDLA fabric was washed 2 times 4 minutes in 99.5% alcohol (Etax Aa; Altia, Rajamäki, Finland) in an ultrasonic cleaner (FinnSonic, Lahti, Finland), after which the scaffolds with diameters of 10 mm and 12 mm were punched from the moist fabric. The scaffolds were then dried at room temperature. The average height of dry non-woven scaffolds was measured to be around 2.5 mm, although there was significant variation between different scaffolds.

The **knitted PLDLA** scaffolds were also made from PLDLA 96/4 (Purac Biochem). The 4-filament fibers were manufactured by extrusion and knitted later using special machinery. The fiber diameter was approximately 70 μm. In Figure 9, a piece of the knit can be seen behind the scaffolds. Suitable lengths were cut from the knit with respect to the desired scaffold size. The knits were then rolled into cylindrical shapes and the ends were fixed to the roll by heat sealing. Finally, the knitted scaffolds were heat treated for 30 minutes at 80°C in a mold to obtain their final shape. Depending on the width of the knit, the scaffold heights varied to some extent. Being the most common value, an average height of 3.6 mm was used in the calculations when dealing with the knitted scaffolds.

5.2   A novel cell seeding model with iron-labeled microspheres and micro-CT

Iron-labeled microspheres (FerroTRACK; BioPAL Inc., Worcester, MA, The United States) of sizes 15 μm and 100 μm were used in the preliminary modeling tests. The tests were conducted using $ScCO_2$ processed scaffolds to model their seedability and pore interconnectivity. The aim of this analysis was to confirm that the microspheres are able to

infiltrate into the pores in different depths of the scaffold, and to test the hypothesis of modeling cell seeding with these particles.

The scaffolds were pre-wetted in distilled water (Milli-Q Biocel A10; Millipore, Molsheim, France) before seeding (pre-wetting is described in section 5.4.1) and incubated in a +37°C water bath for some hours before seeding the microspheres. 10 000 particles with a diameter of 100 µm were seeded per scaffold. In the case of 15 µm particles, a number of 60 000 microspheres was used. Thus, when interpreting the results it must be taken into account, that the combined total volume of the larger particles is almost 50 times higher than that of the smaller 15 µm particles.

Before seeding the microspheres, their saline buffer was changed into distilled water to prevent salt crystal formation when drying the sample (salt crystals could disturb micro-CT imaging results). This was done by centrifuging the microspheres to the bottom of a microcentrifuge tube, removing the supernatant and washing the microspheres with distilled water. After repeating this cycle several times, the particles were suspended in 50 µl of distilled water and seeded to the top surface of the scaffold using the static seeding method (presented in section 5.4.2.). The scaffolds were left to dry for at least 2 days in room temperature before they were imaged using micro-CT technology. The scaffolds were imaged individually and the resolution range used was from 5.0 to 6.0 µm.

5.3 Cell isolation and culture

Cell culturing was performed in the Adult Stem Cell Group laboratories at the Institute of Biosciences and Medical Technology (BioMediTech), University of Tampere. The cells were cultured in an incubator (Binder CB210; Binder GmbH, Tuttlingen, Germany) in a humidified atmosphere at +37°C with 5% CO_2.

5.3.1 Human adipose-derived stem cell isolation

Human adipose-derived stem cells (hASCs) were isolated from adipose tissue samples derived from 3 different female donors aged between 32-49 years. The adipose tissue was obtained from the patients in accordance with the Ethics Committee of Pirkanmaa Hospital District (Tampere, Finland). Using scissors, the samples were first chopped small and transferred into 50 ml falcon tubes (Cellstar; Greiner Bio-One, Switzerland). Fibrous and bloody sites were avoided.

The samples were then digested using collagenase type I (1.5 mg/ml; Invitrogen, Carlsbad, CA, The United States) at +37°C. After centrifuging (10 min, 1800 rpm) with Labofuge 400R centrifuge (Kendro Laboratory Products, Osterode, Germany), the resulting pellet was filtrated (Cell Strainer 100 µm nylon filter; BD Falcon, Franklin Lakes, NJ, The United States) and the red blood cells were lysed in 1 ml of sterile water (Baxter

Healthcare SA, Zürich, Switzerland), after which 9 ml of medium was added. After centrifuging again (10 min, 1800 rpm), the new pellet was suspended in 10 ml of medium, filtrated and transferred into T75 cell culturing flasks. The flasks were placed into the incubator at +37°C and washed twice with Dulbecco's Phosphate Buffered Saline (DPBS; Lonza, Verviers, Belgium) the next day.

5.3.2 Characterization of the adipose-derived stem cells

The identification and characterization of the human adipose-derived stem cells was performed at passage 1 after cell isolation and it was done by BioMediTech laboratory specialists. All the three cell lines that were used in the experiments were analyzed. The flow cytometric surface marker expression analysis was performed with a fluorescent-activated cell sorter (FACSAria; BD Biosciences, Erembodegem, Belgium) using 10 000 cells per sample.

The probes used in the FACS analysis included monoclonal antibodies against CD3-Phycoerythrin (PE), CD14-Phycoerythrin-Cyanine (PE-Cy7), CD19-PE-Cy7, CD45R0-Allophycocyanin (APC), CD54-fluorecein isothiocyanate (FITC), CD73-PE, CD90-APC (BD Biosciences, San Jose, CA, The United States); CD11a-APC, CD80-PE, CD86-PE, CD105-PE (R&D systems, Minneapolis, ME, The United States); CD34-APC and HLA-DR-PE (Immunotools GmbH, Friesoythe, Germany).

5.3.3 Cell maintenance and passaging

The cells were cryopreserved in nitrogen gas phase storage and thawed when needed in a +37°C water bath. Since the freezing solution contained dimethyl sulfoxide (DMSO; Sigma Aldrich, St. Louis, MO, The United States), the cells were suspended immediately after thawing in 6 ml of cell culturing medium, centrifuged for 5 minutes at 1000 rpm, suspended into 10 ml of cell culturing medium and put into a T75 cell culturing flask (Nunc, Roskilde, Denmark). The cell culturing medium was optimized for hASCs and composed of Dulbecco's Modified Eagle Medium (DMEM/F-12 1:1; Gibco by Life Technologies, Paisley, The United Kingdom) supplemented with 1% L-glutamine (GlutaMAX; Gibco by Life Technologies), 5% Human Serum type AB (Paa Laboratories GmbH, Pasching, Austria) and 1% penicillin-streptomycin antibiotics (Biowhittaker Pen-Strep; Lonza).

The culturing medium for the cells was changed every 3 or 4 days. Typically half of the medium in each flask was changed, but in case it was desirable to try to hinder cell proliferation, the whole amount was changed. When confluent, the cells were passaged by washing the cells first with 5 ml of DBPS (Lonza) and then detaching the cells using 3 ml of TrypLE Select enzymes (Gibco by Life Technologies, Grand Island, NY, The United States). The cells were incubated with TrypLE Select (Gibco by Life Technologies) for approximately 10 minutes at +37°C. The enzyme was inactivated with 6 ml of medium

per each flask, the suspensions were collected and centrifuged for 5 minutes at 1000 rpm. The resulting cell pellet was then suspended in medium and divided into new cell culturing flasks containing altogether 10 ml of medium per flask.

5.3.4   USPIO-labeling of the cells

Ultrasmall Superparamagnetic Iron Oxide (USPIO) nanoparticles (Magnetizable 50nm nanoparticles, 25 mg/ml; Kisker GmbH, Steinfurt, Germany) were used to label hASCs in order to make them visible in micro-CT images. The amounts of USPIO particles used were based on optimization tests of M.Sc. Mimmi Patrikoski.

The cells were first left to attach and accommodate in their culturing flasks for 3 or 4 days, after which their number was estimated using a light microscope (Nikon Eclipse TE2000-S; Nikon Instruments Europe). For this work, the cell number estimations were provided by BioMediTech laboratory technologist Anna-Maija Honkala. Based on the estimated number of cells, the amount of nanoparticles were calculated using 1000 µg of USPIO particles per 100 000 cells as a basis. The nanoparticles were diluted in cell culturing medium to a concentration of 1 mg/ml of USPIO particles. Poly-D-lysine (PDL, 1 mg/ml; Millipore) was then added to an extent of 3750 ng per 100 000 cells.

The working solution obtained was incubated in room temperature for 3×10 minutes, mixing it gently after every 10 minutes. During this incubation, poly-D-lysine should attach to the USPIO nanoparticles and thus facilitate the uptake of nanoparticles into the hASCs. Finally, this working solution was diluted with medium to a final USPIO nanoparticle concentration of 200 µg/ml. The culturing medium of the cells was then replaced with this USPIO-PDL solution. After an incubation of 48 hours, the USPIO-PDL medium was removed and replaced with 10 ml of fresh medium to let the cells recover. Figure 10 presents adipose-derived stem cells just before adding the USPIO-PDL medium and 48 hours after adding the USPIO particles.
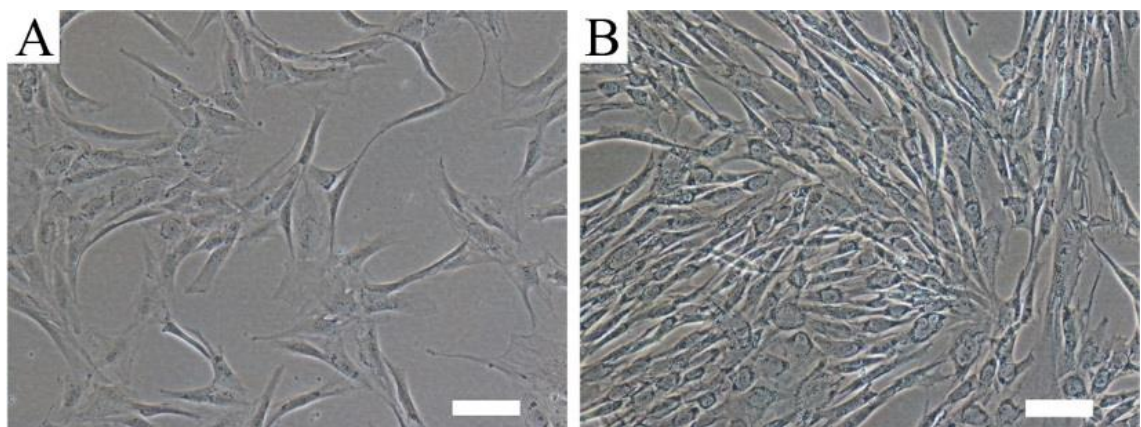

Figure 10. *Light microscopy images of hASCs in a cell culturing flask (A) just before and (B) 48 hours after USPIO-labeling. Scale bars 100 µm.*

The cells were allowed to recover for 1 day in fresh media before they were seeded. In addition to seeding cells into scaffolds, an applicable number of USPIO-labeled hASCs were seeded on a glassy cover slip on a 6-well plate with 3 ml of cell culturing medium. The cover slip was cultivated for 3 days like the scaffolds, after which the Prussian blue staining was performed to evaluate the success of the USPIO-labeling.

5.4 Cell seeding methods

The 6 different cell seeding methods used in this work are explained in this chapter. A graphic illustration of the methods is provided in Figure 11.
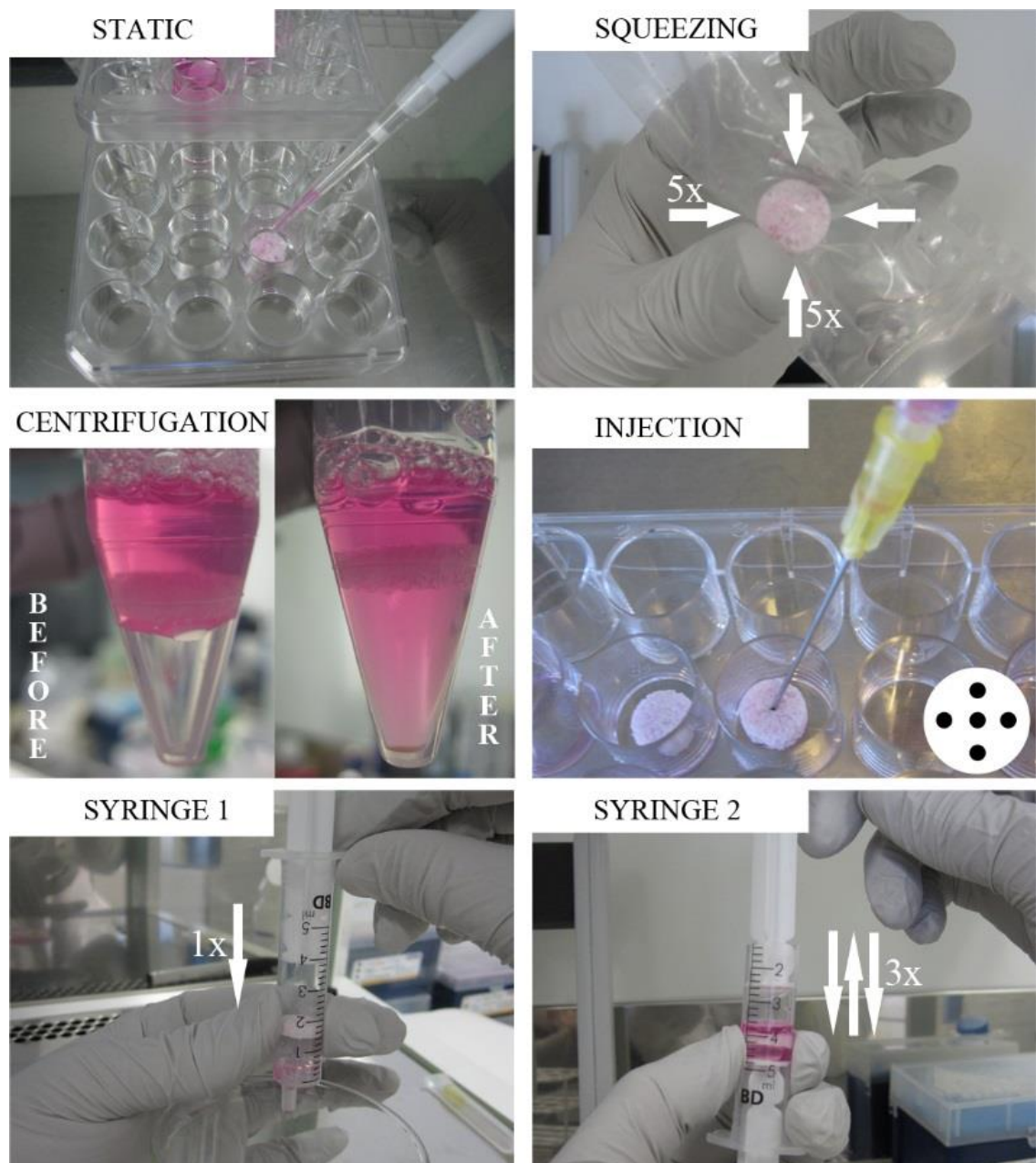

Figure 11. *Illustration of the cell seeding methods used in this work.*

After cultivating and expanding human adipose-derived stem cells in sufficient amounts, the cells were detached from their flasks as in passaging (section 5.3.3) and counted using a Bürker chamber. Based on the estimated scaffold volumes, different numbers of cells were used in each scaffold. As presented later in Table 3, a total of 3 experiments were made with the $ScCO_2$ processed scaffolds, whereas the analyses were done only once with the PLDLA 96/4 scaffolds. The experiment series was started exceptionally by seeding 60 000 hASCs into Sc-PLCL scaffolds, but the rest of the experiments were done with an increased cell number of 120 000, as implied in Table 2.

Table 2. *Scaffold volumes and cell amounts used. The 12 mm scaffolds were used in the two syringe methods.*

Scaffold type	The amount of cells seeded	Average scaffold height	Average scaffold volume ($V=\pi \cdot r^2 \cdot h$, ⌀=10mm)	Average scaffold volume ($V=\pi \cdot r^2 \cdot h$, ⌀=12mm)	Cell seeding density (⌀=10mm)	Cell seeding density (⌀=12mm)
Sc-PLCL	60 000 / 120 000	3.0 mm	75π mm^3	108π mm^3	509 cells/mm^3	354 cells/mm^3
Sc-COMP50	120 000	3.0 mm	75π mm^3	108π mm^3	509 cells/mm^3	354 cells/mm^3
Non-woven PLDLA 96/4	100 000	2.5 mm	$62,5\pi$ mm^3	90π mm^3	509 cells/mm^3	354 cells/mm^3
Knitted PLDLA 96/4	144 000	3.6 mm	90π mm^3	130π mm^3	509 cells/mm^3	354 cells/mm^3

The cell seeding density indicates the amount of cells found per cubic millimeter of a scaffold in an ideal case where all the cells are attached to the scaffold. The cell numbers were chosen based on the scaffold volumes with the aim of getting a similar cell seeding density. It needs to be taken into account, that also scaffolds with a diameter of 12 mm were used with the syringe cell seeding methods. The amount of cells was still kept the same, which led to a different cell seeding density.

5.4.1 Scaffold pre-wetting

Before cell seeding, the scaffolds were pre-wetted in cell culture medium 2 days in advance. This was done by adding approximately 20 ml of cell culture medium into a 50 ml falcon tube (Greiner Bio-One) and adding an applicable number of scaffolds, typically

from 10 to 12. The bottom of the falcon tube was knocked against a table until the scaffolds had sunken to the bottom of the tube. This indicated that the air in the scaffold pores was removed and replaced by medium. The scaffolds were then transferred to 24 well-plates (Nunc) with 1 ml of medium per each well, after which the plates were kept in an incubator at +37°C until the cell seeding process. This was done to enable protein adsorption from the medium to the scaffold.

5.4.2   Static method

In the static seeding method, an appropriate number of cells in a volume of 50 µl cell suspension were pipetted to the top surface of the scaffold. In practice, the surface of the scaffold was touched with the cell suspension drop hanging from the pipette tip. Typically, 50 µl of cell suspension corresponded to 3-5 drops of cell suspension that were spread as evenly as possible to the surface of the scaffold. This widely used static cell seeding method was considered as a control method.

5.4.3   Squeezing method

The squeezing method was based on the assumption of getting a more homogenous cell distribution by inducing suction inside the scaffold, created by the elastic nature of the scaffolds. The scaffold was first put into a small gamma-sterilized (25 kGy, BBF Sterilisationsservice GmbH) plastic "squeezing pouch". It was first squeezed from the sides 2×5 times before adding any cells. The squeezing was done using an index finger and a thumb: the scaffold was squeezed from the sides five times with a relatively fast release after each squeeze. After five squeezes, the scaffold was rotated 90º around its axis and the squeezing was repeated. The squeezing directions are illustrated in Figure 11.

The scaffold was then oriented so that its top surface was pointing up towards the opening of the pouch. The cells in a volume of 50 µl were pipetted onto the top surface similarly to that on static seeding. In practice, it was more difficult to spread cell suspension to the perimeter of the scaffold surface, because the cell suspension drop adhered easily to the sides of the squeezing pouch. After spreading the cell suspension to the top, the scaffold was again squeezed 2×5 times. The squeezing was done in a similar manner compared to the pre-cell pipetting phase.

5.4.4   Centrifugation method

Centrifugation seeding was performed by pressing the scaffold gently from its sides to fit a 15 ml falcon tube (Cellstar; Greiner Bio-One). The fit was supposed to be tight enough to prevent the cell suspension from flowing to the bottom of the tube before centrifugation, but loose enough to not close the porous structure of the scaffold. A cell suspension volume of 1000 µl with an applicable cell amount was then pipetted on top of the scaffold

and centrifuged for 5 minutes at 1000 rpm. After centrifugation, the cell suspension had flowed to the bottom of the tube as in the Figure 11.

5.4.5 Injection method

In a preliminary test, it was noticed that a liquid volume of approximately 10 µl was left inside the syringe. That led to choosing a cell suspension volume of 110 µl for the injection method. Using an injection needle (KD Medical GmbH, Berlin, Germany) and a 1 ml syringe (Omnifix-F; B.Braun Melsungen AG, Melsungen, Germany), the aim was to inject 20 µl of cell suspension evenly into five different spots in the scaffold. The pattern of the injection sites is presented in Figure 11. The injection needle was not pressed all the way through the scaffold in order to prevent the cell suspension from flowing out from the bottom of the scaffold.

5.4.6 Syringe 1 method

The principal idea behind the two different syringe methods is close to that of the centrifugation method: to force the flow of cell suspension through the pores of the scaffold. In syringe 1 method, the plunger of the syringe (BD Discardit II; Becton Dickinson, Mequinenza, Spain) was pulled out, the scaffold was placed into the syringe using tweezers and 1000 µl of cell suspension was pipetted to the top of the scaffold. The plunger was then pushed until it almost touched the scaffold to create pressure that would possibly enable the cells to go deeper into the pores of the scaffold. The principal idea was to keep the scaffolds at the 2 ml mark instead of letting them slide to the bottom. This was done by gently pressing the syringe from outside with two fingers. However, only the Sc-COMP50 scaffolds fitted the syringe tightly enough to permit this. For this method, scaffolds with diameters of 12 mm were used.

5.4.7 Syringe 2 method

In the syringe 2 method, a syringe (Becton Dickinson) was taken and its tip was cut off using a sterile scalpel. The scaffold was placed into the syringe from the newly formed opening, after which 1000 µl of cell suspension was pipetted to the top of the scaffold. A plunger from a new syringe was taken and used to push the cell suspension through the scaffold. This phase was repeated altogether 3 times. After each cycle, the syringe system was always turned in a way that the cell suspension was above the scaffold. Each time the upper plunger was pushed and the lower one only controlled in a manner that prevents it from falling off the system. The scaffold was kept still by pushing the syringe from the sides, as in the syringe 1 method. Again, some of the scaffolds did not hold still, which changed the nature of the seeding method. For this method, scaffolds with diameters of 12 mm were used.

5.4.8 Post cell seeding treatment

After the seeding process, the cell-scaffold constructs were transferred to clean, dry 24-well plates in order to discard the cells that did not reach the scaffold. The constructs were incubated at +37°C to enable cell attachment. After an incubation of 3±0.5 hours, 1 ml of fresh medium per well was added. The constructs were then cultured for 3 days before performing the analyses.

5.5 Analyses

All the analyses were performed at a time point of 3 days after cell seeding. Cell distribution and cell viability were assessed qualitatively, whereas the cell number analysis was quantitative. The amount of experiments performed on each scaffold type is presented in 0. Essentially, microsphere analyses were only performed for the supercritical CO_2 processed scaffolds: both microsphere sizes of 15 μm and 100 μm were tested on Sc-PLCL, whereas only the larger 100 μm microspheres were tested on Sc-COMP50 scaffolds. The cell seeding experiments were carried out with 3 different cell lines when it comes to these scaffolds. Only one cell line was used for the two PLDLA scaffold types.

Table 3. *The number of experiments performed on each scaffold type.*

Scaffold type	Cell seeding model with iron-labeled microspheres	Cell viability and 2D distribution (Live/Dead)	Cell number (CyQUANT)	3D cell distribution (Micro-CT)
Sc-PLCL	15 μm and 100 μm	3x	3x	3x
Sc-COMP50	100 μm	3x	3x	-
Non-woven PLDLA 96/4	-	1x	1x	1x
Knitted PLDLA 96/4	-	1x	1x	1x

5.5.1 Cell viability and distribution in 2D (Live/Dead staining)

The viability of the cells as well as their attachment and distribution on the top, bottom and cross section of the scaffolds were studied using Live/Dead staining at the time point of 3 days after cell seeding. For each cell seeding method, 2 parallel Live/Dead specimens were used.

The method is based on two probes, calcein acetoxymethyl ester (calcein AM) that produces a green fluorescence in live cells and ethidium homodimer-1 (EthD-1) inducing a red fluorescence in dead cells. The cell permeable calcein AM is conversed to fluorescent calcein by intracellular esterase activity in live cells, whereas EthD-1 cannot permeate through an intact cell membrane of viable cells. EthD-1 enters thus only cells with damaged membranes and binds to nucleic acids, which results in a 40-fold increase in fluorescence of the dye. (Invitrogen Molecular Probes 2005)

The seeded scaffolds were washed once gently with DPBS, after which 1 ml of Live/Dead working solution per scaffold was added. They were then dark incubated at room temperature in gentle shaking for 45 minutes. The working solution was a mixture of 0.25 mM EthD-1 and 0.5 mM calcein AM (LIVE/DEAD Viability/Cytotoxicity Kit for mammalian cells; Invitrogen Molecular Probes, Eugene, OR, The United States) in DPBS prepared according to the manufacturer's instruction.

After incubation, the working solution was replaced with DPBS and the scaffolds were imaged using a fluorescence microscope (Olympus IX51). The top and bottom of each scaffold was always first imaged, after which the scaffold was cut vertically along the diameter of the top surface using a scalpel. The cross sectional area was then imaged as 3 different images and arranged later computationally into one continuous image. Living cells appeared green in the images, dead cells correspondingly showed red fluorescence.

5.5.2　Quantitative cell proliferation assay (CyQUANT assay)

In order to evaluate the amount of hASCs in the seeded scaffolds 3 days after the seeding process, CyQUANT cell proliferation assay was utilized. The method is based on a CyQUANT GR fluorescent dye, which binds to cellular nucleic acids. The content of nucleic acids in the culture reflects the number of cells. For each cell seeding method, 3 parallel specimens were used with 3 parallel samples measured from each specimen.

At the time point of 3 days after cell seeding, the scaffolds were washed once gently with DPBS and transferred then to clean 24-well plates. 500 µl of 0.1% Triton-X-100 (Sigma-Aldrich) in DPBS was then added per culture well. The well plates were stored at -70°C for at least 1 day to enable efficient cell lysis. They were then thawed at room temperature and the buffer solution was pipetted 5 times on both sides of the scaffolds in order to incorporate all the cells also from inside the scaffolds into the analysis. After this, the well plates were frozen again at -70°C and then thawed in a similar manner before starting the analysis.

The triton lysates were collected into small microcentrifuge tubes and centrifuged shortly for 5 seconds. Out of each individual specimen, 3 parallel samples of 20 µl were pipetted into a 96-well plate (Nunc). Then, 180 µl of CyQUANT working solution was added. The working solution was prepared using distilled water, CyQUANT GR dye and cell-lysis

buffer (CyQUANT Cell Proliferation Assay Kit; Life Technologies) according to the manufacturer's instructions. The air bubbles were broken using a pipette tip and the samples were protected from light. The fluorescence measurement was done using a multi-plate reader (Victor 1420 Multilabel Counter; Wallac, Turku, Finland).

5.5.3 3D cell distribution of the USPIO-labelled cells (Micro-CT)

A novel method for evaluating the 3D cell distribution inside scaffolds after cell seeding was designed: adipose-derived stem cells were labeled with USPIO particles (labeling process described in section 5.3.4.) and then seeded into the scaffolds. The cells were fixed to the scaffold after 3 days of cultivation. The scaffolds were then imaged using micro-CT technology, which detects the iron oxide nanoparticles inside the cells providing an insight into the distribution of the cells. When imaging single scaffolds, the micro-CT resolution range was typically between 5.0 - 6.0 µm. Multiple scaffolds were imaged with resolutions in the range of 17.0 – 18.0 µm.

Before starting the actual cell seeding experiments, preliminary tests were performed by seeding 3 500 ASCs into a well on a 48-well plate (Nunc). The cells were then USPIO-labeled according to the protocol - the amounts of USPIO-labeling reagents were calculated using 3 500 cells as a reference instead of estimating the true number of cells on the well. The cells were then fixed, washed and dried before imaging the sample. These steps were done in a similar manner than with the scaffolds, described next. After the well-plate test, also preliminary scaffold test was performed by seeding 60 000 USPIO-labeled cells statically into a Sc-PLCL scaffold. The cells were fixed after 1 day instead of the 3-day time point used later in the experiments.

In the actual experiments, the USPIO-labeled cells in the scaffolds were first fixed with 4% paraformaldehyde and washed 3 times with DPBS afterwards. In order to prevent salt crystal formation that could disturb micro-CT imaging, the external salts originating from DPBS were removed from the scaffold. This was done by incubating the scaffolds in 0.1% Tween 20 (Sigma-Aldrich) in DPBS for 1 hour at room temperature in a gentle shaking, rinsing the scaffolds first with distilled water, washing 3 times with distilled water in gentle shaking for 4 minutes and finally removing the water and letting the samples dry. Dry scaffolds were then imaged using a micro-CT scanner (MicroXCT-400; Xradia, Pleasanton, CA, United States).

5.5.4 Prussian blue staining for iron

The Prussian blue staining was performed to assess the presence of iron inside the cells, that is, to evaluate the level of success in USPIO-labelling. After seeding the USPIO-labeled ASCs into the scaffolds, a glass coverslip was placed into a 6-well plate (Costar; Corning Incorporated, Corning, NY, United States) with 3ml of cell culturing medium, after which approximately 70 cells/mm^2 were seeded onto the coverslip.

On the day of the experiment time point, the cells on the coverslip were fixed with 2.5% glutaraldehyde (25% glutaraldehyde in H_2O; Sigma-Alrich) in H_2O for 10-15 minutes. The cells were then stained in an equal mix of 10% potassium ferrocyanide in H_2O and 20% HCl in H_2O by immersing the coverslip in the solution for 20 minutes. After 3 washes in distilled water, the cells were counterstained with Nuclear Fast Red (Sigma-Aldrich, Egham, The United Kingdom) for 5 minutes, rinsed twice with distilled water and dehydrated through 95% alcohol (Etax Aa diluted in distilled water) and 2 changes in 99.5% alcohol (Etax Aa; Altia). After clearing the sample 2 times 3 minutes in xylene, the coverslip was fixed onto a glass plate with vectamount (Eukitt; O.Kindler GmbH & CO, Freiburg, Germany). The sample was then imaged with light microscopy – bright blue indicated the presence of iron, whereas cell nuclei and cytoplasm were colored red and pink, respectively.

6. RESULTS

6.1 Pore interconnectivity analysis with microspheres

The distribution of the iron-labeled microspheres was determined from the micro-CT images. Figure 12 shows 15 μm microparticles being relatively evenly distributed inside the scaffold.
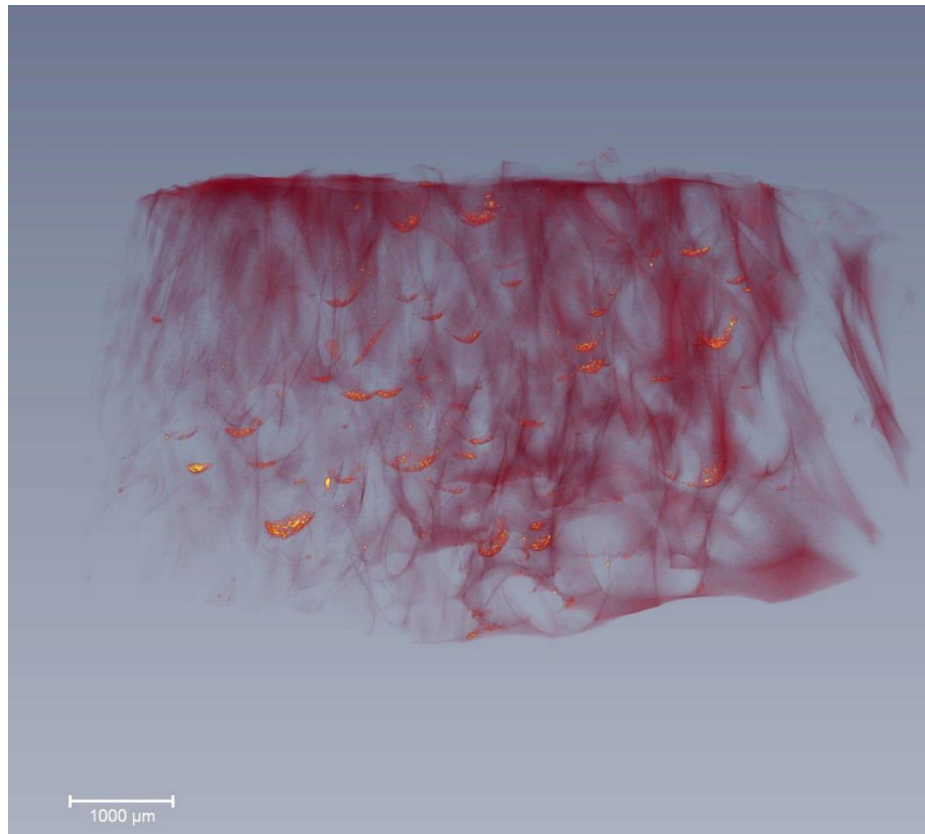

Figure 12. *Micro-CT image of a Sc-PLCL scaffold seeded with 15μm iron-labeled microspheres. The image is taken from the side of the scaffold with microspheres appearing goldish on the bottom of the pores.*

Altogether 60 000 microspheres were statically seeded, but instead of the whole scaffold, only part of the scaffold (approximately 6×6×3 mm in size) was imaged in order to obtain a better resolution and thus ensure the visibility of the particles. Figure 12 obviously shows crescent-shaped clusters of iron-labeled microspheres in different depths of the scaffold. It was thus clear, that the interconnectivity of the pores in these scaffolds is on a good level. A similar test was performed with 10 000 microspheres with a size of 100 μm. The result is shown in Figure 13, with the whole scaffold being imaged. Similarly to the previous Figure 12, the 3D view is from the side with the scaffold material partly faded to see the microspheres in the pores.
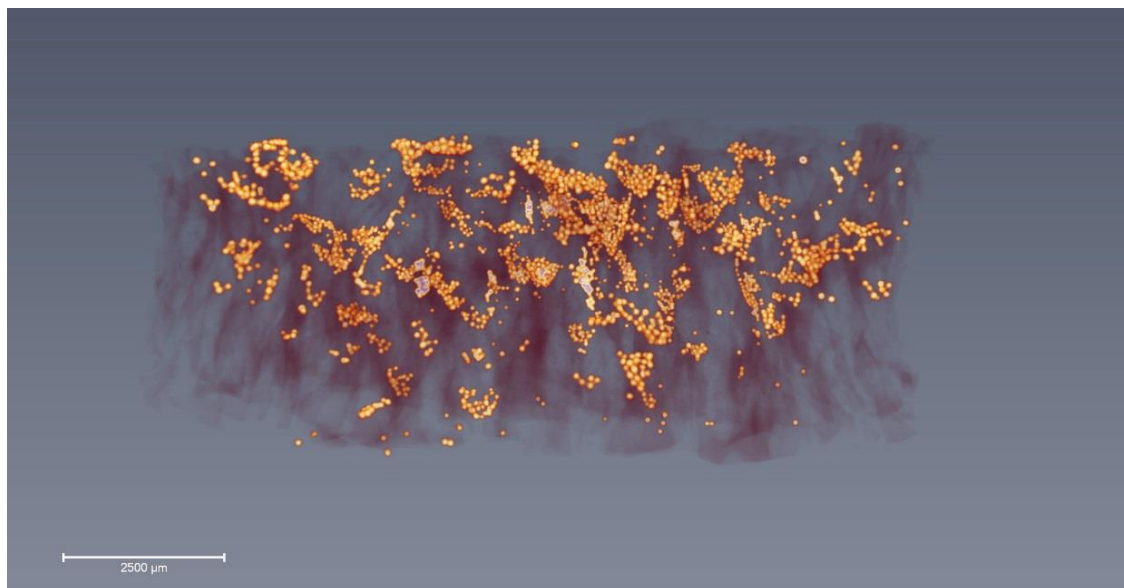
Figure 13. *Iron-labeled microspheres with a diameter of 100 µm inside a Sc-PLCL scaffold. The whole scaffold is seen in the image in a dark purple color.*

Again, the microspheres ended up into the pores deep in the scaffold confirming the result of good pore interconnectivity. The lower corners of the scaffold are emptier: this might be due to pipetting the particles in a center-oriented way. Nonetheless, in general the particles have occupied the scaffold evenly. This also indicates that most of the pore interconnections are undoubtedly larger than a 100 µm. The brighter appearance of the 100 µm microspheres results from their size. The total volume of 10 000 microspheres of size 100 µm is approximately 50 times the volume occupied by 60 000 microspheres of size 15 µm.

The Sc-COMP50 scaffolds were examined only using microspheres of size 100 µm. Because of the TCP particles disturbing the image, a similar 3D view from the side compared to the PLCL scaffolds was not meaningful. Figure 14 shows a representative sight into a crosscut of a Sc-COMP50 scaffold seeded with 10 000 microspheres.
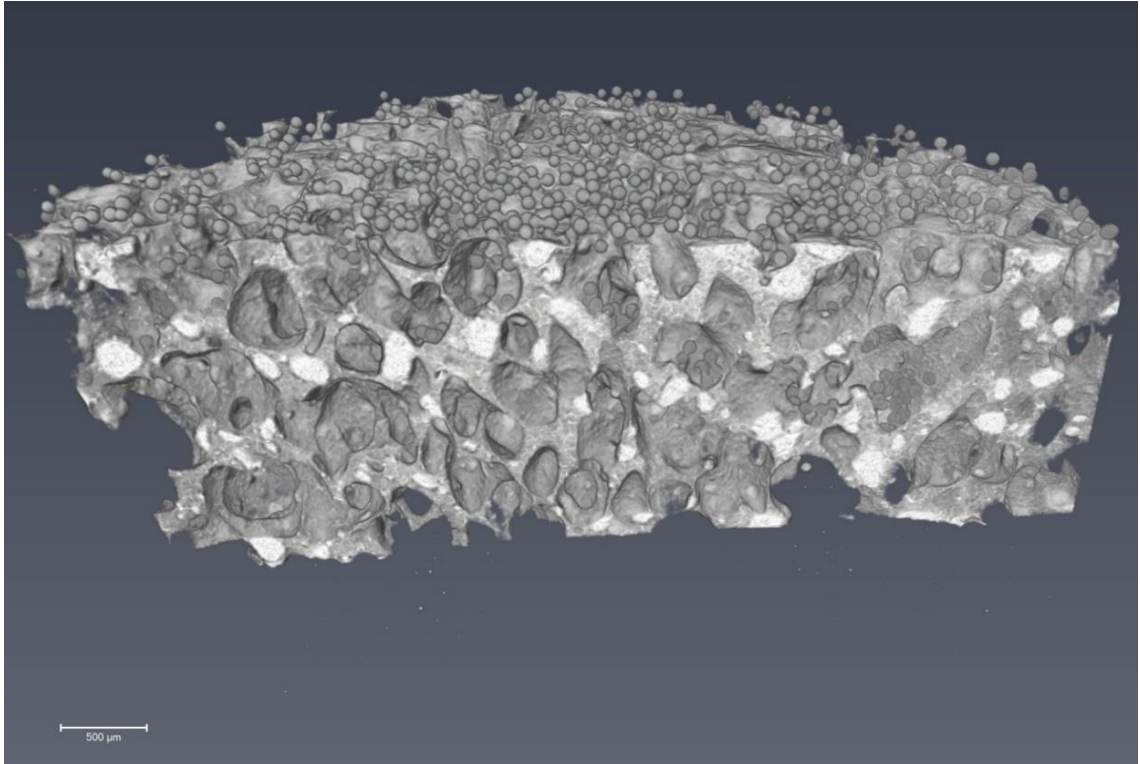
Figure 14. A cross sectional image of an Sc-COMP50 scaffold seeded with 100 µm iron-labeled microspheres. Some of these spheres can be seen in the pores at the cross section of the scaffold. Scale Bar 500 µm.

There are clearly many particles on top of the scaffold, but some can be spotted also inside the structure in the pores. In the undermost quarter of the scaffold, only few particles were seen.

6.2   Characterization of the hASCs

0 lists the three cell lines used in this work as well as their expressions of different surface markers as analyzed by flow cytometry. The cell lines are named as human fat stem cells (HFSC) with a unique number indicating their isolation order and year. Cell line 3 was used with the third Sc-PLCL and Sc-COMP50 experiments, as well as with the PLDLA 96/4 scaffolds.

Table 4. Surface marker expressions of different cell lines used in this study. The ASC criteria indicates the minimal requirements for adipose-derived stem cells as introduced by the ISCT in (Dominici et al. 2006)*.*

Surface protein	Cell line 1 HFSC1/14 (%)	Cell line 2 HFSC40/12 (%)	Cell line 3 HFSC2/14 (%)	ASC criteria (2006)
CD3	0.4	0.2	0.2	
CD11a	0.8	0.7	0.6	
CD14	0.7	0.8	0.3	≤2%
CD19	0.6	0.6	0.3	≤2%
CD34	9.7	48.5	35.4	≤2%
CD45	1.1	0.7	1.4	≤2%
CD54	2.8	32.2	6.6	
CD73	98.4	97	96.7	≥95%
CD80	0.6	0.8	0.4	
CD86	0.5	0.6	0.3	
CD90	99.6	99.7	99.7	≥95%
CD105	99.4	99.3	97.5	≥95%
HLA-DR	0.7	1.2	0.6	≤2%

According to the analysis, all the cell lines expressed the markers CD73, CD90 and CD105 strongly (≥95%). At the same time, the expression of the surface markers CD14, CD19, CD45 and HLA-DR is very weak (≤2%). All of these values are perfectly in line with the minimal criteria for adipose-derived stem cells, proposed by the ISCT (Dominici et al. 2006). However, contrariwise to the criteria, the hematopoietic marker CD34 shows moderate expression in all of the cell lines.

6.3 Cell seeding results

All the analyses were performed at a time point of 3 days. Before performing the experiments, the well plates were always imaged using light microscopy to ensure there were no bacterial contaminations. The well plate images of the COMP50 scaffolds are presented in Appendix 1. Typically, a large amount of cells growing on the well were noticed in the case of scaffolds seeded with static and squeezing methods. The syringe methods resulted mainly in a low number of cells growing outside the scaffold. Black specks, interpreted as dead cells, were seen in the case of squeezing and centrifugation methods.

6.3.1 Cell viability and 2D distribution

At a 3 day time point, cell viability and distribution in 2D were qualitatively analyzed using Live/Dead staining. Green fluorescence represents viable cells, whereas dead cells

are seen in red. Along with the top and bottom surfaces, the cross sections were imaged. Figure 15 illustrates the results from the third Sc-PLCL experiment. The results of the two previous experiments are shown in Appendix 2.
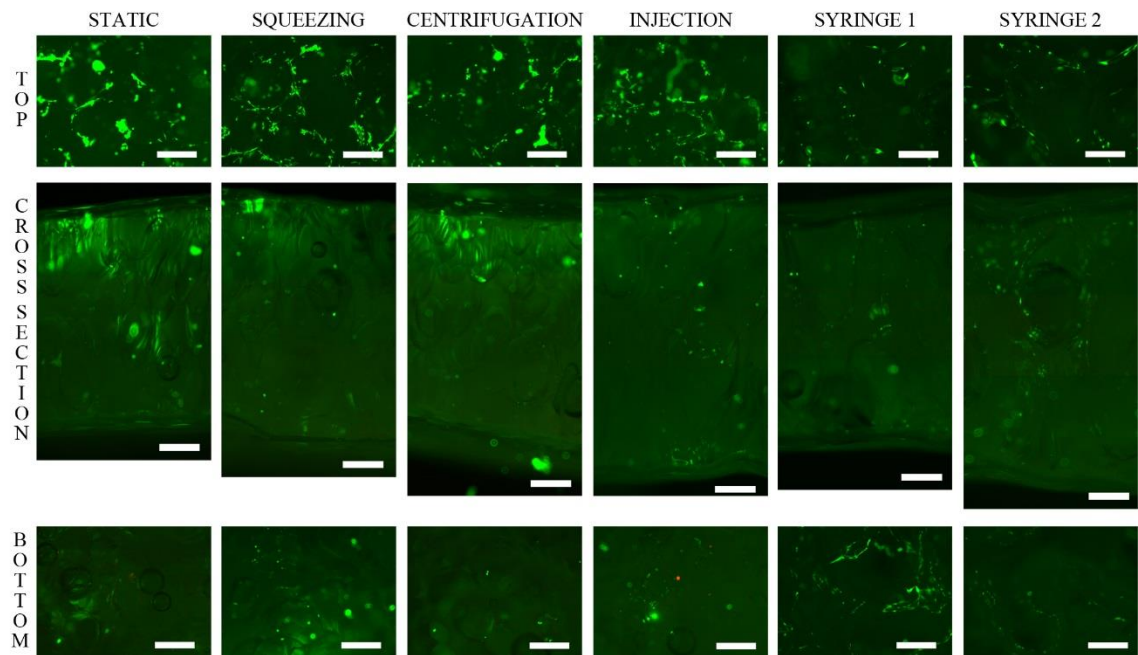

Figure 15. *Representative Live/Dead images from one of the three Live/Dead experiments performed on Sc-PLCL scaffolds. Scale bars 500 μm.*

The syringe methods resulted in less cells on the top of the scaffold than the other seeding methods. In the cross sectional view, they also showed some cells in every depth from the bottom to the top. The statically seeded scaffold cross cut in Figure 15 also demonstrated quite a lot of cells distributed relatively evenly - however from the two parallel samples, the other one performed significantly poorer. No significant differences were seen in the bottom surfaces. The other two experiments showed essentially similar results even in the case of the first experiments with only 60 000 seeded cells. Some dead cells were seen in the case of centrifuged scaffolds. Some individual large cell clusters were occasionally spotted on the bottom or in the middle of the cross section images of the statically seeded scaffolds.

Figure 16 presents the results of the third Sc-COMP50 experiment. The two other repetitions are again available in Appendix 2.
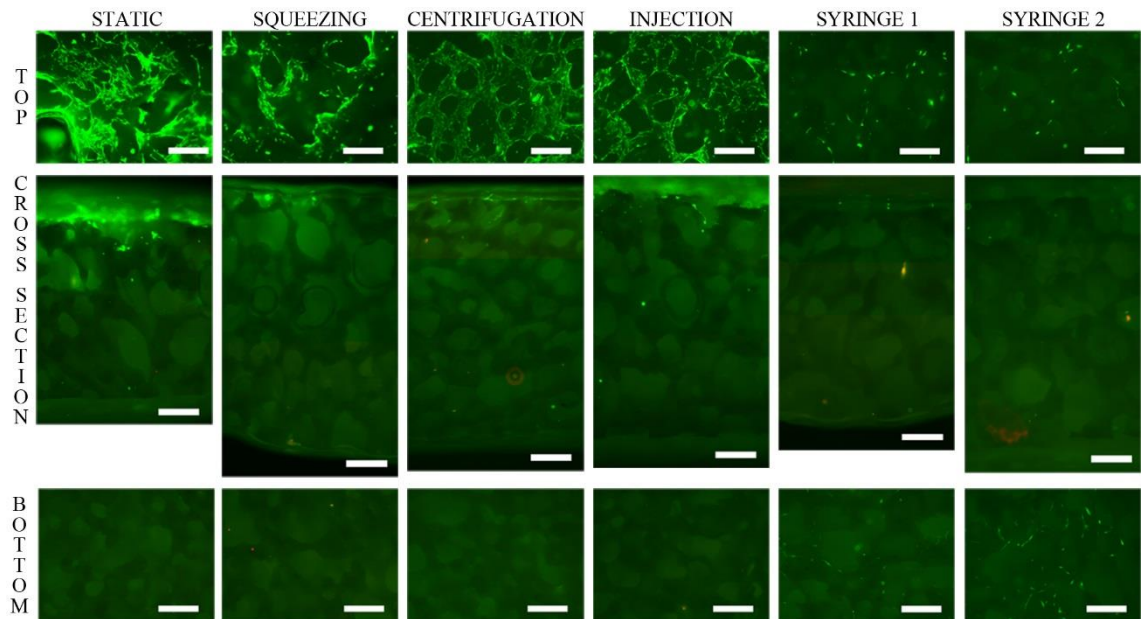

Figure 16. *Representative Sc-COMP50 Live/Dead images. Scale bars 500 μm.*

The static, squeezing, centrifugation and injection methods result in a smooth cell sheet on the top surface of the scaffold. The scaffolds seeded with the syringe methods have again less cells on the top surface, but it can be seen that there are some cells at least inside the uppermost pores. The cross cut pictures show very few cells: the syringe methods have some individual small clusters in the middle of the scaffold. The clusters are typically yellowish due to part of the cells being viable and some already dead. Also the cross sectional view demonstrates how for example the static method has a lot of cells on the top, but not many deeper in the scaffold. Again the other experiments performed quite similarly. Some more clusters with dead and alive cells are seen in the cross section images.

The knitted PLDLA 96/4 scaffolds showed desirable results in terms of cell distribution and viability, as shown in Figure 17. Single dead cells were seen, but the absolute majority was viable. All the images including the cross sections indicated an even, relatively frequent cell distribution regardless of the cell seeding method.
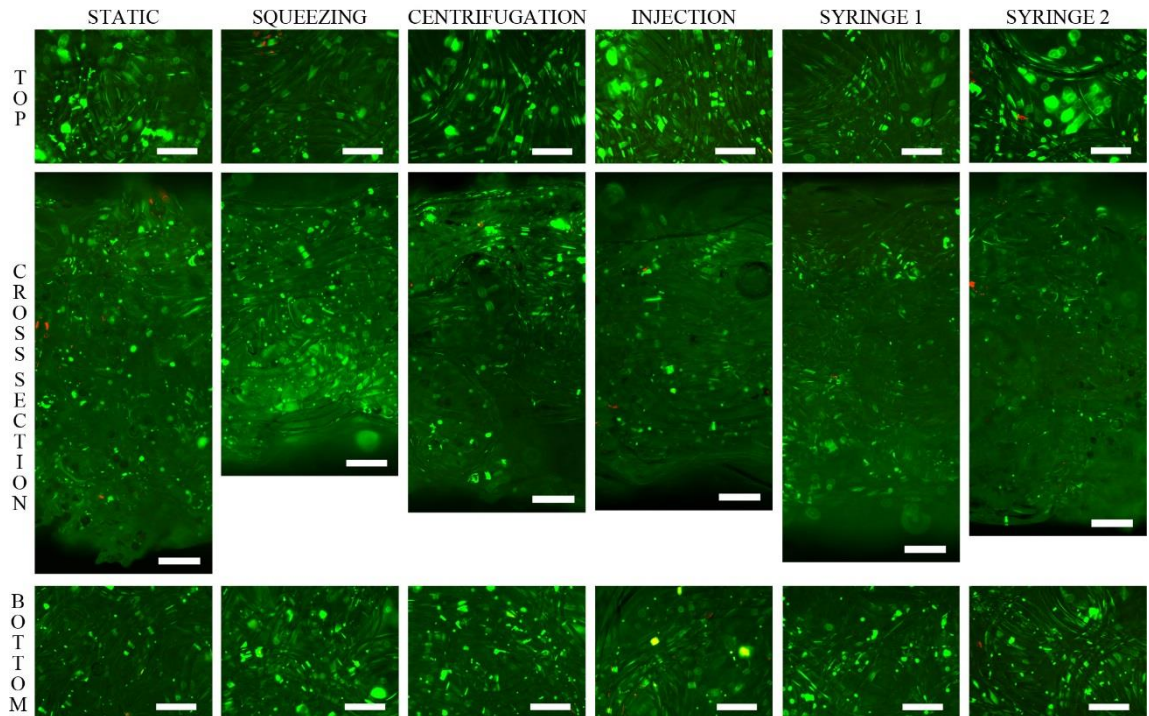

Figure 17. Knitted PLDLA 96/4 scaffold Live/Dead images. Scale bars 500 μm.

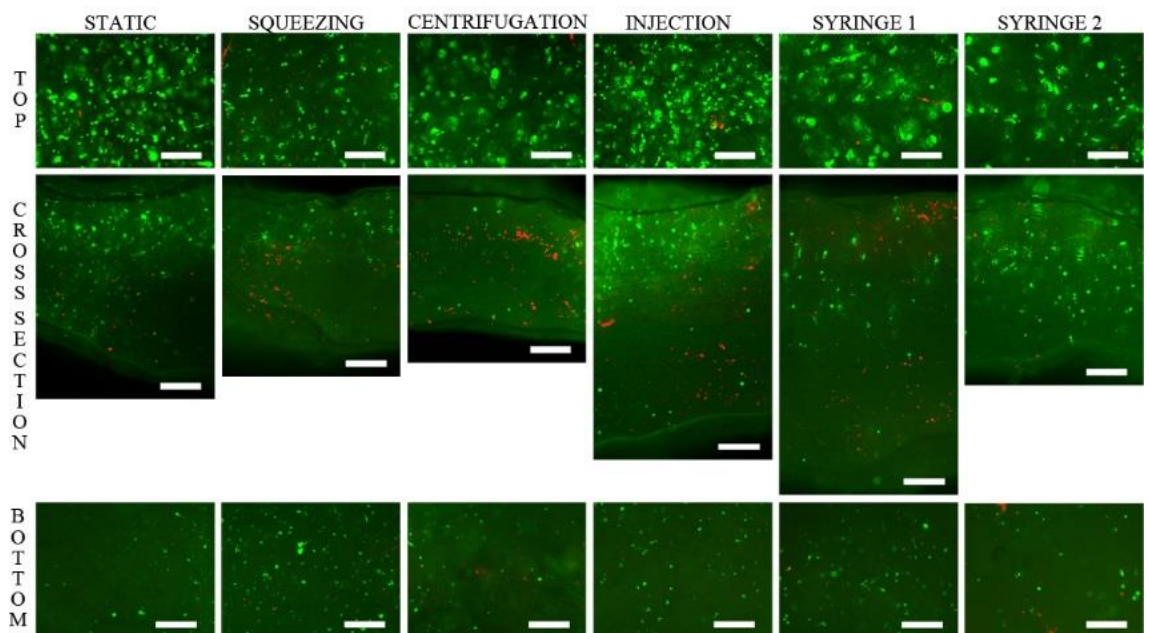The non-woven PLDLA fabrics showed quite many dead cells, as seen in Figure 18.

Figure 18. Cell viability in non-woven PLDLA 96/4 scaffolds. Scale bars 500 μm.

The actual number of dead cells was even higher, since some of the cells were stained only lightly and thus could not be included in the final images. Dead cells were found in all of the scaffolds regardless of the seeding method. The distribution of the cells however seems very even. The top and bottom surfaces show similar results between different seeding methods and there are adipose-derived stem cells in every depth of the cross section.

6.3.2 Quantitative cell number

The amount of DNA in the scaffolds was quantitatively examined applying the CyQUANT analysis. The amount of DNA reflects the number of cells in the sample. The relative cell number results are presented in Figure 19 with respect to the static seeding method, which is considered to be the standard seeding method and is thus fixed into the value 1. Three experiments were performed with both of the ScCO$_2$ processed scaffolds. The results of the missing two experiments are presented in Appendix 3.

Figure 19. Relative CyQUANT results with respect to the static method, which is considered as the control sample.

The absolute results are presented in Figure 20, with again the remaining ScCO$_2$ processed scaffold experiments 1 & 2 attached to Appendix 3.

Figure 20. *Absolute CyQUANT results. The Y Axis shows fluorescence values resulting from the CyQUANT GR dye, which binds to cellular nucleic acids.*

The results concerning Sc-PLCL scaffolds showed different absolute results, but similar relationship between each cell seeding method. As the first experiment was done using 60 000 adipose-derived stem cells per scaffold, 120 000 cells were used in the later sets. In the experiment 2 the scaffolds were also cut into 4 pieces to facilitate getting all the DNA material from inside the relatively dense scaffolds into the samples. Since the relative results did not change dramatically between these two experiments, the chopping step was left out from the last experiment. Comparing the second and the third experiment reveals, that there actually is a difference depending whether the scaffolds are chopped into pieces or not. Still, the relative results between different cell seeding methods remain unaffected.

Clearly there were 3 methods (static, squeezing and centrifugation) that performed the best in this analysis regarding both ScCO$_2$ processed scaffold types. Typically these results fit into the error margins of each other. This was also the case in Sc-COMP50 scaffolds, where the squeezing method seems to perform a bit worse at a first glance. The reason for this and to the relatively large error margin was the fact that in each of the experiments, one of the three squeezed scaffolds had a significantly lower result than the other two parallel samples. The injection method showed very variant results between

different repetitions, but ranked typically fourth in terms of cell number. The performance of the syringe methods was very poor with both Sc-PLCL and Sc-COMP50 scaffolds, especially in the case of COMP50.

Both knitted and non-woven PLDLA 96/4 scaffolds showed similar results: the static and the squeezing methods ranked the highest with not much difference between each other. Compared to Sc-PLCL and Sc-COMP50 scaffolds, the centrifugation method performed significantly worse. The cell amount by injecting the cells ranked a bit lower than the two best methods. Again, both syringe methods performed the worst, still obtaining better absolute results than in the case of Sc-COMP50 scaffolds.

6.3.3 Micro-CT & Prussian blue

The novel combination of USPIO-labeled adipose-derived stem cells and micro-CT imaging was first tested by seeding 3 500 cells on a well plate. The result, shown in Figure 21, verifies that USPIO-labeled cells can be detected with micro-CT technology. Green roughness on the well piece denotes iron oxide particle clusters inside the cells.
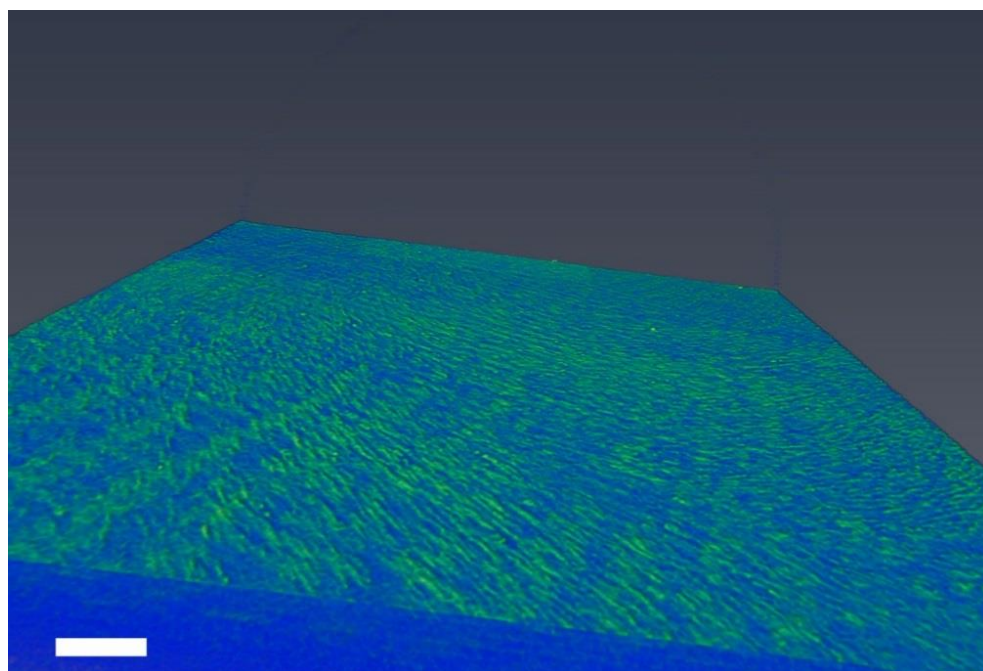

Figure 21. *Micro-CT image of USPIO-labeled cells on a well plate. The green-colored signals are USPIO particles. Scale bar 250 μm.*

Along with the succesful well plate test, the method was tested with a Sc-PLCL scaffold. The result is shown in Figure 22.
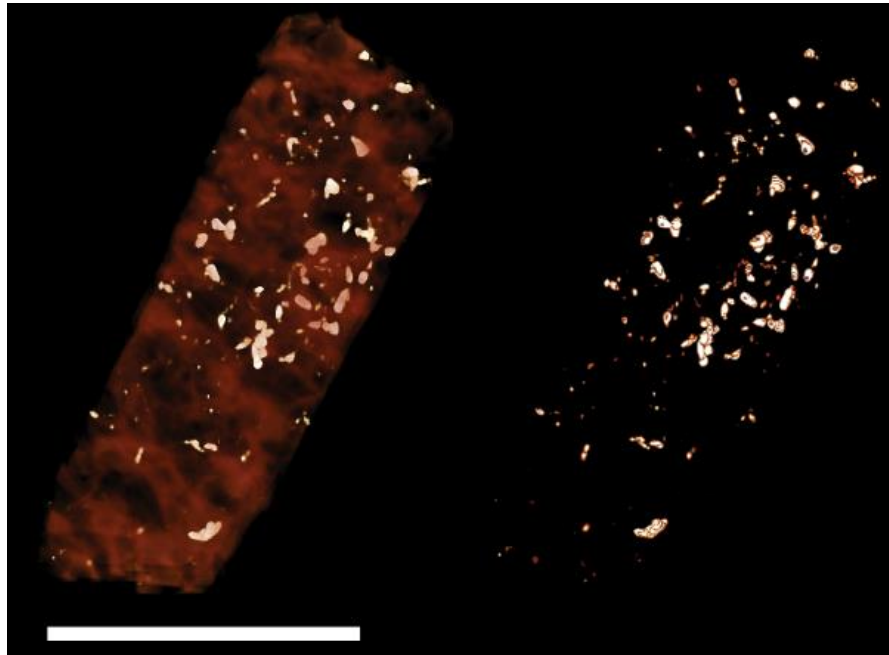

***Figure 22.** Sc-PLCL scaffold with statically seeded USPIO-labeled ASCs at a time point of 1 day. Both images show the same scaffold, with the PLCL matrix being faded out on the right side. Scale bar 5.0 mm.*

When testing the visibility of the USPIO-labeled cells in Sc-COMP50 scaffolds, it became clear that the USPIOs cannot be distinguished from the scaffold. As seen in Figure 230 where the PLCL bulk has been faded out from the picture, the dense tricalcium phosphate granules dominate the image with their high intensity.
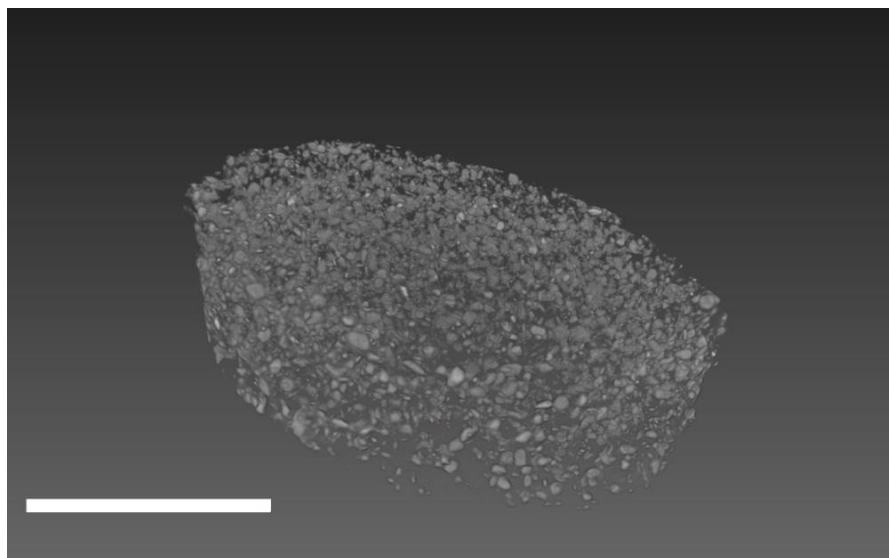

***Figure 23.** β-TCP granules inside a COMP50 scaffold. The PLCL matrix has been faded out from the image. Scale bar 5.0 mm.*

Detecting the nanoparticle clusters from polymeric scaffolds was easier. Figure 24 shows Sc-PLCL scaffolds seeded with different methods. The other two experiments are presented in Appendix 4. The scaffolds are gradually faded away from the pictures: the piles on the left show the polymer, whereas on the right only the USPIO nanoparticles are seen.

When looking the pictures closely, there were USPIO nanoparticles in the middle of the scaffold to some extent in almost every scaffold - only the injection method showed poor results. In the experiment 2 (Appendix 5), all the other methods performed equally well. Still, when evaluating the 3 experiments as a whole, the Syringe 1 method resulted in best results when it comes to the 3D distribution of the cells. Because of this, Figure 24 was considered to be a good representative of all the experiments.

The prussian blue results from all of the experiments are presented in Appendix 5. Any iron in the samples is colored in blue. The cytoplasm shows pink and the nuclei bright red. Based on the Prussian blue images, the USPIO-labeling in Sc-PLCL experiment 2 had succeeded somewhat better than in the other repetitions. The appearance of the USPIO-labeled cells used with the knitted and non-woven PLDLA 96/4 scaffolds showed an unusual appearance. Still, blue iron could be seen in the Prussian blue images.

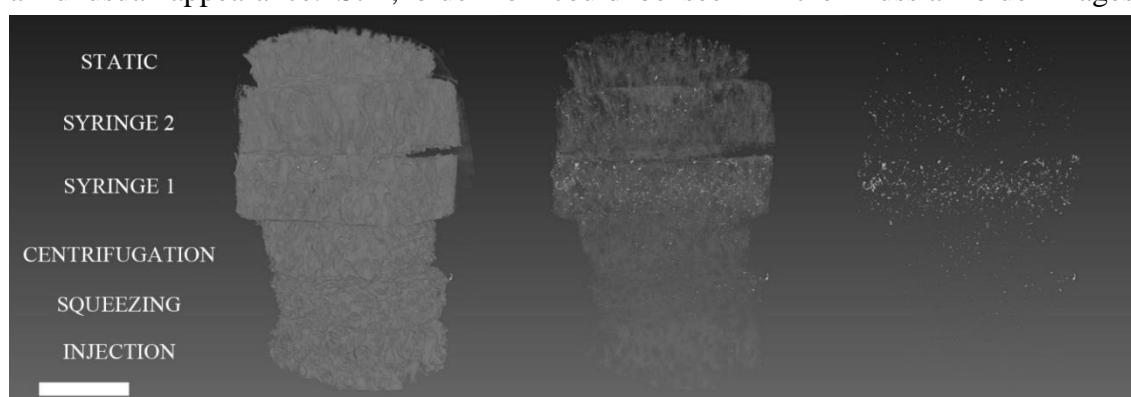*Figure 24. Scaffolds seeded by different cell seeding methods. The three piles represent same scaffolds with different kind of image processing. The first pile from the left shows the scaffold - from the second pile some nanoparticles can be detected inside the scaffold that is faded. In the last pile, the scaffold material has been completely faded away with only USPIO particle signals left in the image. Scale bar 5.0 mm.*

The micro-CT results of the knitted PLDLA scaffolds were controversial to those obtained with the Live/Dead staining: only very few, if any, USPIO-labeled cells are seen. Figure 25 illustrates the situation.
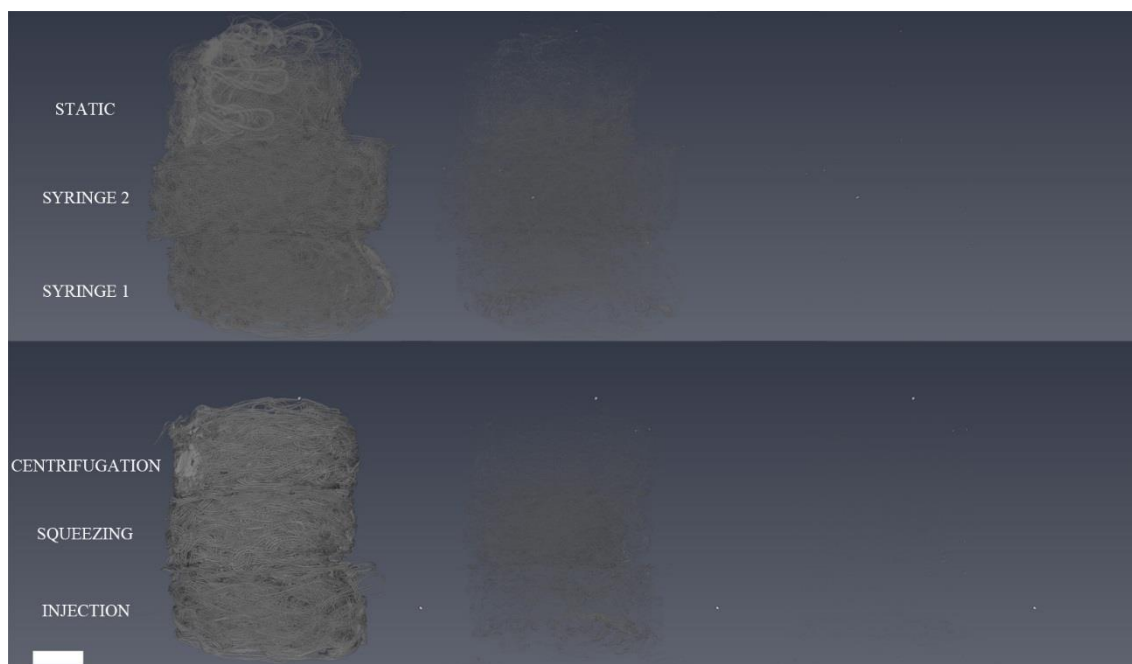

Figure 25. *Micro-CT images of the knitted PLDLA scaffolds seeded with USPIO-labeled cells. Again, the scaffold piles on the left show the scaffold only, whereas the piles on the right are processed to show only USPIO particle signals. In the middle, only part of the scaffold has been faded away with some visible signals from the USPIO particles as well. In the statically and centrifugally seeded scaffolds, the seams obtained by heat sealing are seen. Scale bar 5.0 mm.*

In the case of non-woven PLDLA fabrics, some USPIO-labeled cells were detected. Also the variation in scaffold heights becomes clear when looking at the Figure 26. Both syringe methods show an even yet relatively loose 3D cell distribution, but the comparison of the methods is very difficult due to the differences in the scaffolds. The statically seeded scaffold also contains some USPIO particles, but not much is seen in the scaffolds seeded with centrifugation, squeezing or injection methods. These three scaffolds were also significantly thinner than the rest.

STATIC

SYRINGE 2

SYRINGE 1

CENTRIFUGATION
SQUEEZING
INJECTION

Figure 26. Non-woven PLDLA 96/4 fabrics as imaged with micro-CT technology. Para-film sheets used to hold the sample still during the imaging process can be seen on the left pile. The scaffold material has partly been faded away to show some signals from the USPIO-labeled cells as well. On the right, only USPIO particle signals are seen. Scale bar 5.0 mm.

7. DISCUSSION

Successful cell seeding enables uniform ECM deposition and tissue growth throughout the engineered construct. In the case of non-uniform seeding, unwanted nutrient and metabolite gradients are formed around the scaffold. (Bueno et al. 2007) When choosing for a suitable cell seeding method, the effect of the cell type, scaffold structure and material need to be taken into account. In an ideal case the method is also simple, fast and reproducible (Soletti et al. 2006). The more additional equipment and scaffold handling the cell seeding method requires, the bigger is also the contamination risk.

7.1 Scaffold properties and microsphere cell seeding model

In this study, 4 different scaffold types were used. Sc-PLCL and Sc-COMP50 scaffolds were made with supercritical carbon dioxide processing, whereas knitted PLDLA and non-woven PLDLA scaffolds were produced from different PLDLA 96/4 fibers by applying knitting and non-woven technologies, respectively. The Sc-PLCL and Sc-COMP50 scaffold types had similar porosities of 65%, as analyzed from the micro-CT data. However, micro-CT image analysis showed that the COMP50 scaffolds had smaller pore sizes.

One challenge in these scaffolds is that the micro-CT analysis does not take a stance on the shape of the pores or their interconnectivity, which is difficult to determine because of the limitations in the micro-CT resolution. If the wall thickness or a pore is smaller than the micro-CT can identify, the result of the analysis is misleading (Darling & Sun 2004). Partly for this reason, the microsphere seeding tests were performed. The results are however not directly comparable with each other: the 15 µm microspheres occupied a 50 times lower volume compared to the 100 µm particles. Thus, the larger particles can be seen to a larger extent in the images. Also the field of view is smaller in the image of Sc-PLCL scaffold seeded with 15 µm particles (only part of the scaffold is shown). Due to the dense β-TCP particles and their strong signals in the micro-CT images, a comparable 3D view of the COMP50 scaffolds was not reasonable. This not only makes the comparison between these two scaffold types difficult, but also complicates the objective evaluation of the particle distribution inside the COMP50 scaffolds, since only a single crosscut image at a time can be evaluated.

Based on the microsphere analysis, the interconnectivity of the Sc-PLCL scaffold pores was high. Even with static seeding only, there were microspheres in every depth of the scaffold. The reason for the lower 100 µm particle frequency on the sides probably resulted from the seeding method: pipetting suspension drops to the absolute periphery of the scaffolds without wasting microspheres was challenging. The particle distribution is

more difficult to evaluate with the COMP50 scaffolds, but it was noticed that there were only few 100 μm microspheres in the undermost third of the scaffold. Another finding was that there were multiple pores so small, that only one microsphere fit the pore. This result was consistent with the micro-CT analysis, which demonstrated smaller pore size of Sc-COMP50 scaffolds compared to the Sc-PLCL scaffolds.

Besides the interconnectivity analysis, another interesting but tricky question regarding microsphere seeding is whether or not they can be used to model actual cell seeding. The microspheres sediment so quickly in both PBS and distilled water, that their behavior can be expected to be dominated by gravity in the scaffolds as well. This is not always the case with living cells (Ghavidel Mehr et al. 2014). Another crucial difference between the microsphere and cell seeding experiments is the fact that the microspheres are not attached or fixed to the scaffold. This might permit their movement deeper into the scaffold during the drying phase, as the water in the pores evaporates. Also the spherical shape of the microspheres might facilitate their infiltration deeper into the scaffold compared to the cells.

Another group has performed similar tests with 10 μm polystyrene microspheres imaged with phase contrast microscopy: they concluded that the microspheres provide a baseline for non-aggregated, trypsinized cell seeding, but it must be remembered that cells do not always behave as single entities (Ghavidel Mehr et al. 2014). Indeed, one concern about cell seeding of Sc-COMP50 scaffolds was, whether the cells permeate to the inner pores of the scaffold or aggregate rather on the surface. Cell aggregates might prevent nutrient transport or cell infiltration into the scaffold (Ding et al. 2008; Ghavidel Mehr et al. 2014).

According to the hypothesis that cell seeding could be modeled with iron-labeled microspheres, the microsphere results promise easy seedability of the PLCL scaffolds with hASCs as well. For evaluating the 3D cell distribution in cell seeding, a novel method was proposed utilizing USPIO-labeled hASCs and micro-CT technology. Previously, ultrasmall iron oxide nanoparticles have mostly been used as contrast agents in magnetic resonance imaging both *in vivo* and *in vitro* (Oude Engberink et al. 2007; Mathiasen et al. 2013; Weissleder et al. 1995). When comparing the microsphere results to the statically seeded USPIO-labeled cell images, a lot of similarities were seen. Especially in the preliminary cell test after 1 day, cells are seen quite evenly distributed in the scaffold. This is also the case with the 3-day experiments, although the amount and intensity of the signals is lower. Both microsphere sizes show signals in the scaffold in an even more comprehensive manner, which is intuitively understandable since the amount of iron is higher in the microspheres and not all of the cells are successfully USPIO-labeled.

As a result, in the case of Sc-PLCL scaffolds the iron-labeled microspheres imply better seeding results than can be produced with the USPIO-labeling method. Keeping in mind the seemingly better tendency of microspheres to infiltrate into the scaffold pores and especially their better visibility in the micro-CT images, it appears that the microparticles

offer a functional way to model cell seeding in this type of scaffolds. The situation might be different with Sc-COMP50 scaffolds. As already discussed, the 100 µm microspheres did not occupy the COMP50 scaffolds as evenly as they did with PLCL scaffolds. The lack of an adequate 3D imaging method for composite scaffolds makes it challenging to compare the cell distribution to that of the microspheres. Still, the 2D Live/Dead images of the cells indicate again a worse distribution compared to the microspheres: a sheet of cells can be seen on the top of many scaffolds. As a conclusion, the microspheres are potential candidates for providing an excellent model of the interconnectivity and seed-ability of the $ScCO_2$ processed scaffolds, but caution must be obeyed when the results are used to model cell seeding results (Ghavidel Mehr et al. 2014).

Naturally the material properties also have an impact on the scaffold properties. When comparing the two $ScCO_2$ processed scaffold types, the COMP50 scaffolds are under-standably more rigid, yet they still show an elastic and ductile behavior. The embedded β-TCP granules increase their hydrophilicity compared to the hydrophobic Sc-PLCL scaf-folds. (Ahola et al. 2012) When the scaffolds are cut into their final dimensions, it is done with a scalpel by hand, leading to variations in the scaffold heights. In cell seeding, this can have an impact on the final outcome (Bryant & Anseth 2001). Cutting the COMP50 scaffolds might also reveal more surface area of bioactive β-TCP on the cut surface, which might attract the cells and thus reduce their migration willingness deeper into the scaffold.

Despite the hydrophobicity of polylactide, both knitted and non-woven PLDLA scaffolds sunk effortlessly to the bottom of the falcon tube in the pre-wetting phase, which clearly addresses their loose structure. The knitted scaffolds varied a lot in height depending on the width of the knit. Also the non-woven fabric was patchy resulting in significant height variations of the non-woven scaffolds. It also needs to be taken into account, that the height measurements were done dry and the dimensions of the non-woven scaffolds change when wetted.

7.2 Stem cells and cell culturing

Characterization of the adipose-derived stem cells showed the mesenchymal origin of the cell lines used in the experiments. Only the hematopoietic surface marker CD34 showed higher expression values than suggested in the ISCT criteria for adipose-derived stem cells, which is typical when human serum is included in the culturing media. The expres-sion of this marker is shared by endothelial cells and hematopoietic stem cells (Bourin et al. 2013). Since the absolute majority (99%) of the hematopoietic cells should not adhere to cell culturing dishes (Gordon et al. 2006) and the endothelial cells in general are very dependent on shear stress and supplements, they may dedifferentiate or trigger apoptosis when cultured statically (Baer & Geiger 2012). Since the analyzed cells were at passage 1, it can be assumed that the expression of CD34 would decrease along passaging.

The 3 different cell lines showed distinct proliferative properties. Cell line 1 proliferated particularly fast - the cells started readily to curl on top of each other and the flasks were confluent only a few days after passaging. Cell line 2 had a moderate cell proliferation rate. The third cell line, used for the third set of $ScCO_2$ processed scaffold experiments and for the PLDLA 96/4 scaffolds, showed quite fast proliferation, although not as active as the first cell line. These differences might affect the results of the cell number analysis and the efficiency of the USPIO-labeling, as the iron oxide particles become diluted (Küstermann et al. 2008).

7.3   Cell seeding methods

The study was based around 6 different cell seeding methods. Out of these, the **static method** was considered to be the standard control method due to its easiness and simplicity (Dai et al. 2009; Vitacolonna et al. 2013). In this method, no external forces are applied to the cells, which in some cases leads to non-uniform cell distribution (Ding et al. 2008). However, it also means that the cells are not subjected to forces that could possibly alter their viability or function. A uniform distribution of cells using static seeding requires a loose enough scaffold structure to enable cell migration and passive diffusion of cells into the scaffold. Another advantage of the method is that it is not dependent on the scaffold type.

The **squeezing method** was hypothesized to lead to better seeding results by means of suction forces created by squeezing the elastic $ScCO_2$ processed scaffolds. Squeezing before the cells were applied clearly had an effect on these scaffolds: especially the Sc-COMP50 scaffolds felt hard at the beginning despite the pre-wetting at +37ºC. After the pre-squeezing, the scaffolds were softer and more elastic. In addition to the sectional forces, it was postulated that the inner microstructure of the scaffolds might get broken during the pre-squeezing, which could result in an even better interconnectivity of the pores. The squeezing method was also applied to the knitted and non-woven PLDLA 96/4 scaffolds, but the knitted scaffolds could not be squeezed much without breaking the scaffold structure. Even low force squeezing resulted in deformation of the scaffold shape. As expected, the non-woven scaffolds recovered poorly from the stress.

One concern with the squeezing method was the usage of the sterile plastic pouches. Handling and orienting the scaffold in a desired way was often complicated due to the slippery pouch. Touching the sides of the pouch with the top side of the scaffold (where the cells were seeded) was tried to be avoided, often unsuccessfully. This, as well as the flow of medium and cell suspension from the scaffold during the squeezing process admittedly led to losing some of the cells to the pouch during the seeding process.

One of the methods with a significantly larger cell suspension volume was **centrifugation**. The way it was done in this work is partially dependent on the scaffold shape and mechanical properties. Soft non-woven fabrics and knitted scaffolds seemed to detach

from the bottom of the falcon tube. At the same time, pressing the scaffolds too tightly needs to be avoided or the openness of the pores might be compromised. Some minor problems were related in removing the scaffold from the tube – caution was needed to avoid contaminations and to keep track which was the top side where the cells were seeded. One question regarding this method is associated with the hypothesized fluid flow through the scaffold: of the cell suspension volume, how much actually flows through the pores and what portion goes directly to the bottom of the falcon tube from the sides? To avoid wasting cells, it is possible to re-suspend the cells from the bottom of the tube between centrifugation (Roh et al. 2007), but this makes the process also more time-consuming and complicated.

Similar problems with the fluid flow were encountered with both of the syringe methods. Before starting the cell seeding experiments, the methods were tried out with distilled water and Sc-COMP50 scaffolds. These scaffolds fit the syringes tightly enough to prevent the liquid from flowing past the scaffold before applying pressure with the syringe plunger. Later it was noticed that this was not the case with the other scaffold types, or even with some of the COMP50 scaffolds. Instead, the cell suspension flowed often freely past the scaffold. Also the COMP50 scaffolds fitting the syringe tightly raised a question whether the fluid actually flows through the scaffold - some signs were noticed that at least part of it slips past the scaffold. Ideally, this should be prevented by tight-fitting the scaffold into the syringe, yet leaving the porous structure open for fluid flow.

Concerning **syringe 1 cell seeding method**, the looseness of the scaffold-syringe construct meant that most of the 1 ml cell suspension had already flown out from the syringe before the plunger was used. The effect of the pressure created by the plunger was anyhow clearly seen, as the remaining cell suspension splashed forcefully out from the syringe. At the same time, the appearance of the more loosely structured pre-wetted knit and nonwoven scaffolds turned paler and drier, due to the cell culturing media partly escaping the scaffold.

The larger cell suspension volume means that a large amount of cells are wasted with the excess cell suspension. The rationale behind it was to create fluid flow inside the pore network of the scaffolds and to avoid too high cell densities in the suspension, which might result in aggregates on top of the scaffold. In **syringe 2 method,** the idea was to actualize the fluid flow from both sides of the scaffold. With most of the scaffolds, the tightness of the construct was not sufficient. In practice, this meant that the seeding method turned out to be a semi-static seeding method: the scaffolds floated in cell suspension as the syringe constructs were handled according to the protocol.

Out of these 6 seeding methods, the **injection method** was probably the most dissatisfying in terms of repeatability. First of all, the injection depth needed to be estimated in every injection. Pushing the needle too far resulted in injecting most of the cell suspension directly to the bottom of the well. Another concern was dividing the cell suspension

evenly into the 5 injection spots. Not only estimating such small volumes was hard, but achieving the even division in practice required extreme precision. In addition, the method damages the scaffold structure slightly. In the case of Sc-COMP50 scaffolds, dark traces of metal particles were left to the injection sites, indicating that the needle is ground by the ceramic content.

7.4 Cell viability and 2D distribution analysis

Live/Dead staining was used as a qualitative method to assess the viability and distribution of the cells seeded into the scaffolds. Some caution must be kept in mind when interpreting the results, as there are a few concerns related to the method. Although the washing steps and staining were performed very carefully, it is possible that the dead cells might be washed away. The two-dimensional nature of the analysis is an even bigger limitation, leading easily to misinterpretations. It is also questionable whether the dyes diffuse into the center of the scaffold: there were some lightly colored cells to be seen with the microscope, but the staining was not strong enough to be shown in the final images. Moreover, one reason for the better-looking crosscuts of the PLCL scaffold is due the transparency of the polymeric material. Some viable cells can be seen in the PLCL scaffolds although the cells were a bit deeper in the material. The composite material lacks this feature and practically shows only the cells on the same plane.

The experiment series was started with seeding 60 000 cells per **Sc-PLCL** scaffold. The Live/Dead results for this experiment 1 showed only a moderate amount of cells on the scaffold crosscut images, which were used to evaluate the distribution of the cells. Still, as discussed it needs to be remembered that these images represent only a 2D vision. Both syringe 1 and syringe 2 methods along with centrifugation showed the best results in terms of obtaining the most cells on the plane of the crosscut. Perhaps even more importantly, these methods seemed to result in cells locating from the top to the bottom of the scaffold. On the other hand, the possibility that some of the cells have been transferred from the top surface via the scalpel needs to be taken into account. A low number of dead cells were seen in the scaffold seeded by centrifugation and some individual ones in other scaffolds.

With the aim of seeing more cells on the crosscuts, the amount of cells seeded was doubled after the first experiment. Contradictory, the Sc-PLCL Live/Dead experiment 2 revealed qualitatively evaluated even less cells on the crosscut images. Only the syringe 1 method seemed to perform better. In this experiment, the centrifuged scaffold has possibly flipped during its removal from the falcon tube, showing more cells on the bottom than on the top of the scaffold. The third experiment showed more cells, with all of the methods performing in a tolerable manner. In all of the experiments, static, squeezing and centrifugation methods resulted in aggregates being formed on the top surface of the scaf-

fold, denoting a better seeding efficiency and possibly the fact that most of the cells remain on the top surface after seeding. As expected, the injection method demonstrated very varying results.

All the 3 experiments performed with the **Sc-COMP50** scaffolds showed quite similar results with each other, with hardly any cells on the crosscut images. The static and centrifugation seeding methods as well as partly the squeezing method all lead to a smooth sheet of cells on top of the scaffold. On one side the smoothness of the sheet implies that the material is more desirable to the cells. On the other side, combined with the crosscut image results it suggests that these methods might be unable to seed the cells deeper into the scaffold. This is probably partly attributed to the smaller pores of the COMP50 scaffolds. The top surface images of the squeezing method together with the syringe methods showed clearly living cells inside the outermost pores, which is a good sign but does not justify any definite conclusions about their functionality. All in all, the syringe 1 method would be suggested based on the Live/Dead results, but no definitive conclusions should be made from these 2D pictures.

The viability of the cells on the $ScCO_2$ scaffolds was on a very good level with only few dead cells. This demonstrates the cytocompatibility of the material. The few dead cell aggregates found from the middle of some scaffolds probably result from poor turnover of nutrients and metabolic products. This could probably be improved with bioreactor culturing (Martin et al. 2004). Slow diffusion of culturing media would also support the assumption of imperfect penetration of the dyes into the center of the scaffold.

Owing to their loose structure, the **knitted PLDLA 96/4** scaffolds proved an extremely good seedability with any of the 6 cell seeding methods. The amount of dead cells was again low. Also in the center of the scaffold, only few dead cells were noticed, probably due to the accessibility of cell culturing media inside the scaffold caused by the loose structure. As a conclusion, all of the tested methods are suitable for seeding these scaffolds. Thus, the static method is recommended due to its simplicity and rapidity (Vitacolonna et al. 2013). Correspondingly, the squeezing method is not suggested because of the scaffold deformation and damage risk.

The **non-woven PLDLA 96/4** fabric scaffolds demonstrated also very good seedability. The top and bottom surfaces both had living cells attached regardless of the cell seeding method. Also the crosscut images proved that there are cells throughout the whole height of the scaffold. However, the non-woven scaffolds also showed a significantly higher number of dead cells than the other scaffold types. Even more lightly colored dead cells were seen at the fluorescence microscope, but not all could be displayed in the final Live/Dead images. Since the raw material and the cell line were the same than those used with the knitted scaffolds, the most probable reason lies in the structure of the scaffold. The PLDLA fiber diameter in the non-wovens was more than 5 times lower compared to the 4-filament fibers used to produce the knit. Most probably the small fiber diameter has

caused problems in the attachment of the relatively large hASCs, which is also supported by the spherical shape of the cells (Karageorgiou & Kaplan 2005). On the other hand, the closed scaffold structure makes it also more difficult for the dead cells to shed from the scaffold during the staining process, leading to their visibility in the images.

In addition to the actual analyses, the well plates were always light microscopy imaged at the time point of 3 days before performing the analyses. This was done to ensure that there were no bacterial contaminations and to evaluate the amount of cells growing out from the scaffolds. Those wells with scaffolds seeded using the centrifugation and squeezing methods contained black specks, which were interpreted to be dead cells. It was thus concluded that these methods are the most stressful ones for the cells. The effect was especially clear with the Sc-COMP50 scaffolds (Appendix 1). Previously, a small decrease in cell viability as a result of increased cycles of squeeze-loading has been reported (Xie et al. 2006). Also the individual dead cells in the Live/Dead images favor this theory.

7.5 Cell number analysis

The cell number analysis was done quantitatively. The utilized CyQUANT analysis however does not take any stance on the distribution of the cells, which is a very important measure when evaluating the success of cell seeding. Another concern is whether all the DNA from inside the scaffold can be included into the analysis. Accordingly, using CyQUANT only is not a sufficient measure for evaluating cell seeding. It provides anyhow useful, quantified and accurate information about the cell number in different samples. The amounts of DNA presented in this work result not only from initial cell attachment, but also from 3 days of cell proliferation, which should be noted (Vunjak-Novakovic et al. 1998).

The CyQUANT analysis performed on dense 3D scaffolds is assumed to favor cell seeding methods that seed the cells on top of the scaffold. Firstly, the cells on the top surface have a better access to the nutrients in the cell culturing medium compared to those deeper in the scaffold. Thus, the cells on the scaffold periphery can be expected to proliferate faster (Bueno et al. 2007). Secondly, the question about getting all the DNA material deep from the scaffold is valid, despite the fact that the detergent solution is pipetted quite forcefully from both sides of the scaffolds when collecting the sample. If there are problems getting the cell suspension into the pores, it should also be challenging to pipette the detergent solution into the pores (and getting it out from there). This assumption is supported by the observations of lightly colored cells in the Live/Dead analysis: the dyes probably did not diffuse into some scaffold types in adequate amounts.

In all of the 3 CyQUANT experiments performed with the **Sc-PLCL** scaffolds, there were three seeding methods, namely static, squeezing and centrifugation methods that resulted in higher amount of cells compared to the other methods. The most important reason for

the success of static and squeezing methods in cell numbers is probably related to the amount of wasted cells. A cell suspension volume of 50 µl can be effectively seeded to the scaffold with a great number of cells being offered a realistic chance to attach to the scaffold. On the contrary, the cell suspension volume of 1000 µl in centrifugation and both syringe methods inevitably led to most of the cell suspension ending up as wasted material. In this respect, the great cell numbers in centrifugally seeded scaffolds might seem odd at first. Conversely, the centrifugal forces undoubtedly separate the cells from the medium by pressing them down. Intuitively it thus makes sense that a lot of cells end up in contact with the scaffold. Previous experiments have also shown increased cell attachment when applying centrifugation (Roh et al. 2007) In the case of the syringe seeding methods, not even the bigger scaffold volume and surface area facilitated adequate cell numbers.

The Live/Dead images showed repeatedly, that the top three methods (static, squeezing, centrifugation) result in a large number of cells on the top surface of the scaffold. This is one factor supporting their success in CyQUANT analysis. The injection method showed relatively versatile results throughout the experiments. This is undoubtedly related to the challenges in repeatability of the method. The relatively low volume of 110 µl ensures that at least a moderate amount of cells can always be brought in good contact with the scaffold. On the other hand, some of the cells were always lost into the syringe and when part of the injected cell suspension spilled out from the scaffold. When pressing the needle too deep, most of the suspension had the chance to flow directly to the bottom of the well. As the scaffolds were always transferred to clean wells after seeding (and after 3 days before collecting the CyQUANT samples), this has an impact on the cell number.

The same static, squeezing and centrifugation methods generated the best results also in Sc-COMP50 scaffolds. In addition, the injection method stood up to the same group in two out of three experiments, but again showed variant results due to the low repeatability of the method. The seemingly varying results of the squeezing method can be explained by the challenging handling of the scaffold inside the squeezing pouch: in some cases more cells are simply lost to the slippery pouch as the scaffold often twirls inside the pouch. The scaffold top surfaces in the Live/Dead images support these results, as static and centrifugation seeding lead to a smooth sheet of cells. In COMP50 experiments 1 and 2, the squeezing method lacks the sheet, which might indicate more lost cells or a more even cell distribution with cells ending up deeper into the scaffold.

When comparing any of the experiments performed with COMP50 scaffolds to the PLCL experiment 3 (PLCL experiments 1 and 2 were differently executed), the absolute cell amounts of the static and centrifugation methods are generally higher in the COMP50 scaffolds. Not only the Live/Dead images from the top of the scaffold show the cell sheet, but also the crosscut images imply that these methods seed most of the cells to the top in COMP50 scaffolds. In addition, bioactive TCP granules are better exposed when the scaf-

folds are cut into shape, which might accelerate cell proliferation and slow down the migration of the cells deeper into the scaffold. These cell number and 2D distribution results together address the better material properties but harder seedability of COMP50 scaffolds compared to the PLCL scaffolds.

The syringe methods show practically negligible cell amounts. The presumably smaller pores of the COMP50 scaffold could lead to increased flow resistance in the scaffold, and thus result in most of the cell suspension slipping past the scaffold. Also the probability of DNA remaining in the scaffold instead of being included into the Triton samples rises as the scaffold porosity decreases. Since its effect on the results was seen with the PLCL scaffolds, cutting the COMP50 scaffolds into 4 pieces when collecting the samples could provide useful data about the supposed cell distribution as well. Comparing the results between the two $ScCO_2$ processed scaffold types could reveal differences between the amounts of cells inside the two scaffold types.

The cell numbers of knitted and non-woven scaffolds were quite similar with each other. On the other hand the looser structure of the scaffolds enabled a more reliable analysis by making it possible to collect most of the cells into the samples. Then again, it also allows some of the cells to flow through the scaffold to the well plate bottom. This is seen especially in the case of knitted scaffolds seeded with static and squeezing methods: the well plate images show dense cell clusters curled on top of each other on the wells. The flow through the scaffold is probably also the reason why the absolute cell amount on knitted PLDLA scaffolds was not superior compared to the non-woven scaffolds, despite the larger number of cells seeded. The syringe methods again lead to a low number of cells due to many cells being flushed away with the excessive cell suspension. Also the centrifugation method led to a similar outcome with these scaffold types, because the scaffolds did not tightly fit the falcon tube. Thus, compared with the $ScCO_2$ processed scaffolds, a bigger portion of the centrifuged cells ended up to the bottom of the tube.

7.6   USPIO-labelled cells and the 3D distribution

Although still a great indicator for 3D cell distribution inside scaffolds, the novel method of detecting cells inside a scaffold using USPIO-labeled adipose-derived stem cells and micro-CT imaging technology has some concerns that need to be considered when interpreting the results. First of all, not all cells take USPIO particles inside, and as the cells proliferate, the concentration of these cells increases. At the same time, proliferation of the successfully labeled cells dilutes the USPIO nanoparticle concentration inside these cells as mentioned before. This is insignificant up to a certain threshold level, where the cells contain enough iron oxide nanoparticles to be visible within the given resolution. The resolution of the micro-CT sets also other limitations: single nanoparticles cannot be detected, and on the other hand it is impossible to say how many cells are located on each spot with a visible signal. Similar challenges have been reported when imaging bony

fragments with sizes close to the resolution. (Petrie Aronin et al. 2009; Küstermann et al. 2008)

The method is also applicable only with scaffold materials that are not too dense (Ho & Hutmacher 2006) to disturb the signal of the USPIO nanoparticles. In the preliminary tests where individual COMP50 scaffolds were imaged, it was soon noticed that the signal intensity of the TCP granules was much stronger than that of the USPIO particles. Because of this, the COMP50 scaffolds needed to be excluded from the micro-CT experiments. Since the Live/Dead staining provides only results of the 2D distribution with controversies as described earlier, an imaging method for evaluating the 3D cell distribution would be necessary. Meanwhile, iron-labeled microspheres can be used to give practical support to the micro-CT scaffold analysis, which gives accurate quantitative information about the scaffold porosity. It is also hypothesized, that when the structure of the Sc-COMP50 scaffolds can be brought to the same level with the Sc-PLCL scaffolds, also the cell seeding results should be comparable.

As explained in the results section, all the seeding methods besides the injection methods showed, to some extent, evenly distributed cells in the Sc-PLCL scaffold micro-CT images. Still, the syringe methods had the best performance in this regard. Out of the 3 experiments performed, the USPIO labeling was done a bit differently in the first one. As the amount of USPIO particles was based on the original amount of cells seeded to the cell culturing flask and the particular cell line was extremely proliferative, the concentration of well labeled cells in the scaffolds was lower than in the other experiments, which shows in the Prussian blue staining (Roeder et al. 2014). This explains the relatively low intensities and seemingly low amount of signals from inside the scaffolds.

The experiment 1 is still in line with the experiment 3, as the syringe methods showed the biggest amount of nanoparticle-based signals, but also centrifugation, squeezing and static methods had even cell distributions. In the experiment 3, syringe 1 method stood out from the rest. The cell line used in the third experiment was also fast proliferating. The experiment 2 was a bit different showing a very good result in most of the scaffolds. Prussian blue of the second experiment proved that the labeling was successful, which probably was one reason for the better-looking results compared to the other experiments. Again, the cell line could be a reason to this, as it proliferated slower than those used in the other experiments.

It needs to be remembered that all the analyses are done at an early time point of 3 days. Depending on the end application, it should be evaluated whether the easiest static seeding method provides starting conditions good enough for the development of functional tissue. In any case, the cell distribution inside the Sc-PLCL scaffolds can be improved by forcing the cell suspension to flow deeper into the scaffold by applying a syringe. Out of the two syringe methods, the simpler one where the syringe plunger is pushed only once is recommended due to its easier and faster use and slightly better results.

In addition to the micro-CT results, also the Live/Dead images show even distribution of the cells when using the syringe 1 seeding method. The cell numbers using this method, as obtained by the CyQUANT analysis, show poor results. It would be interesting to see if the cell numbers and perhaps also the 3D distribution as well could be improved by reducing the cell suspension volume - that is, by combining the static and syringe 1 methods. Even though most of the 1000 µl cell suspension goes to waste in the syringe methods, it is also possible that the small cell suspension volumes such as 50 µl simply lead to aggregates on top of the pores (Ding et al. 2008). Even if that was the case, it is possible that the pressure created in the syringe 1 method could break the aggregates. Decreasing cell suspension volume could lead to even better results, less wasted valuable cells and improved user-friendliness.

The micro-CT results of the knitted PLDLA scaffolds were unexpected: hardly any USPIO-based signals were seen in the images. This contradicts the Live/Dead results notably, as in the Live/Dead analysis all the scaffolds proved to have a respectable amount of viable cells inside of them. When looking at the Prussian blue staining images, it can be seen that the cells look unusual compared to the others. The USPIO-labeling itself seems to be successful, as there is blue colored iron inside the cells and the micro-CT images of the non-woven scaffolds show clear signals from inside some scaffolds. Still, the fixed cells in the Prussian blue images seem to be struggling - for one reason or another they have probably detached from the scaffolds.

Cells from the same batch were used with both of the PLDLA scaffold types. The same cell line was successfully used with the $ScCO_2$ processed scaffolds. As the USPIO labeling of the cells was performed with one exception compared to the Sc-PLCL experiments 2 and 3, this exception could also be the reason for the unexpected Prussian blue images. A non-sterile coverslip was used, after it was sterilized using 70% ethanol in the laminar hood. It is thus possible, that some ethanol residues have been left to the coverslip despite letting it dry before usage. This might have caused the changes in cell morphology. No contaminations or any other unusual occurrences were seen with light microscopy when visualizing the samples.

8. CONCLUSIONS

The aim of this work was to find an optimized cell seeding method for different biodegradable polymer-based scaffolds using adipose-derived stem cells. In addition to the two $ScCO_2$ processed scaffold types manufactured with supercritical carbon dioxide technology from poly(L-lactide-co-ε-caprolactone) and its β-tricalcium phosphate composite, two other types, namely knitted and non-woven scaffolds made from polylactide fibers were experimented.

With the aid of iron-labeled microspheres and micro-computed tomography imaging, the interconnectivity of the copolymeric Sc-PLCL scaffolds was first shown. The method was concluded to be a great tool for analyzing the seedability of $ScCO_2$ processed scaffolds. The study also revealed that the cell distribution inside the PLCL scaffolds can be improved by forcing the cell suspension deeper into the pores using a simple syringe method. However, a large number of cells are wasted if this method is applied as such. The 3D distribution of the cells inside the scaffold was evaluated using a novel method where ASCs labeled with iron oxide nanoparticles were detected by micro-CT.

The ceramic content of the composite scaffolds hindered micro-CT imaging in such an extent that determining the USPIO-labeled cells in the scaffolds was not feasible. The results related to cell number and viability as well as non-sterile microsphere seeding showed indications of possibly lower pore size or interconnectivity and thus harder seedability compared to the Sc-PLCL scaffolds. Still, without a functional 3D imaging method no definitive conclusions should be made. Due to their loose structure, both non-woven and knitted polylactide scaffolds proved to be very seedable even with the standard static seeding method. The non-woven PLDLA scaffolds showed a relatively high number of non-viable cells, which raised a question about a too small fiber diameter.

The study suggests a simple method using a syringe to seed cells more evenly into $ScCO_2$ processed scaffolds. With certain scaffold materials, a 3D imaging method applying USPIO-labeled cells and micro-CT can be used for cell distribution evaluation. Although the Sc-COMP50 scaffolds require a 3D imaging method to estimate cell distribution in the scaffolds, it seems that their pore sizes are smaller than those of the PLCL scaffolds. The knitted joint scaffolds admittedly have a functional structure in terms of cell seeding, but further studies are needed to optimize and evaluate the structure of the non-woven scaffolds.

REFERENCES

Adebiyi, A.A., Taslim, M.E. & Crawford, K.D. (2011). The use of computational fluid dynamic models for the optimization of cell seeding processes, Biomaterials. Vol.32, pp.8753-8770.

Ahola, N., Veiranto, M., Rich, J., Efimov, A., Hannula, M., Seppälä, J. & Kellomäki, M. (2012). Hydrolytics degradation of composites of poly(L-lactide-co-ε-caprolactone) 70/30 and β-tricalcium phosphate, Journal of Biomaterials Applications, Vol.28(4), pp.529-543.

Aksu, A.E., Rubin, J.P., Dudas, J.R. & Marra. K.G. (2008). Role of gender and anatomical region on induction of osteogenic differentiation of human adipose-derived stem cells, Annals of Plastic Surgery, Vol.60(3), pp.306-322.

Albrektsson, T. & Johansson, C. (2001). Osteoindution, osteoconduction and osseointegration, European Spine Journal, Vol.10, pp.96-101.

Andersen, T., Markussen, C., Domish, M., Heier-Baardson, H., Melvik, J.E., Alsberg, E. & Christensen, B.E. (2013). In Situ Gelation for Cell Immobilization and Culture in Alginate Foam Scaffolds, Tissue Engineering: Part A, Vol.20(3-4), pp.600-610.

Appel, A.A., Anastasio, M.A., Larson, J.C. & Brey, E.M. (2013). Imaging challenges in biomaterials and tissue engineering, Biomaterials, Vol.34, pp.6615-6630.

Ashammakhi, N., Peltoniemi, H., Waris, E., Suuronen, R., Serlo, W., Kellomäki, M., Törmälä, P. & Waris, T. (2001). Developments in Craniomaxillofacial Surgery: Use of Self-Reinforced Bioabsorbable Osteofixation Devices, Plastic and Reconstructive Surgery, Vol 108 (167), pp.167-180.

Aunoble, S., Clément, D., Fraysinet, P., Harmand, M.F. & Le Huec, J.C. (2006). Biological performance of a new β-TCP/PLLA composite material for applications in spine surgery: In vitro and in vivo studies, Journal of Biomedical Materials Research Part A, Vol.78(2), pp.416-422.

Baer, P.C. & Geiger, H. (2012). Adipose-Derived Mesenchymal Stromal/Stem Cells: Tissue Localization, Characterization, and Heterogeneity, Stem Cells International, Vol.2012, pp.1-11.

Barba, M., Cicione, C., Bernardini, C., Michetti, F. & Lattanzi, W. (2013). Adipose-Derived Mesenchymal Cells for Bone Regeneration: State of the Art, BioMed Research International, Vol.2013, pp.1-11.

Barry, J.J.A., Silva, M.M.C.G., Popov, V.K., Shakesheff, K.M. & Howdle, S.M. (2006). Supercritical carbon dioxide: putting the fizz into biomaterials, Philosophical Transactions of the Royal Society A, Vol.364, pp.249-261.

Bhamidipati, M., Scurto, A.M. & Detamore, M.S. (2013). The Future of Carbon Dioxide for Polymer Processing in Tissue Engineering, Tissue Engineering: Part B, Vol.19(3), pp.221-232.

Bose, S., Roy, M. & Bandyopadhyay, A. (2012). Recent advances in bone tissue engineering scaffolds. Trends in Biotechnology, Vol.30(10), pp.546-554.

Bourin, P., Bunnell, B.A., Casteilla, L., Dominici, M., Katz, A.J., March, K.L., Redl, H., Rubin, J.P., Yoshimura, K. & Gimble, J.M. (2013). Stromal cells from the adipose tissue-derived stromal vascular fraction and culture expanded adipose tissue –derived stromal/stem cells: a joint statement of the International Federation for Adipose Therapeutics (IFATS) and Science and the International Society for Cellular Therapy (ISCT), Cytotherapy, Vol.15(6), pp.641–648.

Bryant, S.J. & Anseth, K.S. (2001). The effects of scaffold thickness on tissue engineered cartilage in photocrosslinked poly(ethylene oxide) hydrogels, Biomaterials, Vol.22(6), pp.619-626.

Bueno, E.M., Laevsky, G. & Barabino, G.A. (2007). Enhancing cell seeding of scaffolds in tissue engineering through manipulation of hydrodynamic parameters, Journal of Biotechnology, Vol.129, pp.516-531.

Buizer, A.T., Veldhuizen, A.G., Bulstra, S.J. & Kuijer, R. (2013). Static versus vacuum cell seeding on high and low porosity ceramic scaffolds, Journal of Biomaterials Applications. Vol.29(1), pp.3-13.

Bunnell, B.A., Flaat, M., Cagliardi, C., Patel, B. & Ripoll, C. (2008). Adipose-derived stem cells: Isolation, expansion and differentiation, Methods, Vol.45(2), pp.115–120.

Burg, K.J.L., Holder Jr, W.D., Culberson, C.R., Beiler, R.J., Greene, K.G., Loebsack, A.B., Roland, W.D., Eiselt, P., Mooney, D.J. & Halberstadt, C.R. (2000). Comparative study of seeding methods for three-dimensional polymeric scaffolds, Journal of Biomedical Materials Research. Vol.51, pp.642-649.

Chapekar, M.S. (2000). Tissue Engineering: Challenges and Opportunities, Journal of Biomedical Materials Research (Applied Biomaterials), Vol.53: pp.617-620.

Choumerianou, D.M., Dimitrou, H. & Kalmanti, M. (2008). Stem Cells: Promises Versus Limitations, Tissue Engineering: Part B, Vol.14(1), pp.53–60.

Costa-Pinto, A.R., Reis, R.L. & Neves, N.M. (2011). Scaffolds Based Bone Tissue Engineering: The Role of Chitosan, Tissue Engineering: Part B, Vol.17(5), pp.331-347.

Coutu, D.L., Yousefi, A.-M. & Galipeau, J. (2009). Three-Dimensional Porous Scaffolds at the Crossroads of Tissue Engineering and Cell-Based Gene Therapy, Journal of Cellular Biochemistry, Vol.108, pp.537-546.

Dai, W., Dong, J., Chen, G. & Uemura, T. (2009). Application of low-pressure cell seeding system in tissue engineering, BioScience Trends. Vol.3(6), pp.216-219.

Dardik, A., Chen, L., Frattini, J., Asada, H., Aziz, F., Kudo, F.A. & Sumpio, B.E. (2005). Differential effects of orbital and laminar shear stress on endothelial cells, Journal of Vascular Surgery. Vol.41(5), pp.869-880.

Darling, A.L. & Sun, W. (2004). 3D microtomographic characterization of precision extruded poly-epsilon-caprolactone scaffolds, Journal of biomedical materials research: Part B, Applied biomaterials, Vol.70(2), pp.311-317.

Davies, O.R., Lewis, A.L., Whitaker, M.J., Tai, H., Shakesheff, K.M. & Howdle, S.M. (2008). Applications of supercritical CO_2 in the fabrication of polymer systems for drug delivery and tissue engineering, Advanced Drug Delivery Reviews, Vol.60, pp.373-387.

Ding, C.-M., Zhou, Y., He, Y.-N. & Tan, W.-S. (2008). Perfusion seeding of collagen-chitosan sponges for dermal tissue engineering, Process Biochemistry. Vol.43, pp.287-296.

Dominici, M., Le Blanc, K., Mueller, I., Slaper-Cortenbach, I., Marini, F.C., Krause, D.S., Deans, R.J., Keating, A., Prockop, D.J. & Horwitz, E.M. (2006). Minimal criteria for defining multipotent mesenchymal stromal cells. The International Society for Cellular Therapy position statement, Cytotherapy, Vol.8(4), pp.315–317.

Dong, J., Uemura, T., Kojima, H., Kikuchi, M., Tanaka, J. & Tateishi, T. (2001). Application of low-pressure system to sustain in vivo bone formation in osteoblast / porous hydroxyapatite composite, Materials Science Engineering C. Vol.17, pp.37-43.

Dutta, D. (2013). Signaling pathways dictating pluripotency in embryonic stem cells, International Journal of Developmental Biology, Vol.57(9-10), pp.667–675.

Ellä, V., Annala, T., Länsman, S., Nurminen, M. & Kellomäki, M. (2011). Knitted polylactide 96/4 L/D structures and scaffolds for tissue engineering: Shelf life, in vitro and in vivo studies, Biomatter, Vol.1(1), pp.102-113.

Ellä, V., Gomes, M.E., Reis, R.L., Törmälä, P. & Kellomäki, M. (2007). Studies of P(L/D)LA 96/4 non-woven scaffolds and fibres; properties, wettability and cell spreading before and after intrusive treatment methods, Journal of Materials Science: Materials in Medicine, Vol.18, pp.1253-1261.

Faulkner, S.D., Vawda, R. & Fehlings, M.G. (2014). Adult-Derived Pluripotent Stem Cells, World Neurosurgery, Vol. 82(3-4), pp.500–508.

Fernández Vallone, V.B., Romaniuk, M.A., Choi, H., Labovsky, V., Otaegui, J. & Chasseing, N.A. (2013). Mesenchymal stem cells and their use in therapy: What has been achieved? ; Differentiation, Vol.85(1-2), pp.1-10.

Fernandez-Yague, M.A., Abbah, S.A., McNamara, L., Zeugolis, D.I., Pandit, A. & Biggs, M.J. (2014). Biomimetic approaches in bone tissue engineering: Integrating biological and physicomechanical strategies, Advanced Drug Delivery Reviews, accepted for publication.

Fiorentini, E., Granchi, D., Leonardi, E., Baldini, N. & Ciapetti, G. (2011). Effects of osteogenic differentiation inducers on in vitro expanded adult mesenchymal stromal cells, The International Journal of Artificial Organs, Vol.34(10), pp.998-1011.

Floren, M., Spilimbergo, S., Motta, A. & Migliaresi, C. (2011). Porous poly(D,L-lactic acid) foams with tunable structure and mechanical anisotropy prepared by supercritical carbon dioxide, Journal of Biomedical Materials Research Part B: Applied Biomaterials, Vol.99B, pp.338-349.

Fonseca, A.C., Gil, M.H. & Simões, P.N. (2014). Biodegradable poly(ester amide)s - A remarkable opportunity for the biomedical area: Review on the synthesis, characterization and application, Progress in Polymer Science, Vol.39(7), pp.1291-1311.

Fortier, L.A. (2005). Stem Cells: Classifications, Controversies, and Clinical Applications, Veterinary Surgery, Vol.34(5), pp.415–423.

Ghavidel Mehr, N., Li, X., Ariganello, M.B., Hoemann, C.D. & Favis, B.D. (2014). Poly(ε-caprolactone) scaffolds of highly controlled porosity and interconnectivity derived from co-continuous polymer blends: model bead and cell infiltration behavior, Journal of Materials Science: Materials in Medicine, vol.25(9), pp.2083–2093.

Godbey, W.T., Stacey Hindy, B.S., Sherman, M.E. & Atala, A. (2004). A novel use of centrifugal force for cell seeding into porous scaffolds, Biomaterials. Vol.25, pp.2799-2805.

Gordon, M.Y., Levičar, N., Pai, M., Bachellier, P., Dimarakis, I., Al-Allaf, F., M'Hamdi, H., Thalji, T., Welsh, J.P., Marley, S.B., Davies, J., Dazzi, F., Marelli-Berg, F., Tait, P., Playford, R., Jiao, L., Jensen, S., Nicholls, J.P., Ayav, A., Nohandani, M., Farzaneh, F.,

Gaken, J., Dodge, R., Alison, M., Apperley, J.F., Lechler, R. & Habib, N.A. (2006). Characterization and Clinical Application of Human CD34$^+$ Stem/Progenitor Cell Populations Mobilized into the Blood by Granulocyte Colony-Stimulating Factor, Stem Cells, Vol.24, pp.1822-1830.

Grayson, W.L., Bhumiratana, S., Cannizzaro, C., Chao, G., Lennon, D.P., Caplan, A.I. & Vunjak-Novakovic, G. (2008). Effects of Initial Seeding Density and Fluid Perfusion Rate on Formation of Tissue-Engineered Bone, Tissue Engineering: Part A. Vol.14(11), pp.1809-1820.

Hasegawa, T., Miwa, M., Sakai, Y., Niikura, T., Lee, S.Y., Oe, K., Iwakura, T., Kurosaka, M., Komori, T. (2010). Efficient cell-seeding into scaffolds improves bone formation, Journal of dental research, Vol.89(8), pp.854–859.

Ho, S.T. & Hutmacher, D.W. (2006). A comparison of micro CT with other techniques used in the characterization of scaffolds, Biomaterials, Vol.27, pp.1362-1376.

Holy, C.E., Shoichet, M.S. & Davies, J.E. (2000). Engineering three-dimensional bone tissue in vitro using biodegradable scaffolds: Investigating initial cell-seeding density and culture period, Journal of Biomedical Materials Research, Vol.51, pp.376-382.

Hong, M.-H., Kim, S.-M., Om, J.-Y., Kwon, N. & Lee, Y.-K. (2014). Seeding Cells on Calcium Phosphate Scaffolds Using Hydrogel Enhanced Osteoblast Proliferation and Differentiation, Annals of Biomedical Engineering, Vol.42(7), pp.1424-1435.

Honkanen, P.B., Tiihonen, R., Skyttä, E.T., Ikävalko, M., Lehto, M.U.K. & Konttinen, Y.T. (2010). Bioreconstructive poly-L/D-lactide implant compared with Swanson prosthesis in metacarpophalangeal joint arthroplasty in rheumatoid patients: a randomized clinical trial, Journal of Hand Surgery (European Volume), Vol.35(9), pp.746-753.

Howard, D., Buttery, L.D., Shakesheff, K.M. & Roberts, S.J. (2008). Tissue engineering: strategies, stem cells and scaffolds, Journal of Anatomy, Vol.213, pp.66-72.

Huttunen, M. (2013). Analysis of the factors affecting the inherent viscosity of oriented polylactides during hydrolytic degradation, Journal of Materials Science: Materials in Medicine, Vol. 24(5), pp.1131–1144.

Huttunen, M. & Kellomäki, M. (2013). Strength retention behavior of oriented PLLA, 96L/4D PLA, and 80L/20D,L PLA, Biomatter, Vol.3(4), pp.1-10.

Ikada, Y. (2006). Challenges in tissue engineering, Journal of the Royal Society Interface, Vol.3, pp.589-601.

Invitrogen Molecular Probes (2005). LIVE/DEAD Viability/Cytotoxicity Kit for mammalian cells, Product Information, Catalog number: MP 03224, pp.1-7. Available: https://tools.lifetechnologies.com/content/sfs/manuals/mp03224.pdf

Jang, J.H., Castano, O. & Kim, H.W. (2009). Electrospun materials as potential platforms for bone tissue engineering, Advanced Drug Delivery Reviews, Vol.61(12), pp.1065–1083.

Ji, C., Khademhosseini, A. & Dehghani, F. (2011). Enhancing cell penetration and proliferation in chitosan hydrogels for tissue engineering applications, Biomaterials. Vol.32, pp.9719-9729.

Jones, J.R., Poologasundarampillai, G., Atwood, R.C., Bernard, D. & Lee, P.D. (2007). Non-destructive quantitative 3D analysis for the optimisation of tissue scaffolds, Biomaterials, Vol.28, pp.1404-1413.

Jung, Y., Park, M.S., Lee, J.W., Kim, Y.H., Kim, S.-H. & Kim, S.H. (2008). Cartilage regeneration with highly-elastic three dimensional scaffolds prepared from biodegradable poly(L-lactide-co-ε-caprolactone), Biomaterials, Vol.29, pp.4630-4636.

Kang, K.S., Hong, J.M., Kang, J.A., Rhie, J.-W., Jeong, Y.H. & Cho, D.-W. (2013). Regulation of osteogenic differentiation of human adipose-derived stem cells by controlling electromagnetic field conditions, Experimental & Molecular Medicine, Vol.45, pp.1-9.

Karageorgiou, V. & Kaplan, D. (2005). Porosity of 3D biomaterial scaffolds and osteogenesis, Biomaterials, Vol.26, pp.5474-5491.

Kellomäki, M., Laine, K., Ellä, V. & Annala, T. (2015). Bioabsorbable fabrics for musculoskeletal scaffolds. In: Blair, T., Biomedical Textiles for Orthopaedic and Surgical Applications: Fundamentals, Applications and Tissue Engineering. Elsevier. Pp.67-85.

Kinner, B. & Spector, M. (2002). Mesenchymal Cell Culture: Cartilage. In: Atala, A., Lanza, R.P., Methods of Tissue Engineering. Gulf Professional Publishing. P.325.

Kokai, L.E., Marra, K. & Rubin, J.P. (2014). Adipose stem cells: biology and clinical applications for tissue repair and regeneration, Translational Research, Vol.163(4), pp.399–408.

Kolk, A., Handschel, J., Drescher, W., Rothamel, D., Kloss, F., Blessmann, M., Heiland, M., Wolff, K.-D. & Smeets, R. (2012). Current trends and future perspectives of bone substitute materials - From space holders to innovative biomaterials, Journal of Cranio-Maxillo-Facial Surgery, Vol.40, pp.706-718.

Kricheldorf, H.R. (2001). Syntheses and application of polylactides, Chemosphere, Vol.43(1), pp.49-54.

Kyllönen, L., Haimi, S., Mannerström, B., Huhtala, H., Rajala, K.M., Skottman, H., Sándor, G.K. & Miettinen, S. (2013). Effects of different serum conditions on osteogenic differentiation of human adipose stem cells in vitro, Stem Cell Research & Therapy, Vol.4(1):17.

Küstermann, E., Himmelreich, U., Kandal, K., Geelen, T., Ketkar, A., Wiedermann, D., Strecker, C., Esser, J., Arnhold, S. & Hoehn, M. (2008). Efficient stem cell labeling for MRI studies, Contrast media & molecular imaging, Vol.3(1), pp.27-37.

Lam, T., Linnes, M. Giachelli, C. & Ratner, B.D. (2007). Mechanical Testing and Optimizing Cell Seeding on Porous Fibrin Scaffolds, Journal of Undergraduate Research in Bioengineering. Vol7(1), pp.22-28.

Larrañaga, A., Diamanti, E., Rubio, E., Palomares, T., Alonso-Varona, A., Aldazabal, P., Martin, F.J. & Sarasua, J.R. (2014). A study of the mechanical properties and cytocompatibility of lactide and caprolactone based scaffolds filled with inorganic bioactive particles, Materials Science and Engineering C, Vol.42, pp.451-460.

Lasprilla, A.J.R., Martinez, G.A.R., Lunelli, B.H., Jardini, A.L., Filho, R.M. (2012). Poly-lactic acid synthesis for application in biomedical devices - A review, Biotechnology Advances, Vol.30(1), pp.321-328.

Lendeckel, S., Jödicke, A., Christophis, P., Heidinger, K., Wolff, J., Fraser, J.K., Hendrick, M.H., Berthold, L. & Howaldt, H.-P. (2004). Autologous stem cells (adipose) and fibrin glue used to treat widespread traumatic calvarial defects: case report, Journal of Cranio-Maxillofacial Surgery, Vol.32(6), pp.370–373.

Li, H., Friend, J.R. & Yeo, L.Y. (2007). A scaffold cell seeding method driven by surface acoustic waves, Biomaterials. Vol.28, pp.4098-4104.

Liao, H.-T. & Chen, C.-T. (2014). Osteogenic potential: Comparison between bone marrow and adipose-derived mesenchymal stem cells, World Journal of Stem Cells, Vol.6(3), pp.299–295.

Locke, M., Feisst, V. & Dunbar, P.R. (2011). Concise Review: Human Adipose-Derived Stem Cells: Separating Promise from Clinical Need, Stem Cells, Vol.29(3), pp.404–411.

Loh, Q.L. & Choon, C. (2013). Three-Dimensional Scaffolds for Tissue Engineering Applications: Role of Porosity and Pore Size, Tissue Engineering: Part B, Vol.19(6), pp.485-502.

Martin, I., Wendt, D. & Heberer, M. (2004). The role of bioreactors in tissue engineering, Trends in Biotechnology, Vol.22(2), pp.80-86.

Martin, Y. & Vermette, P. (2005). Bioreactors for tissue mass culture: Design, characterization, and recent advances, Biomaterials, Vol.26, pp.7481-7503.

Mathiasen, A.B., Hansen, L., Friis, T., Thomsen, C., Bhakoo, K. & Kastrup, J. (2013). Optimal labeling dose, labeling time, and magnetic resonance imaging detection limits of ultrasmall superparamagnetic iron-oxide nanoparticle labeled mesenchymal stromal cells, Stem Cells International, pp.1-10.

Melchels, F.P.W., Barradas, A.M.C., van Blitterswijk, C.A., de Boer, J., Feijen, J. & Grijpma, D.W. (2010). Effects of the architecture of tissue engineering scaffolds on cell seeding and culturing, Acta Biomaterialia. Vol.6, pp.4208-4217.

Mesimäki, K., Lindroos, B., Törnwall, J. Mauno, J., Lindqvist, C., Kontio, R., Miettinen, S. & Suuronen, R. (2009). Novel maxillary reconstruction with ectopic bone formation by GMP adipose stem cells, International Journal of Oral and Maxillofacial Surgery, Vol.38(3), pp.201–209.

Metscher, B.D. & Müller, G.B. (2011). MicroCT for Molecular Imaging: Quantitative Visualization of Complete Three-Dimensional Distributions of Gene Products in Embryonic Limbs, Developmental Dynamics, Vol.240, pp.2301-2308.

Middleton, J.C. & Tipton, A.J. (2000). Synthetic biodegradable polymers as orthopedic devices, Biomaterials, Vol.21(23), pp.2335–2346.

Mitsak, A.G., Kemppainen, J.M., Harris, M.T. & Hollister, S.J. (2011). Effect of Polycaprolactone Scaffold Permeability on Bone Regeneration, Tissue Engineering: Part A, Vol.17(13-14), pp.1831-1839.

Monti, M., Perotti, C., Del Fante, C., Cervio, M. & Redi, C.A. (2012). Stem cells: sources and therapies, Biological Research, Vol.45(3), pp.207–214.

Morrison, S.J. & Kimble, J. (2006). Asymmetric and symmetric stem-cell divisions in development and cancer, Nature, Vol.441(7097), pp.1068–1074.

Murphy, M.B., Moncivais, K. & Caplan, A.I. (2013). Mesenchymal stem cells: environmentally responsive therapeutics for regenerative medicine, Experimental & Molecular Medicine, Vol.45, pp.1-16.

Murphy, C.M., O'Brien, F.J., Little, D.G. & Schindeler, A. (2013). Cell-scaffold interactions in the bone tissue engineering triad, European Cells and Materials, Vol.26, pp.120-132.

Nair, L.S. & Laurencin, C.T. (2007). Biodegradable polymers as biomaterials, Progress in Polymer Science, Vol.32, pp.762-798.

Nguyen, L.H., Annabi, N., Nikkhah, M., Bae, H., Binan, L., Park, S., Kang, Y., Yang, Y. & Khademhosseini, A. (2012). Vascularized Bone Tissue Engineering: Approaches for Potential Improvement, Tissue Engineering : Part B. Vol.18 (5), pp.363-382.

O'Brien, F. (2011). Biomaterials & scaffolds for tissue engineering, Materials Today, Vol.14(3), pp.88-95.

Ohyabu, Y., Adegawa, T., Yoshioka, T., Ikoma, T., Uemura, T. & Tanaka, J. (2010). Cartilage regeneration using a porous scaffold, a collagen sponge incorporating a hydroxyapatite/chondroitinsulfate composite, Materials Science and Engineering B, Vol.173, pp.204-207.

Oude Engberink, R.D., van der Pol, S.M.A., Döpp, E.A., de Vries, H.E. & Blezer, E.L.A. (2007). Comparison of SPIO and USPIO for in vitro labeling of human monocytes: MR detection and cell function, Radiology, Vol.243(2), pp.467–474.

Paakinaho, K., Ellä, V., Syrjälä, S. & Kellomäki, M. (2009). Melt spinning of poly(L/D)lactide 96/4: Effects of molecular weight and melt processing on hydrolytic degradation, Polymer Degradation and Stability, vol.94, pp.438-442.

Paakinaho, K., Heino, H., Väisänen, J., Törmälä, P. & Kellomäki, M. (2011). Effects of lactide monomer on the hydrolytic degradation of poly(lactide-co-glycolide) 85L/15G, Journal of the Mechanical Behavior of Biomedical Materials, Vol.4, pp.1283-1290.

Paakinaho, K. (2013). Processing Derived Control of Hydrolytic Degradation and Generation of Shape-Memory in Lactide Copolymers, dissertation, Tampere University of Technology. Available: http://dspace.cc.tut.fi/dpub/handle/123456789/21651

Park, S.J., Lee, B.-K., Na, M.H., Kim, D.S. (2013). Melt-spun shaped fibers with enhanced surface effects: Fiber fabrication, characterization and application to woven scaffolds, Acta Biomaterialia, Vol.9(8), pp.7719–7726.

Pelto, J., Björninen, M., Pälli, A., Talvitie, E., Hyttinen, J., Mannerström, B., Suuronen Seppänen, R., Kellomäki, M., Miettinen, S. & Haimi, S. (2013). Novel Polypyrrole-Coated Polylactide Scaffolds Enhance Adipose Stem Cell Proliferation and Early Osteogenic Differentiation, Tissue Engineering: Part A, Vol.19(7), pp.882-892.

Petrie Aronin, C.E., Sadik, W.E., Lay, A.L., Rion, D.B., Tholpady, S.S., Ogle, R.C. & Botchwey, E.A. (2009). Comparative effects of scaffold pore size, pore volume, and total void volume on cranial bone healing patterns using microsphere-based scaffolds. Journal of biomedical materials research. Part A, Vol.89(3), pp.632–41.

Pina, S., Oliveira, J.M. & Reis, R.L. (2015). Natural-Based Nanocomposites for Bone Tissue Engineering and Regenerative Medicine: A Review, Advanced Materials, Vol.27, pp.1143-1169.

Puppi, D., Chiellini, F., Piras, A.M. & Chiellini, E. (2010). Polymeric materials for bone and cartilage repair, Progress in Polymer Science, Vol.35, pp.403-440.

Qin, Y., Guan, J. & Zhang, C. (2014). Mesenchymal stem cells: mechanisms and role in bone regeneration, Postgraduate Medical Journal, Vol.90(1069), pp.643–647.

Quirk, R.A., France, R.M., Shakesheff, K.M. & Howdle, S.M. (2004). Supercritical fluid technologies and tissue engineering scaffolds, Current Opinion in Solid State and Materials Science, Vol.8(3-4), pp.313-321.

Reznikov, N., Shahar, R. & Weiner, S., 2014. Bone hierarchical structure in three dimensions, Acta Biomaterialia, Vol.10(9), pp.3815–3826.

Roeder, E., Henrionnet, C., Goebel, J.C., Gambier, N., Beuf, O., Grenier, D., Chen, B., Vuissoz, P.-A., Gillet, P. & Pinzano, A. (2014). Dose-response of superparamagnetic iron oxide labeling on mesenchymal stem cells chondrogenic differentiation: A multi-scale in vitro study, Plos One, Vol.9(5), pp.1-10.

Roh, J.D., Nelson, G.N., Udelsman, B.V., Brennan, M.P., Lockhart, B., Fong, P.M., Lopez-Soler, R.I., Saltzman, W.M. & Breuer, C.K. (2007). Centrifugal Seeding Increases Seeding Efficiency and Cellular Distribution of Bone Marrow Stromal Cells in Porous Biodegradable Scaffolds, Tissue Engineering. Vol.13(11), pp.2743-2749.

Rokkanen, P.U., Böstman, O., Hirvensalo, E., Mäkelä, E.A., Partio, E.K., Pätiälä, H., Vainionpää, S., Vihtonen, K. & Törmälä, P. (2000). Bioabsorbable fixation in orthopaedic surgery and traumatology, Biomaterials, Vol.21, pp.2607-2613.

Romagnoli, C. & Brandi, M.L. (2014). Adipose mesenchymal stem cells in the field of bone tissue engineering, World Journal of Stem Cells, Vol.6(2), pp.144–152.

Romagnoli, C., D'Asta, F. & Brandi, M.L. (2013). Drug delivery using composite scaffolds in the context of bone tissue engineering, Clinical Cases in Mineral and Bone Metabolism, Vol.10(3), pp.155-161.

Russo, V., Yu, C., Belliveau, P., Hamilton, A. & Flynn, L.E. (2014). Comparison of Human Adipose-Derived Stem Cells Isolated from Subcutaneous, Omental, and Intrathoracic Adipose Tissue Depots for Regenerative Applications, Stem Cells Translational Medicine, Vol.3(1), pp.1-12.

Salazar, G.T. & Ohneda, O. (2012). Review of biophysical factors affecting osteogenic differentiation of human adult adipose-derived stem cells, Biophysical Reviews, Vol.5, pp.11-28.

Salgado, A.J., Oliveira, J.M., Martins, A., Teixeira, F.G., Silva, N.A., Neves, N.M., Sousa, N. & Reis, R.L. (2013). Tissue Engineering and Regenerative Medicine: Past, Present, and Future, International Review of Neurobiology, Vol.108, pp.1-33.

Sánchez Alvarado, A. & Yamanaka, S. (2014). Rethinking Differentiation: Stem Cells, Regeneration, and Plasticity, Cell, Vol.157(1), pp.110–119.

Sándor, G.K., Numminen, J., Wolff, J., Thesleff, T., Miettinen, A., Tuovinen, V.J., Mannerström, B., Patrikoski, M., Seppänen, R., Miettinen, S., Rautiainen, M. & Öhman, J. (2014). Adipose Stem Cells Used to Reconstruct 13 Cases With Cranio-Maxillofacial Hard-Tissue Defects, Stem Cells Translational Medicine, Vol.3, pp.530-540.

Schipper, B.M., Marra, K.G., Zhang, W., Donnenberg, A.D. & Rubin, J.P. (2008). Regional Anatomic and Age Effects on Cell Function of Human Adipose-Derived Stem Cells, Annals of Plastic Surgery, Vol.60(5), pp.538-544.

Schliephake, H., Zghoul, N., Jäger, V., van Griensven, M., Zeichen, J., Gelinsky, M. & Wülfing, T. (2009). Effect of seeding technique and scaffold material on bone formation in tissue-engineered constructs, Journal of Biomedical Materials Research. Vol.90A, pp.429-437.

Schmitt, A., van Griensven, M., Imhoff, A.B. & Buchmann, S. (2012). Application of Stem Cells in Orthopedics, Stem Cells International, Vol.2012, pp.1-11.

Serakinci, N. & Keith, W.N. (2006). Therapeutic potential of adult stem cells, European Journal of Cancer, Vol.42(9), pp.1243–1246.

Shimizu, K., Ito, A. & Honda, H. (2007). Mag-Seeding of Rat Bone Marrow Stromal Cells into Porous Hydroxyapatite Scaffolds for Bone Tissue Engineering, Journal of Bioscience and Bioengineering. Vol.104(3), pp.171-177.

Solchaga, L.A., Tognana, E., Penick, K., Baskaran, H., Goldberg, V.M., Caplan, A.I. & Welter, J.F. (2006). A Rapid Seeding Technique for the Assembly of Large Cell/Scaffold Composite Constructs, Tissue Engineering. Vol.12(7), pp.1851-1863.

Soletti, L., Nieponice, A., Guan, J., Stankus, J.J., Wagner, W.R. & Vorp, D.A. (2006). A seeding device for tissue engineered tubular structures, Biomaterials. Vol.27, pp.4863-4870.

Starr, C. & McMillan, B. (2015). Human Biology, Cencage Learning, 11th edition, pp.96-98.

Tan, L., Ren, Y. & Kuijer, R. (2012). A 1-min Method for Homogenous Cell Seeding in Porous Scaffolds, Journal of Biomaterials Applications, Vol.26(7), pp.877–889.

Thevenot, P., Nair, A., Dey, J., Yang, J. & Tang, L. (2008). Method to Analyze Three-Dimensional Cell Distribution and Infiltration in Degradable Scaffolds, Tissue Engineering: Part C. Vol.14(4), pp.319-331.

Tirkkonen, L., Haimi, S., Huttunen, S., Wolff, J., Pirhonen, E., Sándor, G.K. & Miettinen, S. (2012). Osteogenic medium is superior to growth factors in differentiation of human adipose stem cells towards bone-forming cells in 3D culture, European Cells and Materials, Vol.25, pp.144–158.

Tirkkonen, L., Halonen, H., Hyttinen, J., Kuokkanen, H., Sievänen, H., Koivisto, A.-M., Mannerström, B., Sándor ,G.K.B., Suuronen, R., Miettinen, S. & Haimi, S. (2011). The effects of vibration loading on adipose stem cell number, viability and differentiation towards bone-forming cells, Journal of the Royal Society Interface, Vol.8, pp.1736-1747.

Tsuji, W., Rubin, J.P. & Marra, K.G. (2014). Adipose-derived stem cells: Implications in tissue regeneration, World Journal of Stem Cells, Vol.6(3), pp.312–321.

Van Alst, M., Eenink, M.J., Kruft, M.A., van Tuil, R. (2009). ABC's of bioabsorption: application of lactide based polymers in fully resorbable cardiovascular stents, EuroIntervention, Vol.15(5), pp.23-27.

Van Harmelen, V., Röhrig, K. & Hauner, H. (2004). Comparison of proliferation and differentiation capacity of human adipocyte precursor cells from the omental and subcutaneous adipose tissue depot of obese subjects, Metabolism, Vol.54(5), pp.632-637.

Vergroesen, P.-P. A., Kroeze, R.-J., Helder, M.N. & Smitt, T.H. (2011). The Use of Poly(L-Lactide-co-caprolactone) as a Scaffold for Adipose Stem Cells in Bone Tissue Engineering: Application in a Spinal Fusion Model, Macromolecular Bioscience, Vol.11(6), pp.722-730.

Vert, M., Chabot, F., Leray, J. & Christel, P. (1981). Stereoregular bioresorbable polyesters for orthopaedic surgery, Die Makromolekulare Chemie, Vol.5, pp.30–41.

Villalona, G.A., Udelsman, B., Duncan, D.R., McGillicuddy, E., Sawh.Martinez, R.J., Hibino, N., Painter, C., Mirensky, T., Erickson, B., Shinoka, T. & Breuer, C.K. (2010). Cell-Seeding Techniques in Vascular Tissue Engineering, Tissue Engineering: Part B. Vol.16(3), pp.341-350.

Vitacolonna, M., Belharazem, D., Hohenberger, P. & Roessner, E.D. (2013). Effect of static seeding methods on the distribution of fibroblasts within human acellular dermis, BioMedical Engineering OnLine. Vol.12(55), pp.1-13.

Vunjak-Novakovic, G.,Obradovic, B., Martin, I., Bursac, P.M., Langer, R. & Freed, L.E. (1998). Dynamic Cell Seeding of Polymer Scaffolds for Cartilage Tissue Engineering, Biotechnology Progress, Vol.14, pp.193-202.

Vunjak-Novakovic & G., Radisic, M. (2004). Cell Seeding of Polymer Scaffolds. In: Hollander, A.P., Hatton, P.V., Biopolymer Methods in Tissue Engineering. Vol.238. Humana Press. Pp.131-145.

Wang, J., Asou, Y., Sekiya, I., Sotome, S., Orii, H. & Shinomiya, K. (2006). Enhancement of tissue engineered bone formation by a low pressure system improving cell seeding and medium perfusion into a porous scaffold, Biomaterials. Vol.27, pp.2738-2746.

Weissleder, R., Bogdanov, A., Neuwelt, E.A., Papisov, M. (1995). Long-circulating iron oxides for MR imaging, Advanced Drug Delivery Reviews, Vol.16(2-3), pp.321–334.

Xie, J., Jung, Y., Kim, S.H., Kim, Y.H. & Matsuda, T. (2006). New Technique of Seeding Chondrocytes into Microporous Poly(L-lactide-co-ε-caprolactone) Sponge by Cyclic Compression Force-Induced Suction, Tissue Engineering. Vol.12(7), pp.1811-1820.

Yan, X.-Z., van den Beucken, J.J.J.P., Both, S.K., Yang, P.-S., Jansen, J.A. & Yang, F. (2014). Biomaterial Strategies for Stem Cell Maintenance During In Vitro Expansion, Tissue Engineering: Part B, Vol. 20(4), pp.340–354.

Yeatts, A.B. & Fisher, J.P. (2011). Bone tissue engineering bioreactors: Dynamic culture and the influence of shear stress, Bone, Vol.48, pp.171-181.

Yoshii, T., Sotome, S., Torigoe, I., Tsuchiya, A., Maehara, H., Ichinose, S. & Shinomiya, K. (2009). Fresh bone marrow introduction into porous scaffolds using a simple low-pressure loading method for effective osteogenesis in a rabbit model, Journal of Orthopaedic Research, Vol.27(1), pp.1–7.

Zeltinger, J., Sherwood, J.K., Graham, D.A., Müeller, R. & Griffith, L.G. (2001). Effect of Pore Sie and Void Fraction on Cellular Adhesion, Proliferation, and Matrix Deposition, Tissue Engineering, Vol.7(5), pp.557-572.

Zhang, A., Zhang, Q., Bai, H., Li., L. & Li, J. (2014). Polymeric nanoporous materials fabricated with supercritical CO_2 and CO_2-expanded liquids, Chemical Society Reviews, Vol.43, pp.6983-6953.

Zhang, Y., Madhu, V., Dighe, A.S., Irvine, J.N. & Cui, Q. (2012). Osteogenic response of human adipose-derived stem cells to BMP-6, VEGF, and combined VEGF plus BMP-6 in vitro, Growth Factors, Vol.30(5), pp.333-343.

Zhang, Z.-Y., Teoh, S.H., Teo, E.Y., Chong, M.S.K., Shin, C.W. & Tien, F.T., Choolani, M.A., Chan, J.K.Y. (2010). A comparison of bioreactors for culture of fetal mesenchymal stem cells for tissue engineering, Biomaterials, Vol.31, pp.8684-8695.

Zhu, X.H., Arifin, D.Y., Khoo, B.H., Hua, J. & Wang, C.-H. (2010). Study of cell seeding on porous poly(D,L-lactic-co-glycolic acid) sponge and growth in a Couette-Taylor bioreactor, Chemical Engineering Science. Vol.65, pp.2108-2117.

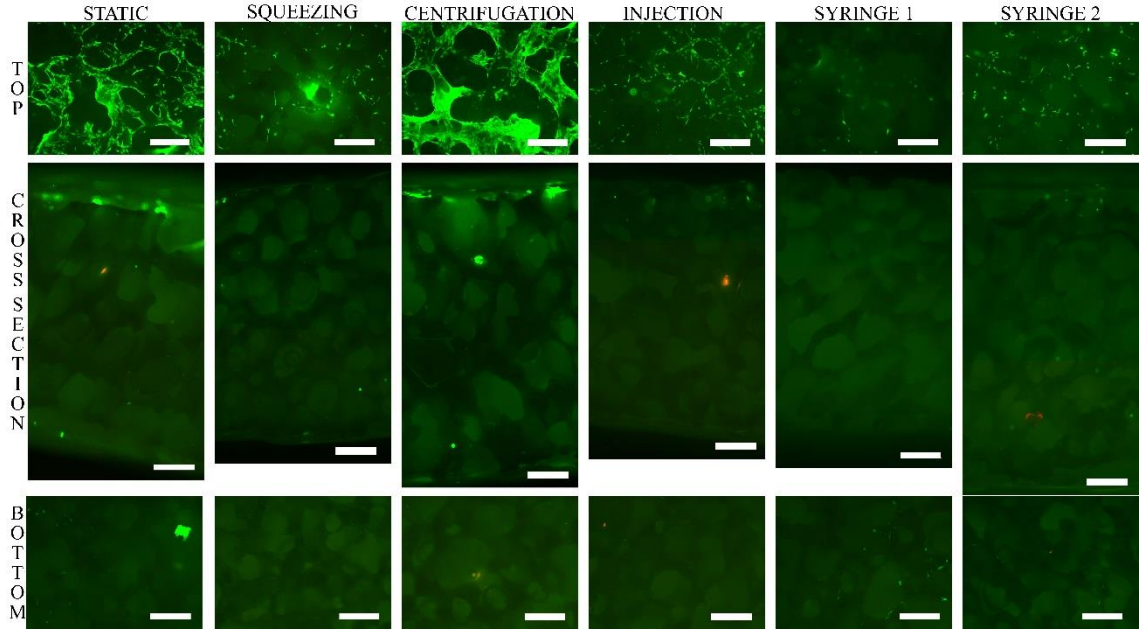## APPENDIX 1: WELL PLATE IMAGES OF COMP50 SCAFFOLDS

STATIC

SQUEEZING

CENTRIFUGATION

INJECTION

SYRINGE 1

SYRINGE 2
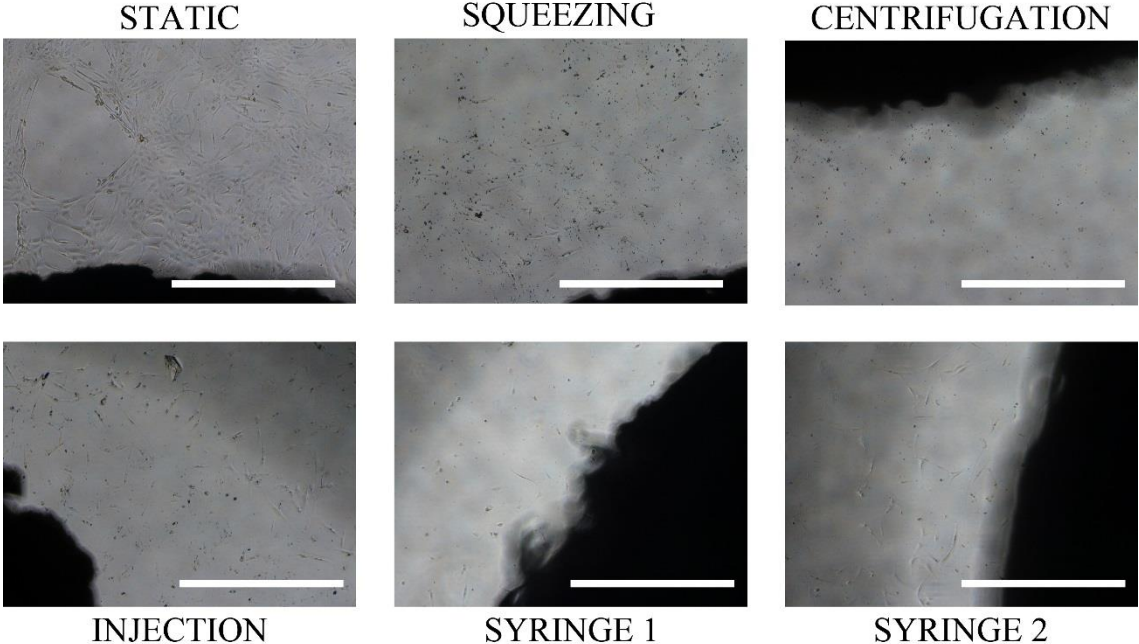
Light microscopy images of the well plates at a time point of 3 days. Scale bars 1.0 mm.
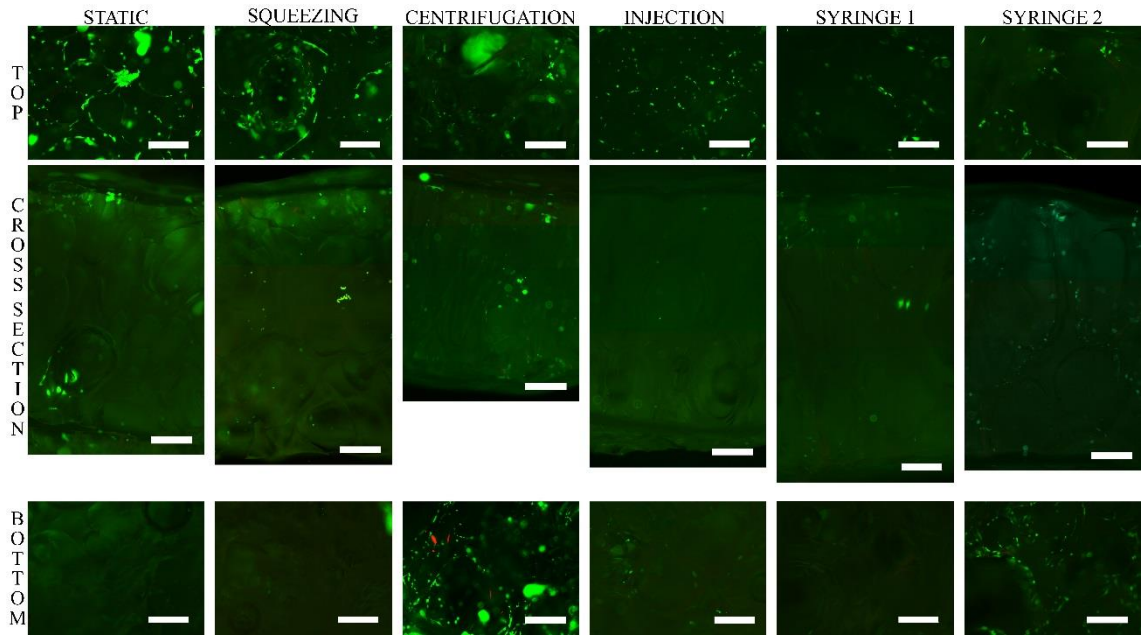
APPENDIX 2: LIVE/DEAD EXPERIMENTS 1 & 2 (1/2)
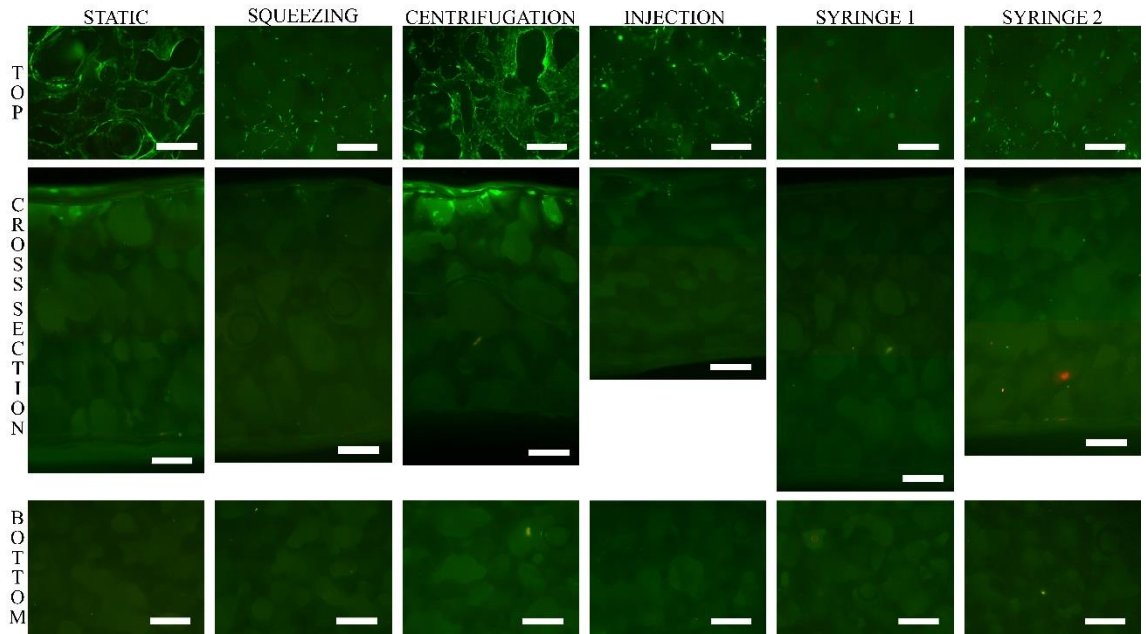
COMP50 Experiment 1 - scale bars 500 µm.

COMP50 Experiment 2 - scale bars 500 µm.

APPENDIX 2: LIVE/DEAD EXPERIMENTS 1 & 2 (2/2)
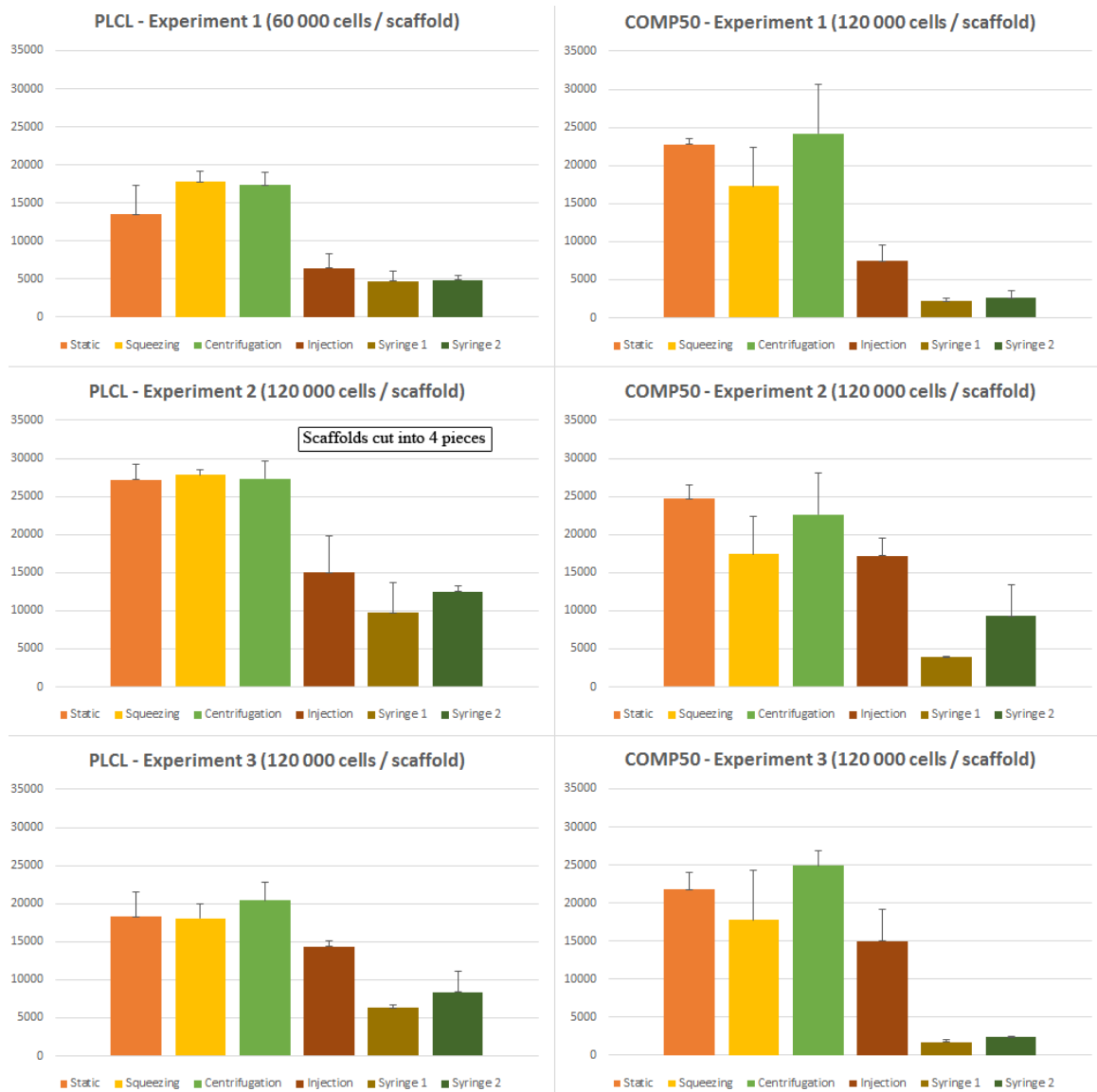

PLCL experiment 1 – scale bars 500 µm.
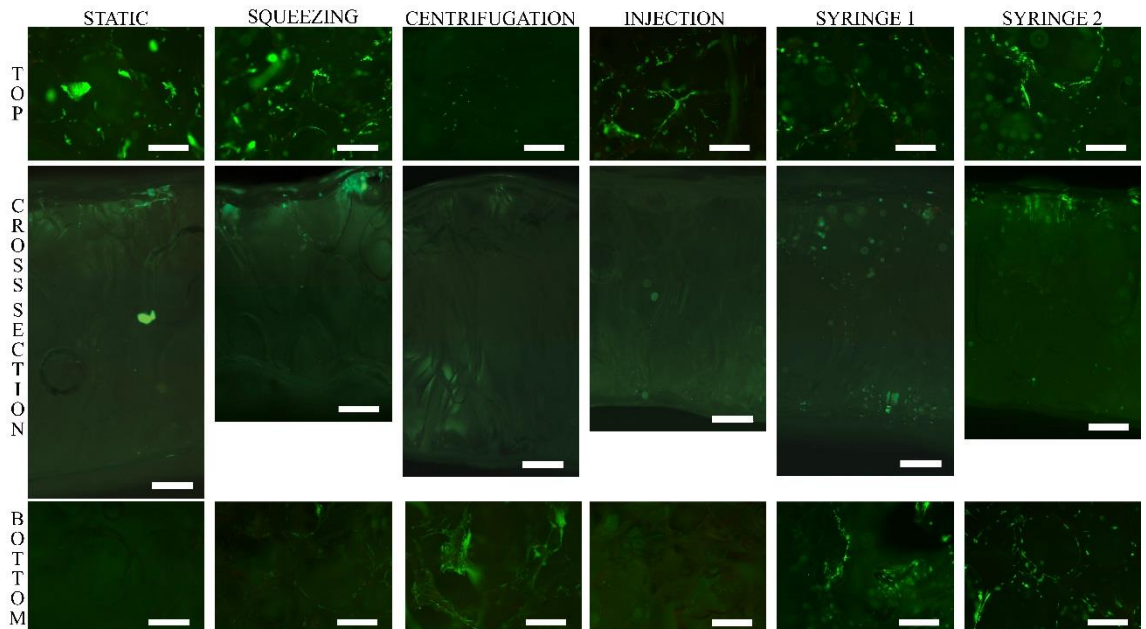
PLCL experiment 2 – scale bars 500 µm.

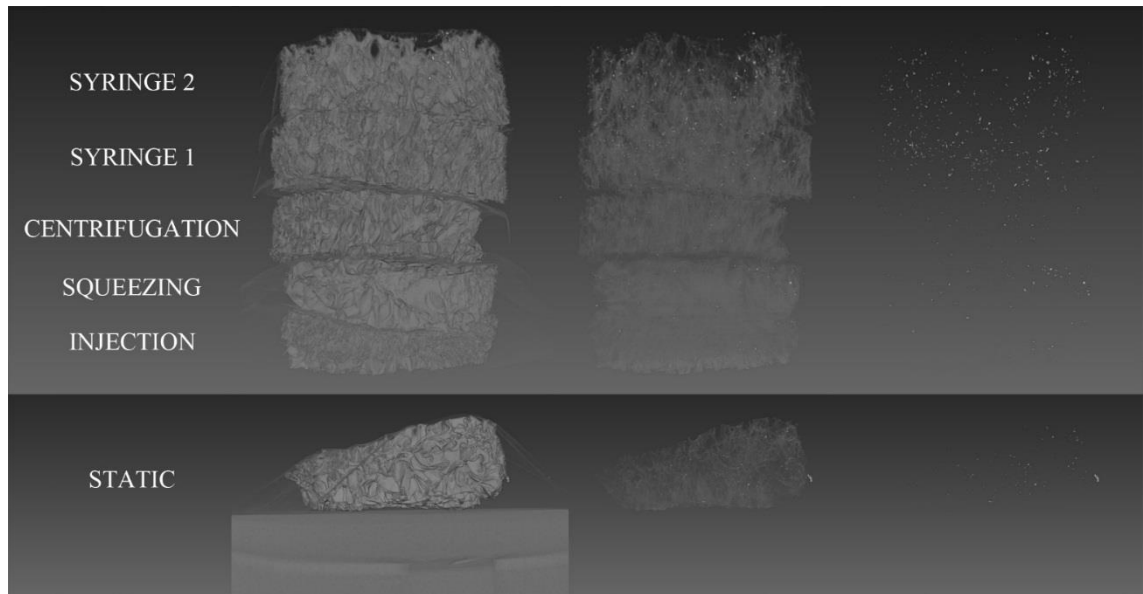# APPENDIX 3: PLCL & COMP50 CYQUANT RESULTS (1/2)
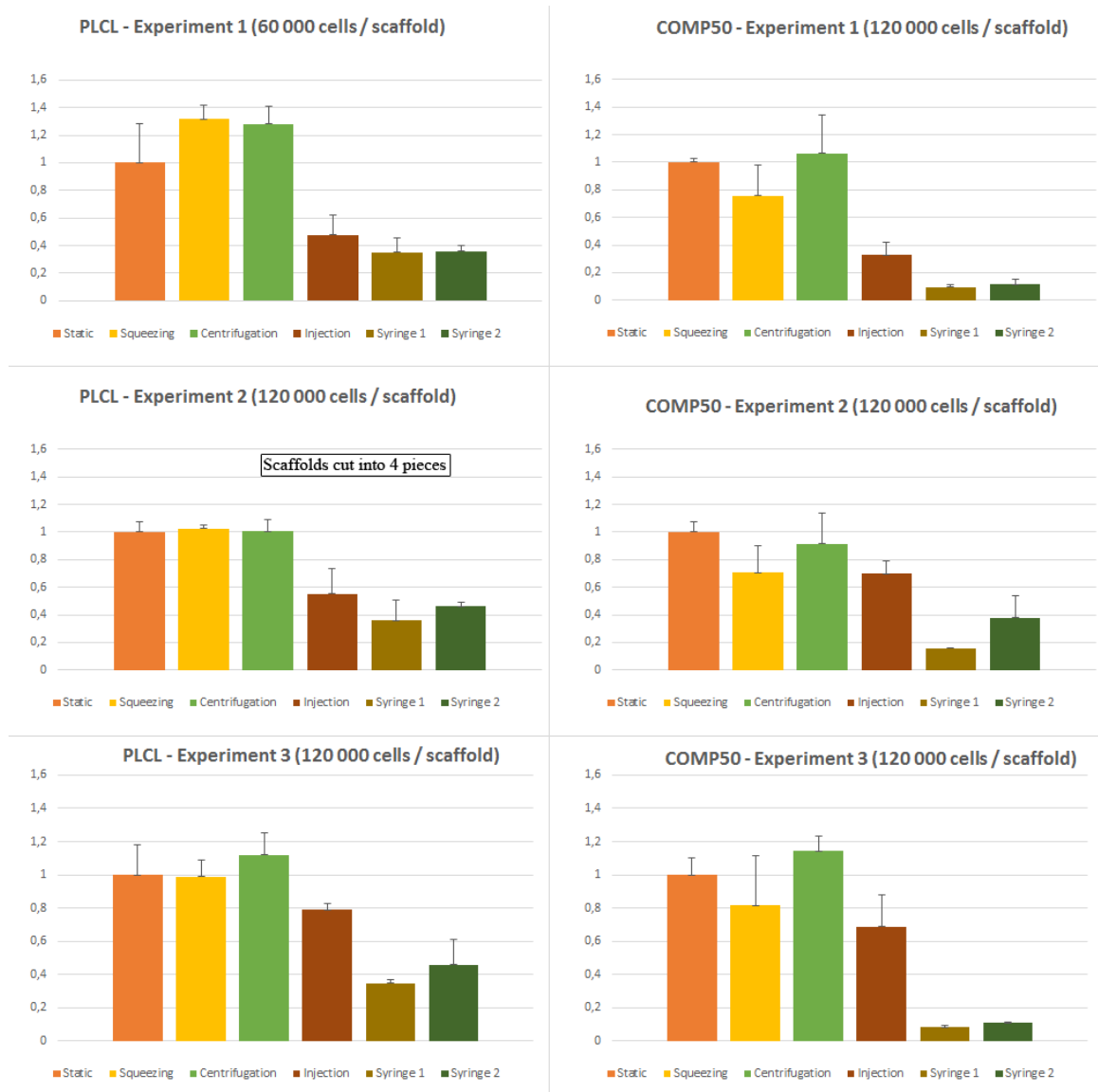
Parallel relative PLCL & COMP50 CyQUANT results.

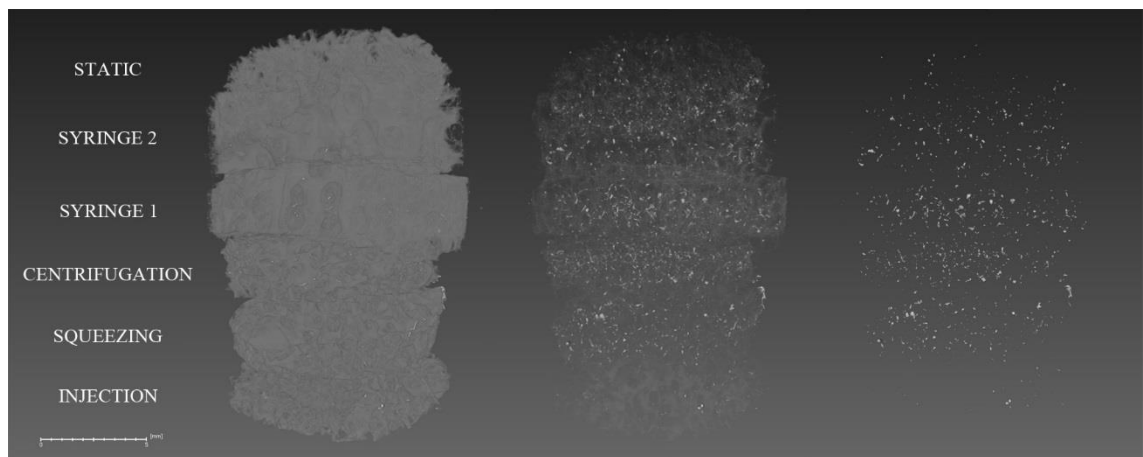# APPENDIX 3: PLCL & COMP50 CYQUANT RESULTS (2/2)

Parallel absolute PLCL & COMP50 CyQUANT results.

APPENDIX 4: PLCL MICRO-CT EXPERIMENTS 1 & 2

Sc-PLCL - Micro-CT Experiment 1. The statically seeded scaffold was individually im-
aged. The piles show the scaffold material being stepwise faded away. On the right, only
signals from the USPIO particles are seen.

Sc-PLCL - Micro-CT Experiment 2. Again, the piles represent the same scaffolds with a
different type of image processing: on the left, only the scaffold is seen. On the right, only
USPIO particle signals are shown. Scale bar 5.0 mm.

APPENDIX 5: PRUSSIAN BLUE RESULTS
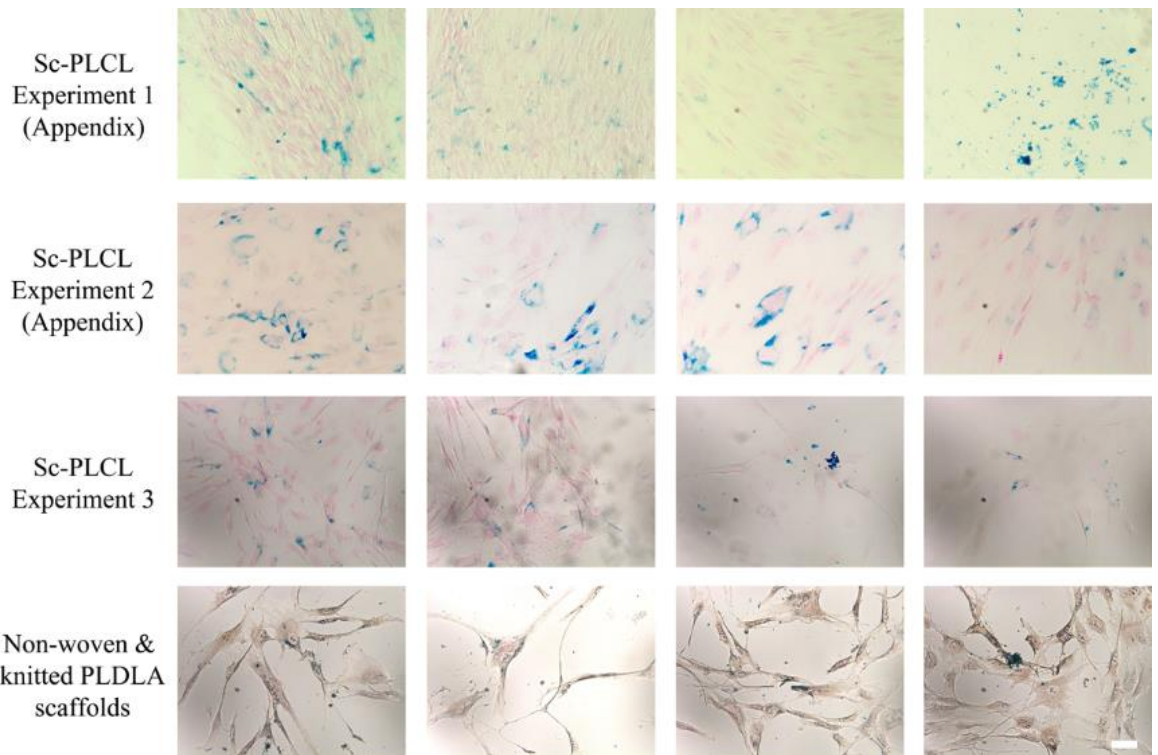
Prussian blue staining results. Each row shows four images from different sites of the same sample. Scale bar 50 μm.